

**COMPREHENSIVE EVALUATION OF FIVE SENSORS USED FOR
PAVEMENT MONITORING**

by

Vivek Tandon

and

Soheil Nazarian

Research Project 913

**DEVELOPMENT OF AN ABSOLUTE CALIBRATION SYSTEM FOR
NONDESTRUCTIVE TESTING DEVICES**

conducted for

Texas State Department of Highways and

Public Transportation

by

Center for Geotechnical and Highway Materials Research

The University of Texas at El Paso

Research Report 913-1F, Volume 1

August 1990

ABSTRACT

The Falling Weight Deflectometer (FWD) and Dynaflect devices are presently being used by highway agencies. The primary function of the FWD and Dynaflect devices is to measure a deflection basin due to a load imparted to the pavement. Deflection basins measured in the field are used in backcalculating modulus profiles of pavement sections. As such, it is critical to determine the deflection basins in the field with great accuracy. Velocity transducers (also called geophones) are used to determine the deflections, and load cells are utilized to measure applied load.

It has become increasingly important in recent years to be able to evaluate the performance of the deflection and load sensors of the Falling Weight Deflectometer or the Dynaflect devices. It has been shown that a small error in the deflections measured in the field may yield significantly erroneous modulus values. As such, a very reliable method for evaluating the accuracy of the sensors used for determining these deflections is necessary.

If geophones are used to determine deflections, the algorithm developed for calculating deflection will also become important. A geophone measures the so-called "raw" particle velocity of the pavement surface directly underneath it. Therefore, the methodology and algorithm employed to obtain the "actual" displacement must be carefully considered. Errors in the load cell measurements are not as important, but should be avoided for reliable results.

In this report, the results of an all around evaluation of five sensors which are commonly used in pavement engineering area are presented. These sensors are: an accelerometer, a LVDT, a proximeter, a geophone and a laser optocator. In the evaluation process, factors such as, cost, accuracy, precision, field-worthiness and ease of mounting were considered. It was found that the geophones are the most suitable sensors amongst the five sensors evaluated.

KEY WORDS: Nondestructive Testing, Performance Monitoring, Geophones, Accelerometers, LVDT's, Sensors, Calibration

METRIC (SI*) CONVERSION FACTORS

APPROXIMATE CONVERSIONS TO SI UNITS

Symbol When You Know Multiply By To Find Symbol

LENGTH

in	Inches	2.54	centimetres	cm
ft	feet	0.3048	metres	m
yd	yards	0.914	metres	m
mi	miles	1.61	kilometres	km

AREA

in ²	square inches	645.2	centimetres squared	cm ²
ft ²	square feet	0.0929	metres squared	m ²
yd ²	square yards	0.836	metres squared	m ²
mi ²	square miles	2.59	kilometres squared	km ²
ac	acres	0.395	hectares	ha

MASS (weight)

oz	ounces	28.35	grams	g
lb	pounds	0.454	kilograms	kg
T	short tons (2000 lb)	0.907	megagrams	Mg

VOLUME

fl oz	fluid ounces	29.57	millilitres	mL
gal	gallons	3.785	litres	L
ft ³	cubic feet	0.0328	metres cubed	m ³
yd ³	cubic yards	0.0765	metres cubed	m ³

NOTE: Volumes greater than 1000 L shall be shown in m³.

TEMPERATURE (exact)

°F	Fahrenheit temperature	5/9 (after subtracting 32)	Celsius temperature	°C
----	------------------------	----------------------------	---------------------	----

APPROXIMATE CONVERSIONS TO SI UNITS

Symbol When You Know Multiply By To Find Symbol

LENGTH

mm	millimetres	0.039	inches	in
m	metres	3.28	feet	ft
m	metres	1.09	yards	yd
km	kilometres	0.621	miles	mi

AREA

mm ²	millimetres squared	0.0016	square inches	in ²
m ²	metres squared	10.764	square feet	ft ²
km ²	kilometres squared	0.39	square miles	mi ²
ha	hectares (10 000 m ²)	2.53	acres	ac

MASS (weight)

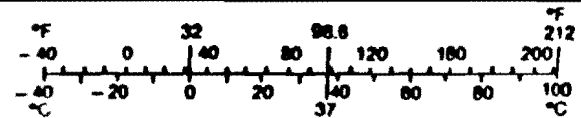
g	grams	0.0353	ounces	oz
kg	kilograms	2.205	pounds	lb
Mg	megagrams (1 000 kg)	1.103	short tons	T

VOLUME

mL	millilitres	0.034	fluid ounces	fl oz
L	litres	0.264	gallons	gal
m ³	metres cubed	35.315	cubic feet	ft ³
m ³	metres cubed	1.308	cubic yards	yd ³

TEMPERATURE (exact)

°C	Celsius temperature	9/5 (then add 32)	Fahrenheit temperature	°F
----	---------------------	-------------------	------------------------	----



These factors conform to the requirement of FHWA Order 5190.1A.

* SI is the symbol for the International System of Measurements

PREFACE

This report is the first of four reports which describes work done on Project 913, "Development of an Absolute Calibration System for Nondestructive Testing Devices." The study is being conducted at the Center for Geotechnical and Highway Materials Research, the University of Texas at El Paso with the cooperation of the Texas State Department of Highways and Public Transportation.

Many people have contributed their help towards the completion of this report. Thanks are extended to Mr. Amin Solehjou for excellent work in preparing the electronic parts, and to all the secretaries in the Department of Civil Engineering for their help and efforts.

Invaluable comments and support were provided by Mr. Robert Briggs, Richard Rogers and all other personnel of SDHPT.

Vivek Tandon

Soheil Nazarian

August, 1990

LIST OF REPORTS

Research Report 913-1F, Volume 1, "Comprehensive Evaluation of Five Sensors Used for Pavement Monitoring," by Vivek Tandon and Soheil Nazarian, presents an extensive testing program to evaluate the accuracy and precision of five deflection sensing transducers used in pavement engineering, for use by Texas State Department of Highways and Public Transportation, August, 1990.

Research Report 913-1F, Volume 2, "An Absolute Calibration System for Nondestructive Testing Devices," by Vivek Tandon and Soheil Nazarian, presents a system developed for the absolute calibration system of the FWD and Dynaflect devices, for use by the Texas State Department of Highways and Public Transportation, August, 1990.

Research Report 913-1F, Volume 3, "User's Manual to Computer Program Calibrat," by Vivek Tandon and Soheil Nazarian, contains a user's manual for a computer program called CALIBRAT, for use by the Texas State Department of Highways and Public Transportation, August, 1990.

Research Report 913-1F, Volume 4, "Appendices and Supporting Data," by Vivek Tandon and Soheil Nazarian, for use by the Texas State Department of Highways and Public Transportation, August, 1990.

SUMMARY

An extensive laboratory testing program was utilized to evaluate the accuracy and precision of five deflection sensing transducers used in pavement engineering. The sensors were tested under steady-state and impulsive loads over wide ranges of amplitudes and frequencies. It was found that the geophones are the most suitable sensors for measuring pavement deformations.

Geophones are rugged enough for the field implementation. Geophones cost less than other sensors. In addition, geophones do not need any special type of mounting fixtures as they can be attached to pavements anywhere with the help of modelling clay. Most importantly, no post and preamplification or signal conditioning is needed.

IMPLEMENTATION STATEMENT

The results of this study were implemented in the development of the calibration system. Also the outcome of this study can be implemented in any upcoming instrumentation project sponsored by the SDHPT.

TABLE OF CONTENTS

	<u>PAGE NO.</u>
ABSTRACT	i
PREFACE	iii
LIST OF REPORT	iv
SUMMARY	v
IMPLEMENTATION STATEMENT	vi
LIST OF FIGURES	ix
LIST OF TABLES	xii
CHAPTER ONE DESCRIPTION OF EQUIPMENT	1
1.1 Introduction	1
1.2 Transducers	1
1.2.1 Accelerometers	1
1.2.2 Linear Variable Differential Transformer	5
1.2.3 Proximeter Probes	8
1.2.4 Laser Optocator	10
1.2.5 Geophone	11
1.3 Load Cell	17
1.4 Recording Device	19
1.5 Waveform Generators	19
1.6 Vibration Source	19
1.6.1 Power Amplifier	19
1.6.2 Exciter	19
CHAPTER TWO LABORATORY TESTS SETUP AND PROCEDURES ...	21
2.1 Introduction	21
2.2 Calibration of LVDT	21
2.3 Calibration of Proximeter	21
2.4 Calibration of Geophone	21
2.5 Calibration of Accelerometer and Laser	23
2.6 Calibration of Load Cell	23

2.7	Laboratory Calibration Setup	24
CHAPTER THREE EVALUATION OF DEFLECTION		
	MEASURING SENSORS	32
3.1	Introduction	32
3.2	Description of Data Collected	32
	3.2.1 Steady State Experiments	32
	3.2.2 Impulse Experiments	39
3.3	Precision and Accuracy of Deflection Sensors	43
	3.3.1 Steady-State Deflections	43
	3.3.2 Half-sine impulse	52
	3.3.3 Square and Triangular Pulses	60
CHAPTER FOUR CONCLUSIONS		
		77
REFERENCES		
		81

LIST OF FIGURES

<u>Figure No.</u>	<u>Page No.</u>
1.1 SCHEMATIC OF SPRING MASS SYSTEM USED IN ACCELERATION TRANSDUCER	2
1.2 GENERAL CONFIGURATION OF AN ACCELEROMETER	3
1.3 BASIC WORKING PRINCIPLE OF LVDT DISPLACEMENT TRANSDUCERS	6
1.4 VARIATION IN OUTPUT VOLTAGE WITH CORE POSITION IN AN LVDT	6
1.5 SCHEMATIC OF LVDT USED IN THIS STUDY.	7
1.6 BLOCK DIAGRAM OF DC-DC CONVERSION CIRCUITRY.	7
1.7 GENERAL CONFIGURATION OF EDDY-CURRENT NONCONTACTING TRANSDUCER.	9
1.8 SCHEMATIC OF A LASER OPTOCATOR.	12
1.9 ELEMENTS OF A GEOPHONE.	13
1.10 IDEALIZED MODEL OF A GEOPHONE	14
1.11 GENERAL CONSTRUCTION OF LOAD CELL	18
2.1 SETUP FOR CALIBRATION OF LVDT	22
2.2 COMPARISON OF LOAD MEASURED WITH LOAD CELL 2 (WITHOUT AN ALUMINUM CASING	25
2.3 A VIEW OF ALUMINUM CASING USED FOR LOAD CELL CALIBRATION	26
2.4 EVALUATION OF EFFECTS OF MOUNTING LOAD CELLS IN AN ALUMINUM PLATE	27
2.5 BLOCK DIAGRAM OF SETUP USED IN THIS STUDY.	28
2.6 SETUP USED FOR COMPARISON OF DIFFERENT SENSORS . . .	29
2.7 SETUP USED FOR MOUNTING LASER OPTOCATOR	30
3.1 EVALUATION OF ACCURACY AND PRECISION OF ACCELEROMETER 1 UNDER STEADY-STATE LOADING. .	46
3.2 EVALUATION OF ACCURACY AND PRECISION OF ACCELEROMETER 2 UNDER STEADY-STATE LOADING. .	47

3.3	EVALUATION OF ACCURACY AND PRECISION OF GEOPHONE 1 UNDER STEADY-STATE LOADING.	48
3.4	EVALUATION OF ACCURACY AND PRECISION OF GEOPHONE 2 UNDER STEADY-STATE LOADING.	49
3.5	EVALUATION OF ACCURACY AND PRECISION OF LVDT UNDER STEADY-STATE LOADING.	50
3.6	EVALUATION OF ACCURACY AND PRECISION OF LASER UNDER STEADY-STATE LOADING.	51
3.7	VARIABILITY IN DEFLECTION MEASURED WITH PROXIMETER AS A FUNCTION OF FREQUENCY AND AMPLITUDE	53
3.8	EVALUATION OF ACCURACY AND PRECISION OF ACCELEROMETER 1 UNDER HALF-SINE PULSE LOADING. . .	54
3.9	EVALUATION OF ACCURACY AND PRECISION OF ACCELEROMETER 2 UNDER HALF-SINE PULSE LOADING. . .	55
3.10	EVALUATION OF ACCURACY AND PRECISION OF GEOPHONE 1 UNDER HALF-SINE PULSE LOADING.	56
3.11	EVALUATION OF ACCURACY AND PRECISION OF GEOPHONE 2 UNDER HALF-SINE PULSE LOADING.	57
3.12	EVALUATION OF ACCURACY AND PRECISION OF OF LVDT UNDER HALF-SINE PULSE LOADING	58
3.13	EVALUATION OF ACCURACY AND PRECISION OF LASER UNDER HALF-SINE PULSE LOADING	59
3.14	VARIABILITY IN DEFLECTION MEASURED WITH PROXIMETER AS A FUNCTION OF HALF-SINE IMPULSE	61
3.15	EVALUATION OF ACCURACY AND PRECISION OF ACCELEROMETER 1 UNDER TRIANGULAR LOADING	62
3.16	EVALUATION OF ACCURACY AND PRECISION OF ACCELEROMETER 2 UNDER SQUARE LOADING.	63
3.17	EVALUATION OF ACCURACY AND PRECISION OF GEOPHONE 1 UNDER SQUARE LOADING.	64
3.18	EVALUATION OF ACCURACY AND PRECISION OF GEOPHONE 2 UNDER SQUARE LOADING.	65
3.19	EVALUATION OF ACCURACY AND PRECISION OF LVDT UNDER SQUARE LOADING	66

3.20	EVALUATION OF ACCURACY AND PRECISION OF LASER UNDER SQUARE LOADING	67
3.21	VARIABILITY IN DEFLECTION MEASURED WITH PROXIMETER AS A FUNCTION OF FREQUENCY AND AMPLITUDE	68
3.22	EVALUATION OF ACCURACY AND PRECISION OF ACCELEROMETER 1 UNDER TRIANGULAR PULSE LOADING.	69
3.23	EVALUATION OF ACCURACY AND PRECISION OF ACCELEROMETER 2 UNDER TRIANGULAR PULSE LOADING.	70
3.24	EVALUATION OF ACCURACY AND PRECISION OF GEOPHONE 1 UNDER TRIANGULAR PULSE LOADING.	71
3.25	EVALUATION OF ACCURACY AND PRECISION OF GEOPHONE 2 UNDER TRIANGULAR PULSE LOADING.	72
3.26	EVALUATION OF ACCURACY AND PRECISION OF LVDT UNDER TRIANGULAR PULSE LOADING	73
3.27	EVALUATION OF ACCURACY AND PRECISION OF LASER UNDER TRIANGULAR PULSE LOADING	74
3.28	VARIABILITY IN DEFLECTION MEASURED WITH PROXIMETER AS A FUNCTION OF HALF-SINE IMPULSE	75
4.1	COMPARISON OF DATA OBTAINED FROM LASER AND GEOPHONE, FOR HALF-SINE, AT 1 MIL DEFLECTION. .	78

LIST OF TABLES

<u>Table No.</u>		<u>Page No.</u>
3.1	SUMMARY OF STEADY-STATE TESTS CARRIED OUT IN THE ABSENCE OF LASER DEVICE . . .	34
3.2	TESTING SEQUENCE USED IN STEADY-STATE DEFLECTION MEASUREMENTS AT EACH FREQUENCY AND AMPLITUDE. .	35
3.3	COMPARISON OF DEFLECTIONS FOR PROXIMETER AND OTHER SENSORS	36
3.4	EVALUATION OF VARIATION IN DEFLECTIONS MEASURED BY EACH SENSOR	36
3.5	SUMMARY OF STEADY-STATE TESTS CARRIED OUT IN THE PRESENCE OF LASER DEVICE	37
3.6	TESTING SEQUENCE USED IN STEADY-STATE DEFLECTION MEASUREMENTS AT EACH FREQUENCY AND AMPLITUDE. .	38
3.7	SUMMARY OF IMPULSE TESTS CARRIED OUT IN THE ABSENCE OF LASER DEVICE	40
3.8	TESTING SEQUENCE USED IN IMPULSE MOTION DEFLECTION MEASUREMENTS AT EACH PULSE WIDTH AND AMPLITUDE.	41
3.9	COMPARISON OF DEFLECTIONS FOR PROXIMETER AND OTHER SENSORS	42
3.10	EVALUATION OF VARIATION IN DEFLECTIONS MEASURED BY EACH SENSOR	42
3.11	SUMMARY OF IMPULSE TESTS CARRIED OUT IN PRESENCE OF LASER DEVICE	44
3.12	COMPARISON OF DEFLECTIONS FROM LASER AND OTHER SENSORS	45
4.1	COMPARISON OF DIFFERENT CHARACTERISTICS OF FIVE SENSORS EVALUATED	79

CHAPTER ONE

DESCRIPTION OF EQUIPMENT

1.1 INTRODUCTION

The accuracy and precision of five transducers used for measuring displacement of pavements were evaluated. The advantages and disadvantages of each transducer are briefly discussed in this chapter. Also a brief overview of recording device, waveform generators, vibration sources used in this experiment are presented in the last three sections of the chapter. The specifications of all the equipment used in this study are included in Appendix A.

1.2 TRANSDUCERS

Accuracy and precision of five different deflection measuring devices were determined. An accelerometer, a linear variable differential transformer (LVDT), a proximeter probe, a laser optocator and geophones were compared. These devices were selected because of their commercial availability and their effectiveness in deflection measurement. In the next section, the theoretical background and working principles behind each device are described.

1.2.1 ACCELEROMETERS

Accelerometers are important vibration measurement sensors which are available in wide ranges of sizes and response characteristics. All accelerometers use a sensing mechanism to measure the acceleration which acts upon a mass (sometimes called proof mass or seismic mass). This mass is restrained by a spring. The motion of mass is usually damped in a spring mass system (Norton, 1982), as shown in Figure 1.1. When a motion is applied to an accelerometer case, the mass moves relative to the case and consequently the spring gets stretched. Under a dynamic motion, the mass is accelerated at a certain rate due to a force exerted on the spring. Since the spring deflection is proportional to the force applied to the mass and the force is proportional to the acceleration of the mass, the spring deflection is a measure of acceleration (Doebelin, 1983).

The general construction of an accelerometer is shown in Figure 1.2. The system consists of a mass, M , connected to the accelerometer case by means of a spring, a dashpot and a relative displacement transducer. The spring is linear and has a spring constant of K_s . The viscous coefficient of damping of the dashpot is B . In order to measure the acceleration, an accelerometer is rigidly fastened to the moving system. The absolute displacement of the system and the accelerometer mass can be assumed to be X_i and X_m , respectively. The relative displacement of the transducer with respect to mass M is denoted as X_0 . Relative displacement transducers are usually made of piezoelectric crystals.

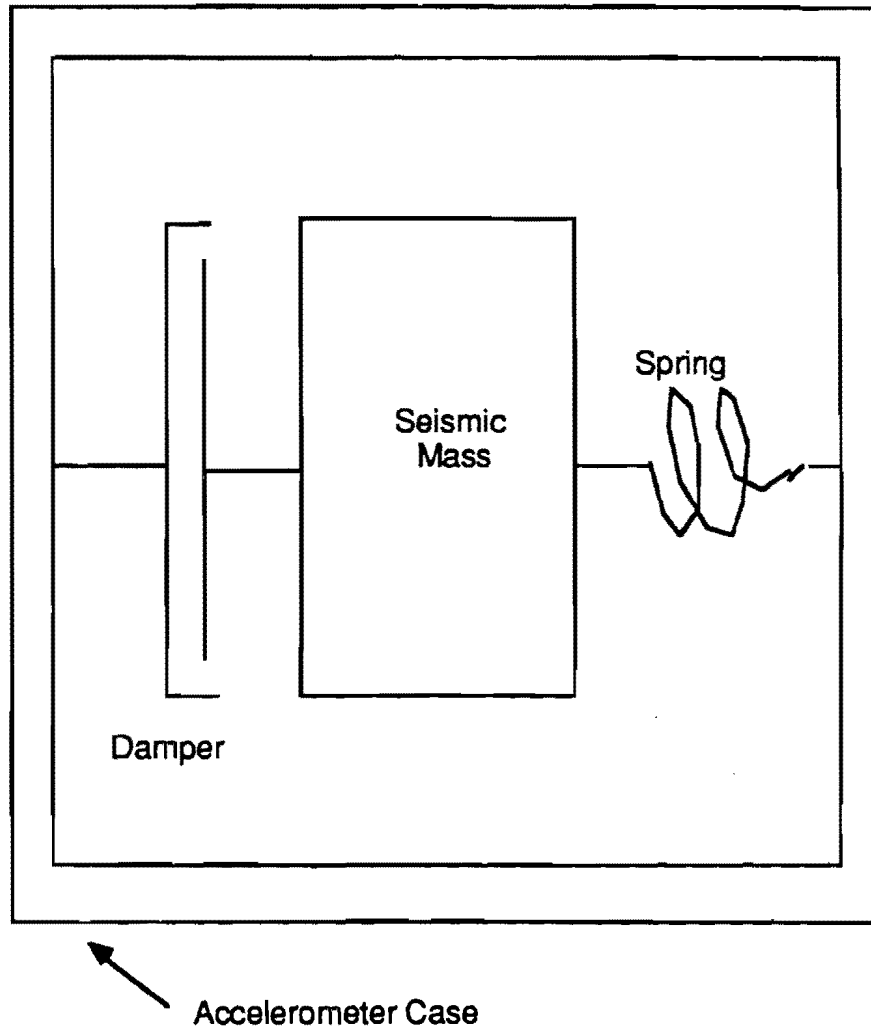


Figure 1.1 Schematic of Spring Mass System Used in Acceleration Transducer (from Norton, 1982)

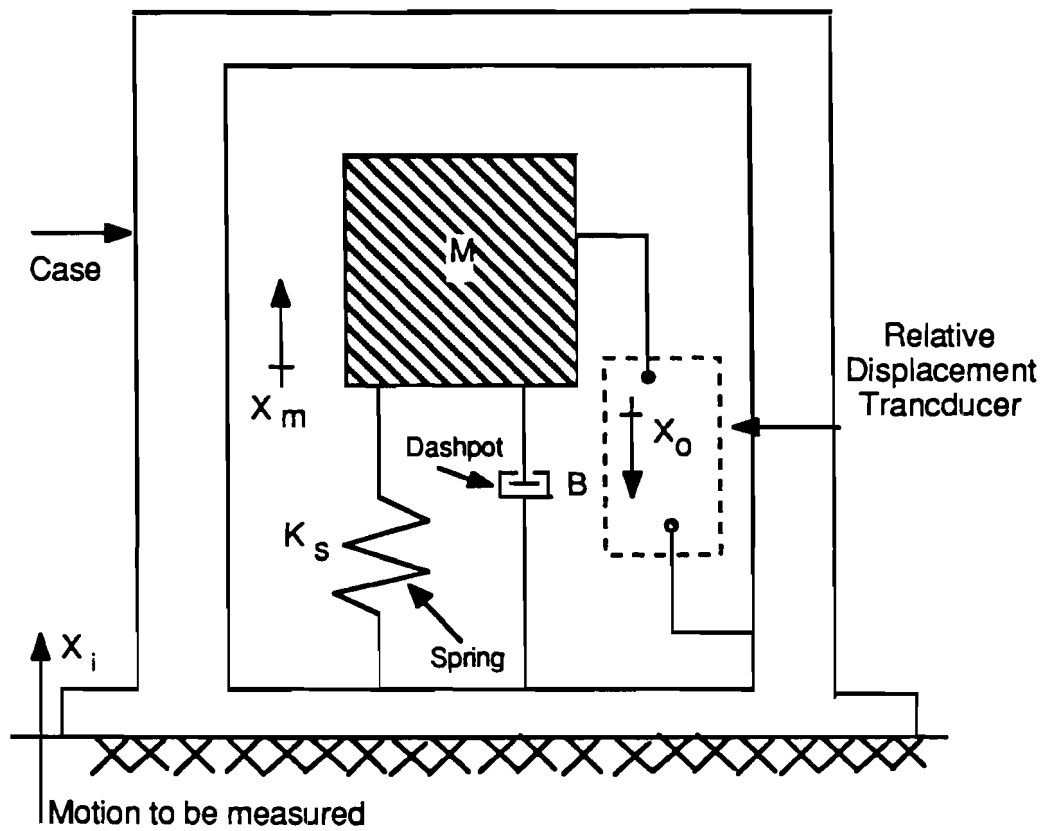


Figure 1.2 General Configuration of an Accelerometer (from Doebelin, 1983)

To derive the theoretical relationship between the absolute displacement of the material to be measured and the accelerometer mass, Newton's law is applied to the seismic mass as follows:

$$B\dot{X}_0 + K_s X_0 - M(\ddot{X}_1 - \ddot{X}_0) \quad (1.1)$$

In Equation 1.1, \dot{X}_0 and X_0 correspond to first and second derivatives of X_0 with respect to time and similarly \ddot{X}_1 is the second derivative of X_1 with respect to time. This equation can be rewritten as:

$$\frac{X_0}{X_1}(S) = \frac{\frac{S^2}{\omega_n^2}}{\frac{S^2}{\omega_n^2} + \frac{2\zeta S}{\omega_n} + 1} \quad (1.2)$$

where,

$$\omega_n \triangleq \sqrt{\frac{K_s}{M}}$$

$$\zeta \triangleq \frac{B}{2\sqrt{K_s M}}$$

Symbols S and \triangleq denote Laplace transform operator and corresponds to, respectively. Symbols ω_n and ζ denote the undamped natural frequency of the accelerometer and the damping ratio of the system, respectively. The sensitivity of the accelerometer can be denoted by K , which is inversely proportional to square of natural frequency, ω_n .

For a piezoelectric transducer Equation 1.2 can be rewritten as:

$$\frac{e_0}{\ddot{X}_1}(S) = \frac{\left[\left(\frac{K_q}{C\omega_n^2}\right)\right]\tau S}{(\tau S + 1)\left(\frac{S^2}{\omega_n^2} + \frac{2\zeta S}{\omega_n} + 1\right)} \quad (1.3)$$

where e_0 is the output voltage generated in the piezoelectric crystal due to mechanical deformation of the mass. Symbol τ is a discharge time constant of piezoelectric element. Symbol K_q is a proportionality constant. The value of K_q can be found from:

$$q = K_q x_i \quad (1.4)$$

where q is charge (in Coulomb) generated in the piezoelectric element, due to mechanical deflection X_i .

There are several advantages to the use of accelerometers. Piezoelectric accelerometers generate large output-voltage signals, are compact, and possess high natural frequencies. These properties make an accelerometer a good tool for accurate shock and vibration measurements. The damping ratio of an accelerometer is very low (about 0.01). This low damping ratio is acceptable because of very high natural frequency associated with the accelerometers.

There are some disadvantages associated with accelerometers. Piezoelectric accelerometers do not respond to constant acceleration. Usually, the response of these accelerometers is not reliable at low frequencies. The lowest frequency that can be accurately measured with an accelerometer depends on the value of discharge time constant. The reliability of piezoelectric accelerometers for pulse waves of large duration is doubtful due to small value of discharge time constant τ . This matter is described in detail in Appendix B.

1.2.2 LINEAR VARIABLE DIFFERENTIAL TRANSFORMER

Linear Variable Differential Transformers (LVDT) uses the principle of change in magnetic coupling or reluctance to determine deflection. A schematic of an LVDT is shown in Figure 1.3. Basically, an LVDT consists of a case and a core. The case of an LVDT contains three coils, one primary and two secondary. The basic function of secondary coils is to produce opposing voltage. When the core is in a neutral or zero position, the voltage induced in the secondary windings are equal and the net output is zero. The output voltage will be non-zero when the core is moved, as shown in Figure 1.4. The output voltage will be positive or negative depending upon the relative position of the case and the core rod.

As the core rod penetrates farther in the core, magnetic coupling between the primary and one of the secondary coils increases meanwhile the coupling between the primary and the other secondary coil decreases. So, the net voltage increases as the core is moved away from the neutral position.

An schematic of the LVDT, which was used in our study is shown in Figure 1.5. The primary and the two secondary coils are wound over a hollow coil form, made of a nonmagnetic and insulating material. The ferromagnetic core is threaded to accept a gage head. The winding assembly is potted with a cylindrical case and the connecting leads are brought out of the potted assembly.

This transducer uses integrally packaged dc-dc conversion circuitry as shown in Figure 1.6. The conversion circuitry, which also provides for internal and external connections,

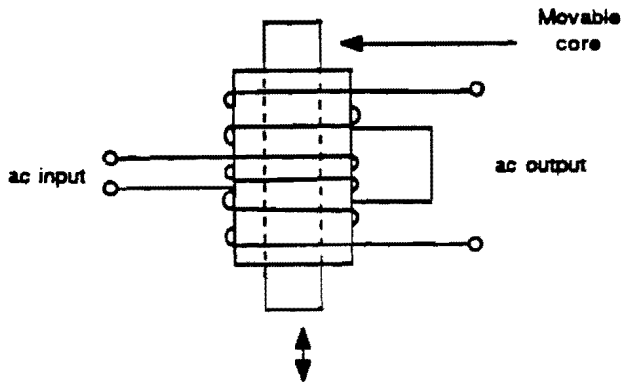


Figure 1.3 Basic Working Principle of LVDT Displacement Transducers (from Hordeski, 1987)

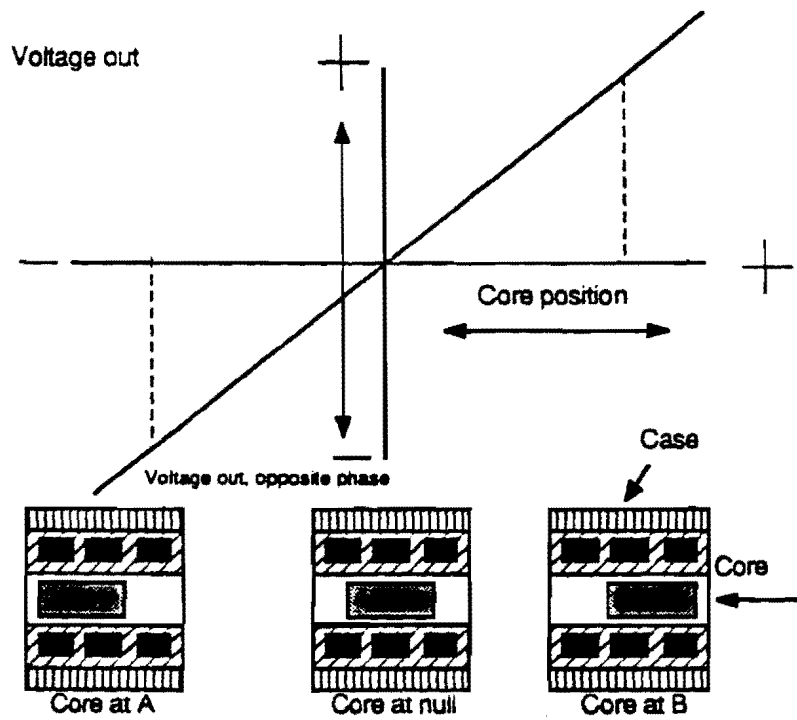


Figure 1.4 Variation in Output Voltage with Core Position in an LVDT (from Herceg, 1976)

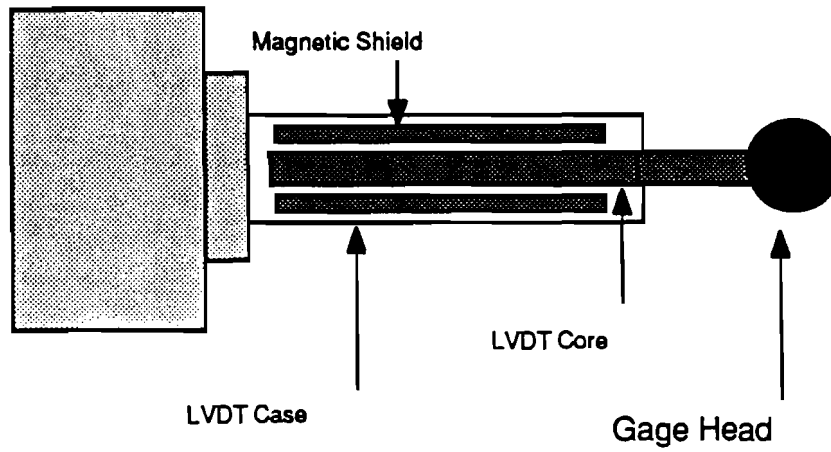


Figure 1.5 Schematic of LVDT Used in This Study

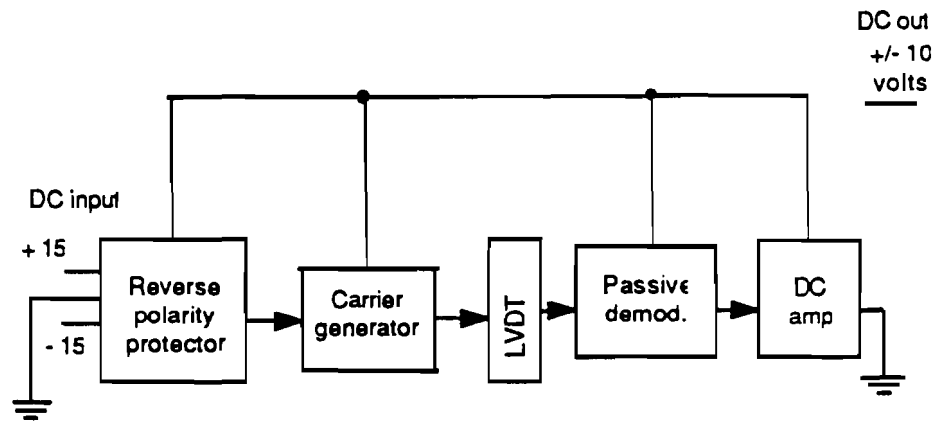


Figure 1.6 Block Diagram of dc-dc Conversion Circuitry (from Hecceg, 1976)

is mounted in the end of the case. The LVDT operates from a ± 15 Volts (dc) power supply and provides an output voltage of ± 10 V dc. As shown in the block diagram (Figure 1.6), a carrier generator is used to convert the direct current wave into the alternating current excitation. The LVDT output is then demodulated into the direct current and is amplified (Herceg, 1986). Reverse polarity protector is included in the design to prevent damage to the dc-dc circuitry due to accidental application of power with a reverse polarity. The resolution of an LVDT is infinitesimal because the core motion is continuous. However, amplification of the output voltage allows detection of a few mils.

The advantages of the LVDT are several. There is no physical contact between the case and the core; thus there is no friction or wear. Also, due to introduction of dc-dc circuitry, the LVDT becomes highly sensitive and extremely rugged at the expense of a reduced reliability.

There are several disadvantages associated with LVDT setup. Dynamic response of an LVDT is limited. Therefore motions with high frequency contents cannot be detected by an LVDT. There are small radial and longitudinal magnetic forces on the core if it is not centered radially and at the null position, which results in less reliability of measured deflection. The utilization of LVDT in the field is difficult and expensive. The output of the LVDT is linear only in a certain range near neutral position of the core. Therefore, the LVDT should be mounted such that the core is positioned near the neutral position. The LVDT also requires a smooth surface for gage head, to provide the continuous contact between the gage head and the surface, of which deflection is to be measured.

1.2.3 PROXIMETER PROBES

Proximeter probes are non-contacting inductive displacement transducers. Generally, the transducer system consists of a proximeter, a probe and an extension cable. The proximeter performs two functions within the transducer system. The first function is to generate a high-frequency signal and transmit the signal to the probe tip. The second function is to receive the signal from the probe tip and process it to produce a dc output proportional to the displacement of the material being observed.

The probe of the transducer system consists of two coils, i.e. active and balance coils, as shown in Figure 1.7. The high frequency signal is generated by the proximeter and is passed through the active coil located in the probe. The coil generates magnetic flux lines around the probe tip. If any conductive material intersects the magnetic field around the probe tip, eddy currents will be induced in the conductive material. Due to generation of eddy currents in the conductive material, the impedance of the active coil changes. This causes a bridge unbalance which is proportional to the strength of the eddy currents being generated. As a result the output voltage of the balance bridge is modulated by the conductive material moving in the magnetic flux around the probe tip. This unbalanced voltage is demodulated and linearized by the proximeter to produce a dc output proportional to target displacement. The essential part of the probe is a small coil located in its tip. This coil is housed in an epoxy fiberglass body which can be mounted in any

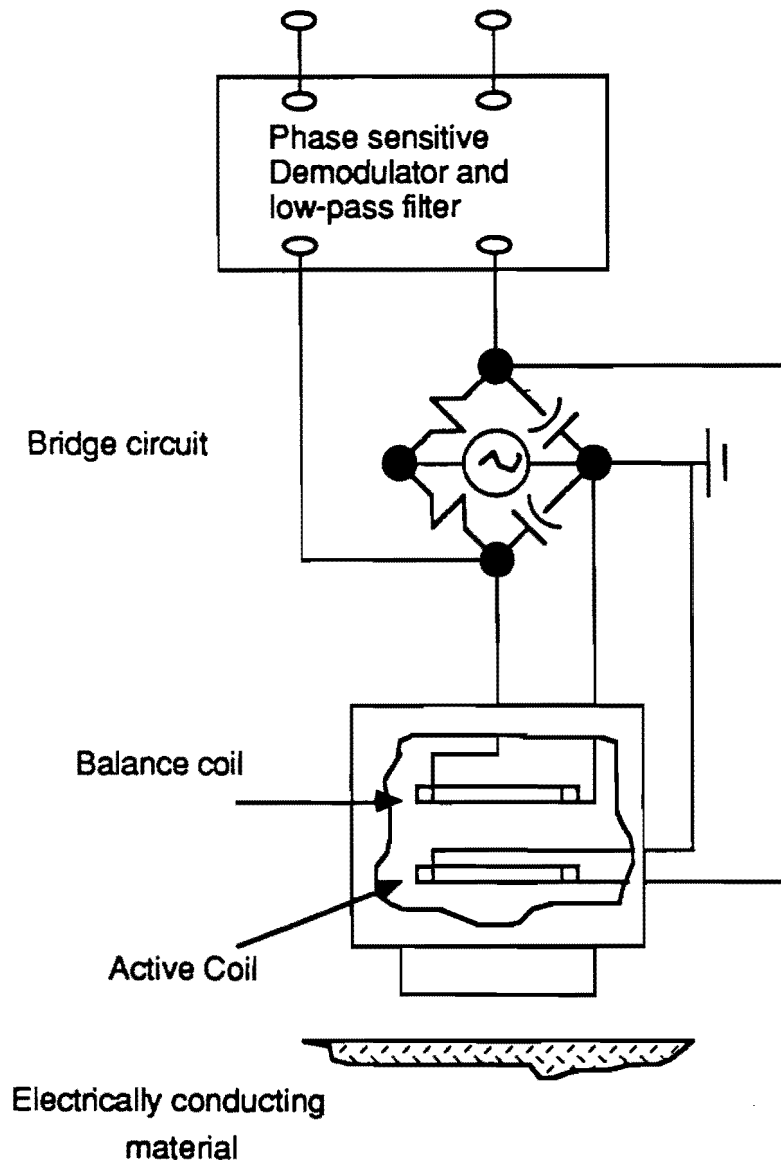


Figure 1.7 General Configuration of Eddy-Current Noncontacting Transducer (from Doebelin, 1983)

metal housing.

The extension cable is a 95-ohm impedance coaxial cable. The proximeter is the driver (oscillator/demodulator) for the transducer system. Its function is to supply energy for the probe and to linearize the signal returned from the probe. The proximeter is designed to operate with a power supply ranging from -18 Volts dc to -24 Volts dc.

The proximeter generates a Radio Frequency (RF) signal, which is transmitted to the coil at probe tip. This signal is radiated into the area surrounding the probe tip through the coil on the tip of probe. If there is no conductive material within the range of the RF signal field, the entire signal is returned to the proximeter. As a conductive material begins to intersect the RF field, eddy currents are induced in the conductive material. Due to generation of eddy currents in the conductive material, the density of signal returned to the proximeter will decrease. Proximeter detects this loss of signal and transmits it as a change in the dc voltage to the proximeter output terminal.

Major advantages of proximeters are as follows. Proximeter output can be read easily with any type of dc voltmeter. Application of high frequency radio signals yields a higher signal-to-noise ratio because more energy is transferred in less time, which immunizes the system from noise. The probe can be connected to proximeter with a long cable, therefore, the probe can be conveniently located near the target (conductive) material.

There are some drawbacks associated with proximeters. The calibration of the proximeter varies based upon the target material used. Also the input voltage needs to be constant and equal to the input voltage supply used while calibrating the proximeter. Proximeters can measure deflections accurately only if the probe is in the close vicinity of the target (within 2 mm). As such the chances of damaging the probe due to sudden increase in the deflection of the target material is high. It is not always easy to maintain a 2-mm gap between the target and probe under field conditions. It is also difficult to mount a proximeter perpendicular to the target in the field. For accurate measurement, the probe should be perpendicular to the target otherwise the deflection obtained may not be reliable.

1.2.4 LASER OPTOCATOR

LASER, which is an acronym formed from the phrase "Light Amplification by Stimulated Emission of Radiation", allows the emission of the entire energy in a narrow beam and in a single direction. The laser optocator is a non-contact displacement transducer. It consists of a light source (either ultra-violet or infra-red) and a photodetector (or light-sensitive transistor) to receive the reflected signal. A beam of light from the light source is aimed at the surface whose position is to be measured. The beam of light is reflected back from the surface. The reflected light is focused on the photodetector through a lens. The photodetector sends a signal to the signal processor according to the position of focused beam on the photodetector.

A laser system consists of a probe, an optocator and a central processing unit. The

optocator gauge probe contains a laser diode, which emits a beam of invisible infra-red (IR) light pulses through a lens assembly (as shown in Figure 1.8). When the light beam hits a surface, part of the light energy will be reflected. This reflected light is collected by the gauge probe's camera unit and focused onto a light-sensitive photodetector. The photodetector provides an output signal proportional to the position of the image on the detector to a central processing unit (CPU). The CPU is equipped with a receiver and a microprocessor board.

The receiver board receives the information from the photodetector in a serial form, converts information to parallel form and acts as an interface between the gauge probe and the microprocessor. The microprocessor board receives the data from the receiver board and converts the measurement data to distance and provides the results on a digital display.

The laser is quite accurate and has a resolution of about 0.025 percent of the measurement range. Pulse durations of approximately 30 microseconds and 16,000 to 32,000 pulse repetitions per second allow the measurements to be made on a moving object.

The laser used in this study is an accurate deflection measuring tool. However, it is not a practical instrument especially for use in the field. To avoid scatter of infra-red laser rays, the observed target should be smooth which is not the case for pavements. Also, good resolution at very low deflection (about 1 mil) could not be obtained in our experiment.

1.2.5 GEOPHONE

Geophones are coil-magnet systems as shown in Figure 1.9. A mass is attached to a spring and a coil is connected to the mass. The coil is located such that it crosses the magnetic field. Due to an impact, the magnet moves but the mass remains more or less stationary causing a relative motion between the coil and magnet. This relative motion generates voltage in the coil which is proportional to the relative velocity between the coil and magnet.

The geophone system can be considered as a Single-Degree-Of-Freedom (SODF) system (Nazarian, 1987). This idealized system is shown in Figure 1.10. Geophone properties that should be addressed are natural frequency, transductivity, and damping. The natural frequency is the undamped natural frequency of the system. Transductivity is the factor of proportionality between the velocity and the output voltage and can be considered as a calibration factor. Damping of the system indicates the attenuation of the motion with time.

The mass, m , in the model (Figure 1.10) is equivalent to the total mass of the spring, suspended mass and the conductor of the geophone. The dashpot, which provides viscous damping in the model, simply corresponds to the electrical resistance of the conductor, pigtail, and any external resistor added to the system. The movement of the

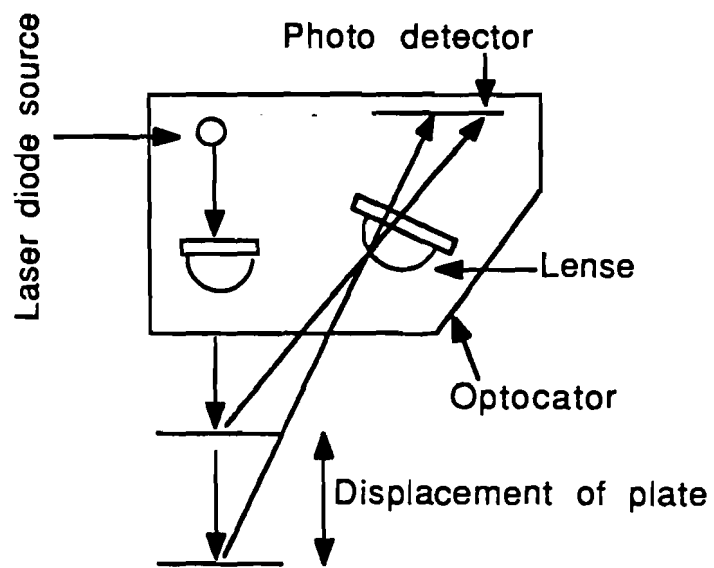


Figure 1.8 Schematic of a Laser Optocator
(Optical Level Sensor) (from Sealecom, 1989)

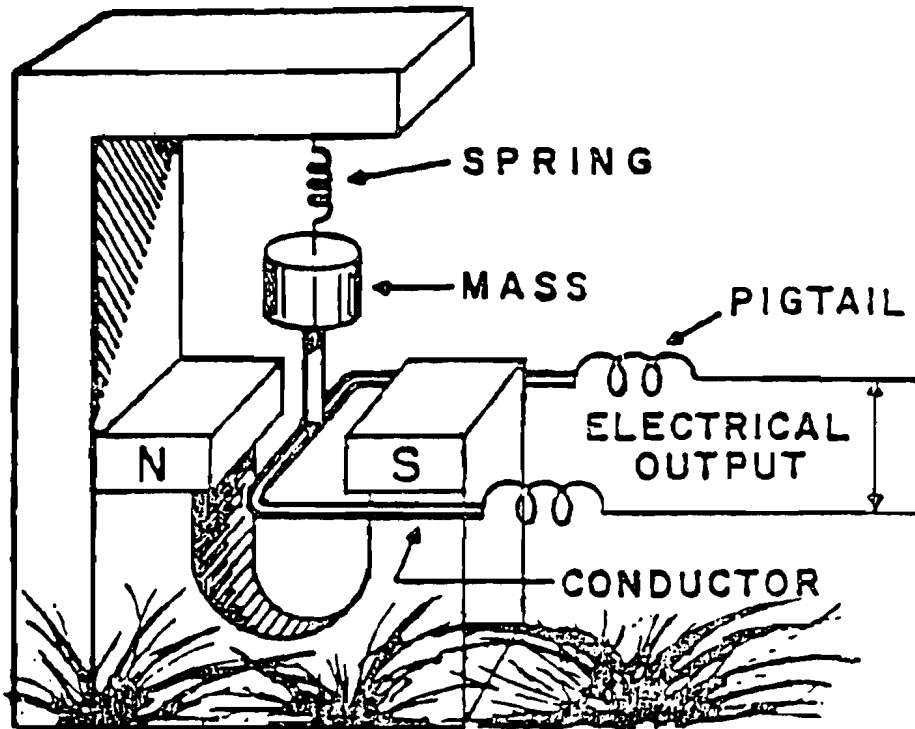


Figure 1.9 Elements of a Geophone (from Mark Products, 1985)

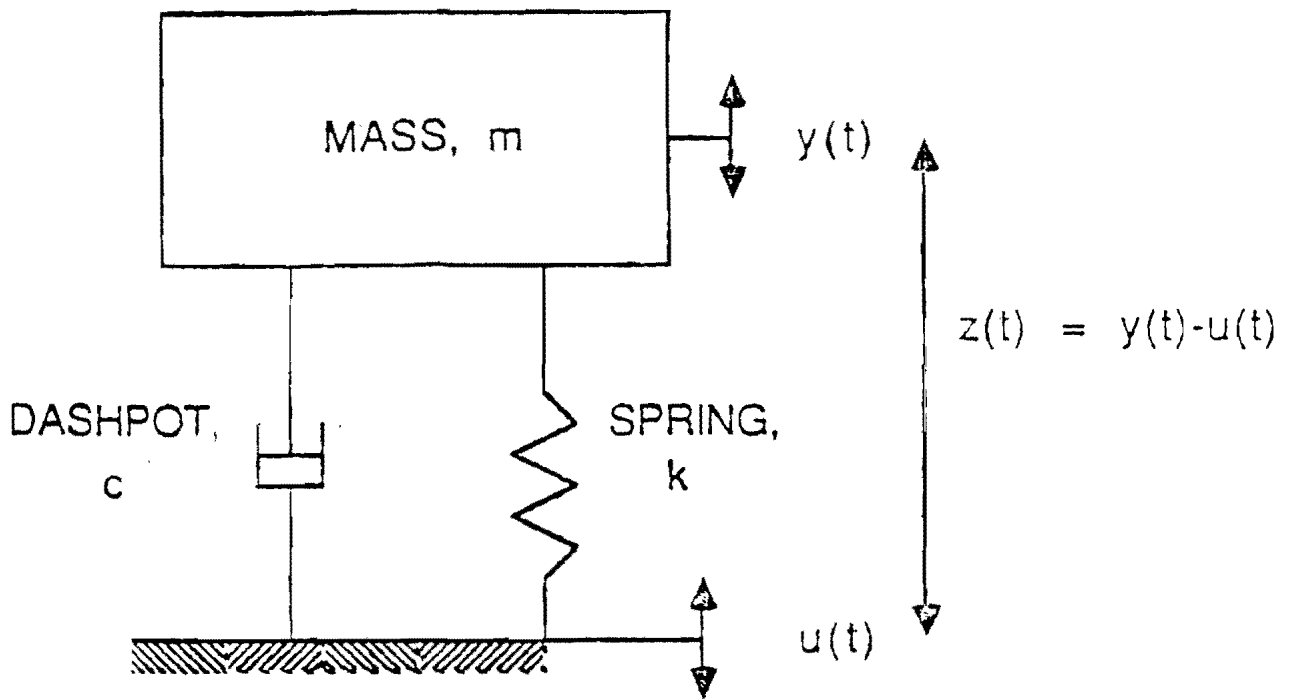


Figure 1.10 Idealized Model of a Geophone

base is shown as a vertical excitation, $u(t)$. The coil-magnet movement (or the voltage output) is equivalent to the relative movement of the mass, m , in the model. The coil-magnet movement is equal to $z(t) = y(t) - u(t)$, if the movement of the base, $u(t)$ and movement of the mass, $y(t)$ are measured relative to a fixed reference datum. The relationship between $z(t)$ and $u(t)$, which is equivalent to the relationship between the output voltage of the geophone and the ground movement, is described below.

The differential equation describing the response motion can be derived by specifying that the sum of all the forces in the system be equal to zero, when the system is excited by a base movement $u(t)$. The forces consist of spring force, $F_k(t)$, damping force, $F_c(t)$, inertial force, $F_m(t)$, and finally the excitation force. The equation of motion can be written as:

$$F_m(t) + F_c(t) + F_k(t) + F(t) = 0 \quad (1.5)$$

If $y(t)$, $\dot{y}(t)$ and $\ddot{y}(t)$ are defined as the inertial motion, velocity and acceleration of the mass, respectively, then:

$$F_k(t) = k[y(t) - u(t)] = k[z(t)] \quad (1.6)$$

$$F_c(t) = c[\dot{y}(t) - \dot{u}(t)] = c\dot{z}(t) \quad (1.7)$$

$$F_m(t) = m[\ddot{y}(t) - \ddot{u}(t)] = m\ddot{z}(t) \quad (1.8)$$

$$F(t) = m\ddot{u}(t) \quad (1.9)$$

Equation 1.5 may now be written as:

$$m\ddot{z}(t) + c\dot{z}(t) + kz(t) = 0 \quad (1.10)$$

Let $u(t)$ be a harmonic motion with a frequency of f , so that:

$$u(t) = u_0 \exp(i 2\pi ft) : [i = \sqrt{-1}] \quad (1.11)$$

Then, the solution to Equation 1.10 can be written as:

$$z(t) = z_0 \exp (i2\pi ft) \quad (1.12)$$

where,

$$z_0 = u_0 \frac{r^2}{[(1 - r^2) + (i2Df)]} \quad (1.13)$$

$$r = \frac{f}{f_n} \quad (1.14)$$

$$D = \frac{c}{c_c} \quad (1.15)$$

Equations 1.13 through 1.15 require clarification. Symbol f_n represents the natural frequency of the SDOF system and can be determined by:

$$f_n = \frac{\sqrt{\left(\frac{k}{m}\right)}}{2\pi} \quad (1.16)$$

The symbol C_c is termed the critical damping. The critical damping can be calculated from:

$$C_c = \sqrt{(2km)} \quad (1.17)$$

Finally, symbol D is called damping ratio.

The response of a geophone to any arbitrary load (such as an impulse) is discussed in detail in Nazarian (1987). The reader is referred to that report for in-depth understanding of the process.

The geophones used in this study are manufactured by Mark Products, Inc. The nominal natural frequency of geophone is 4.5 Hz and a resistor of 6.65 kOhms was used as a shunt to provide a nominal damping ratio of 70 percent.

Geophones are small in size and light in weight. Geophones are inexpensive as compared to other transducers. The output of a geophone can be connected to any recording

device without using any amplifier. Geophones are very rugged and can withstand high temperatures.

1.3 LOAD CELL

Load cells (or force transducers) are load measurement sensors which are available in wide ranges of size and response characteristics. Most force transducers employ a sensing element that converts an applied force into mechanical displacement. Typically, the mechanical displacement is a deformation of an elastic element, which is then converted into an output signal by different elements depending upon the type of load cell used.

The general construction of a load cell is shown in Figure 1.11. The system consists of a mass, M , connected to the load cell case by means of a spring, a dashpot and a relative displacement transducer. The most commonly used displacement transducer is piezoelectric. The model is almost similar to the accelerometer model explained in Section 1.2.1. The only difference is that the force F_i is applied to the mass instead of displacement X_i applied to the system. The relationship between input force F_i and output displacement X_o can be derived by applying Newton's law to the mass as follows:

$$F_i - K_s x_o - B \dot{x}_o - M \ddot{x}_o \quad (1.18)$$

The Equation 1.18 can be rewritten as:

$$\frac{X_o}{F_i}(S) = \frac{\frac{S^2}{\omega_n^2}}{\frac{S^2}{\omega_n^2} + \frac{2\zeta S}{\omega_n} + 1} \quad (1.19)$$

where,

$$\omega_n \triangleq \sqrt{\frac{K}{M}}, \quad K \triangleq \frac{1}{K_s}, \quad \zeta \triangleq \frac{B}{2\sqrt{K_s M}} \quad (1.20)$$

All symbols are defined in Section 1.2.1.

Piezoelectric load cells generate large output-voltage signals, are compact and have high natural frequencies. These properties make them a good tool for accurate dynamic force measurement. Piezoelectric load cells have very low damping ratios nevertheless, this is acceptable because of their high natural frequencies.

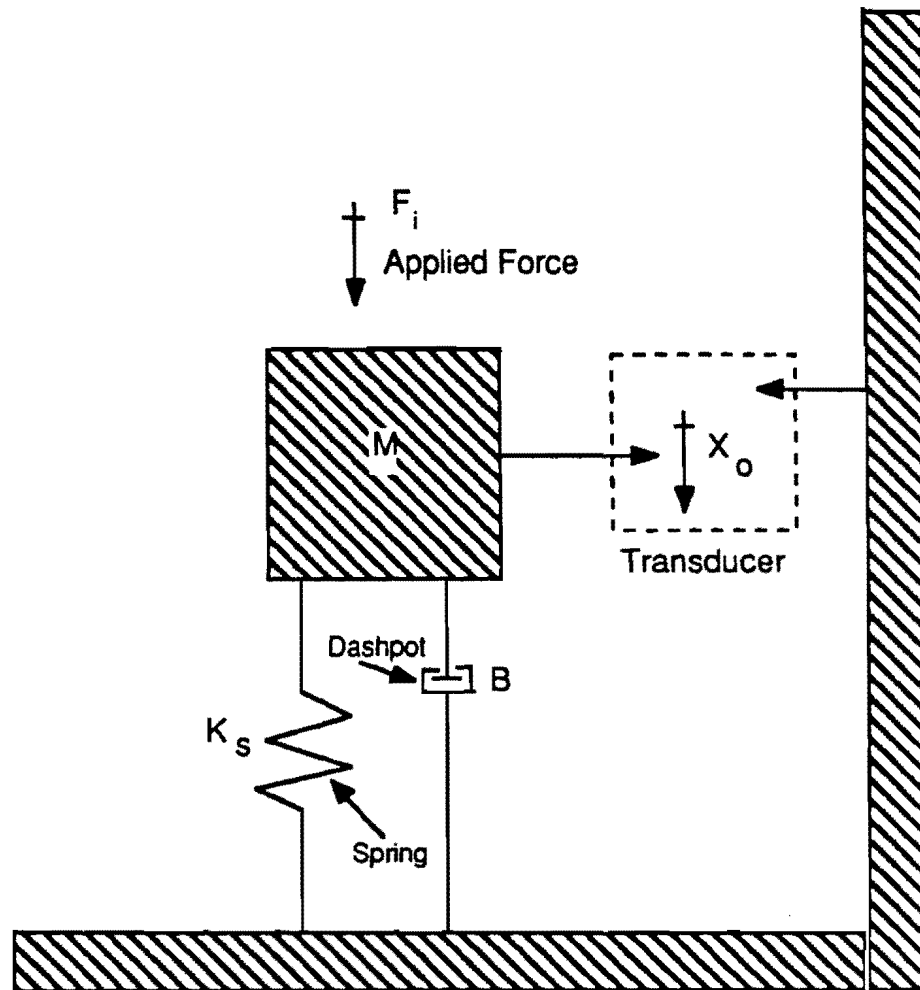


Figure 1.11 General Construction of Load Cell (from Doebelin, 1983)

Piezoelectric load cells do not respond to static forces. These transducers respond only to dynamic compression forces.

1.4 RECORDING DEVICE

The recording device used in this study is a Hewlett-Packard (HP) 3562A Dynamic Signal Analyzer. The HP 3562A is a dual-channel, FFT-based network, spectrum and waveform analyzer which provides analysis capabilities in both the time and frequency domains. The 0-to-100 kHz frequency range, 150 dB measurement range and 80 dB dynamic range of the HP 3562A make it a suitable recording device. This analyzer has a pair of differential input channels and a built-in signal source. The signal source can be used to generate sine waves.

1.5 WAVEFORM GENERATORS

Two waveform generators were used in this study. The signal generator of the HP 3562A analyzer was used in the steady-state tests. A Model 75 Arbitrary Waveform Generator, manufactured by Wavetek, was also used. The Model 75 contains advanced waveform editing features to create and edit complex waveforms from several standard waveforms. The standard waveforms, which are sine, cosine, inverse sine, haversine (inverse cosine), triangle, square, ramp up, and ramp down, can be combined using other editing features of the waveform generator to develop sophisticated wave forms.

1.6 VIBRATION SOURCE

The vibration source used here was a shake table. A shake table is a combination of power amplifier and an exciter. The power amplifier and exciter are described in the next section.

1.6.1 POWER AMPLIFIER

The amplifier is used to amplify the signal obtained from a waveform generator. The amplifier used is capable of delivering 125 watts of output power. This high output power can only be realized at three different stages within the amplifier. The first stage is preamplifier stage. The preamplifier stage can use both single ended and differential inputs and has a gain of approximately 10.4 dB. The output of the preamplifier stage is the input for driver stage. The driver stage amplifier has a gain of approximately 4.3 dB. Finally, the amplified signal from driver stage is sent to the output stage amplifier. The output stage, which provides the final output signal, has a gain of approximately 13.62 dB.

1.6.2 EXCITER

The exciter used in this study is a model PM50A shaker manufactured by MB Dynamics. The design of the exciter is based on the principle that mechanical motion or force can be produced by passing an electric current through a wire placed into a magnetic field.

The body of the exciter is made of ceramic (barium ferrite and iron oxide) magnet, which makes the exciter compact and reduces the chances of damaging the magnet due to overheating.

CHAPTER TWO

LABORATORY TESTS SETUP AND PROCEDURES

2.1 INTRODUCTION

An overview of calibration of all the sensors used in this study is included herein. The setup used for the determination of accuracy and precision of all the sensors is also briefly discussed in this chapter. Finally, the procedures followed to determine deflections from the raw data obtained with each device are presented.

2.2 CALIBRATION OF LVDT

The LVDT was calibrated in the laboratory to establish the voltage/displacement relationship. The characteristics of the instruments used for calibration of the LVDT are included in Appendix C.

The setup used for calibration of LVDT is shown in Figure 2.1. During calibration, a regulated input of ± 15 Volts dc was maintained. Every time that the micrometer was moved 0.10 mm, the output voltage was recorded using a multimeter. The experiment was carried out in the ranges of zero to ten Volts. Linear regression analysis was utilized to obtain the calibration factor (Appendix C).

The calibration factor obtained from the linear regression of laboratory data is 81.026 v/in. while the calibration obtained with the manufacturer's setup (Schaevitz Engineering) was 83.058 v/in.

2.3 CALIBRATION OF PROXIMETER

The calibration of the proximeter was carried out following a procedure similar to that of the LVDT except input power supply of -24 volts dc was used instead of ± 15 volts dc. The raw data as well as its associated best-fit curve are shown in Appendix C.

The proximeter had to be calibrated again due to two complications. First, it was suspected that the proximeter probe was damaged and, secondly, input power supply was changed from -24 volts dc to -20 volts dc. The new calibration of the proximeter is also shown in Appendix C.

The linear factors obtained from the calibration of the proximeter in the laboratory were 198.374 mv/in. and 196.596 mv/in. from the first (February 21, 1989) and second (August 1, 1989) calibration attempts, respectively. The nominal linear scale factor given by manufacturer (Bently Nevada) was 200 mvolts /in.

2.4 CALIBRATION OF GEOPHONE

To calibrate the geophones in the laboratory, a shake table was used. The reference

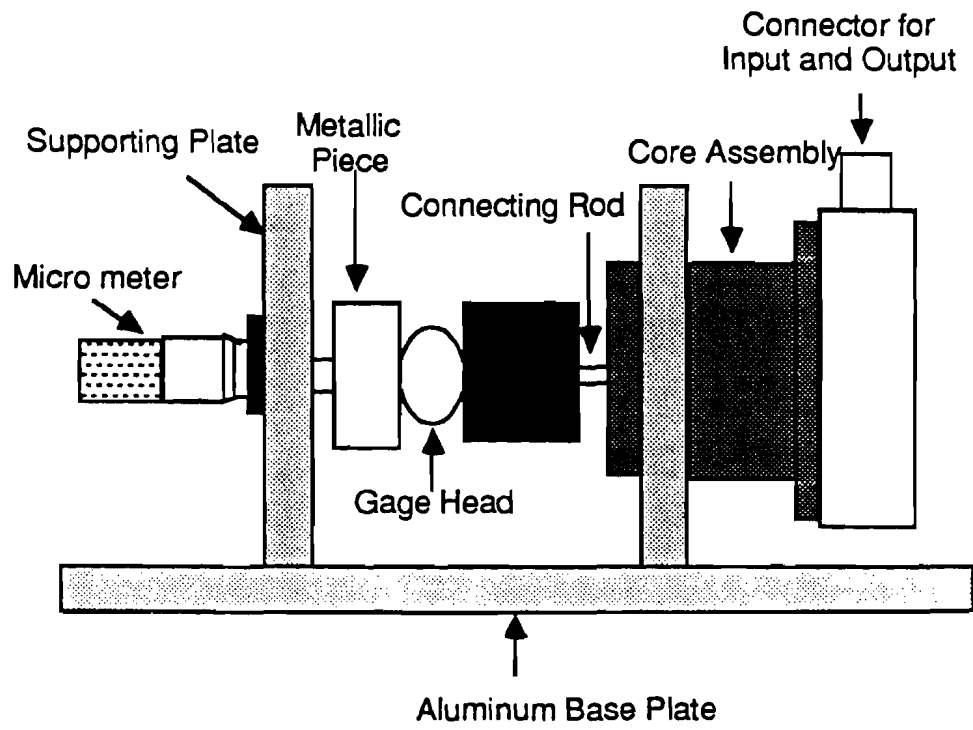


Figure 2.1 Setup for Calibration of LVDT

device for calibration was either an accelerometer or a proximeter.

The shake table was vibrated with a sweep-sine steady-state source. The output voltages of the reference accelerometer (or proximeter) and the geophone were monitored simultaneously. The procedure involved in developing the calibration curve for the geophone is slightly different depending on the reference device used. For better understanding of the process, a detailed theoretical discussion on this matter can be found in Nazarian (1987).

When the accelerometer was used as the reference device, the voltage output of the accelerometer was divided by its calibration factor and was integrated in the frequency domain (using HP 3562A analyzer) to obtain its response in terms of velocity. The ratio of the geophone output voltage to the reduced accelerometer record at each frequency yield the calibration curve for the geophone.

When a proximeter was used as the reference device, the voltage output was divided by the calibration factor of the proximeter and was differentiated in the frequency domain (using HP 3562A analyzer) to obtain its response in terms velocity. The ratio of the geophone output voltage and the reduced proximeter record at each frequency was the calibration curve of the geophone.

Four geophones were used in this study. Geophones named 1 and 2 were calibrated with a proximeter and the calibration of geophones named 5 and 6 were carried out using an accelerometer. The calibration curves obtained for each device are included in Appendix C.

2.5 CALIBRATION OF ACCELEROMETER AND LASER

The accelerometer was purchased from PCB Piezotronics, and the manufacturer provided calibration curves traceable to the National Bureau of Standards (NBS). Calibration specifications are shown in Appendix C.

The laser used in the experiment was not calibrated in the laboratory, and the calibration information given by the manufacturer was used to determine the deflections.

2.6 CALIBRATION OF LOAD CELL

The load cell was purchased from PCB Piezotronics, and the manufacturer provided calibration curves traceable to the National Bureau of Standards (NBS). Nevertheless, the load cells were calibrated in the laboratory for two reasons. First, the accuracy of the load cell's calibration was ensured; secondly, the effects of mounting the load cell in an aluminum casing was studied. The list of equipment used for calibration of the load cell are shown in Appendix C.

In order to determine accuracy of calibration, the load cell was placed between the upper and lower platens of an MTS dynamic testing machine. A seating load of 100 lbs was

applied to the load cell to ensure proper contact between the load cell and the platen. Impulse loads of different magnitude were applied and output voltages from the load cell of the MTS machine and the load cell under calibration were collected. The first impulse load applied was 500 lbs. Thereafter, larger loads were applied in increments of 500 lbs. The calibration curves obtained by this method are shown in Appendix C.

The loads measured with the load cell are plotted against the loads measured by the load cell mounted in the MTS device in Figure 2.2. The slope of line is 1.02.

In the final calibration system, the load cells were placed inside a 1-in. thick aluminum plate. The effect of encasing the load cells in the aluminum plate was also studied. A case as shown in Figure 2.3 was manufactured and the load cell was placed in it. The mounting mechanism of the load cell in the final calibration system is identical to that shown in Figure 2.3. Shown in Figure 2.4 is a comparison of the response of the load cell when it was and was not mounted in the aluminum casing. It can be seen that the slope of the line is .99. As such the effect of mounting the load cell in the aluminum casing is negligible.

2.7 LABORATORY CALIBRATION SETUP

A block diagram of the setup used for determining the accuracy and precision of deflections of all sensors is shown in Figure 2.5. A thick concrete block, as shown in Figure 2.5, was selected and levelled perfectly. Such a structure results in minimal differential movement amongst different components in the system. The PM 50A exciter was kept in between the two walls of the block.

A circular aluminum plate, eight in. in diameter, was screwed securely to the exciter. The geophones were rigidly fastened to the plate using a specially designed casing. An accelerometer was fastened to the top of the casing of each geophone. To place the LVDT and proximeter, a square aluminum plate was fastened to two beams connected rigidly to two steel plates (as shown in Figure 2.6). The two steel plates were securely connected to the concrete. Two holes were bored in this aluminum plate for mounting the LVDT and proximeter. The LVDT was fixed to the top plate, so that the gage head of LVDT was touching the bottom plate attached to the shaker. Since the proximeter had been calibrated using 4140 steel as a target material, a small circular piece of 4140 was screwed in the lower plate providing proper target material for the probe. The proximeter was also attached to the top plate in a similar manner as used for the LVDT, using an adjustable connector.

The second half portion of the bottom plate was reserved for the laser optocator. The laser required sufficient unobstructed area for sending and receiving laser beams. The laser was fixed to the top steel plate with the help of another vertical plate, as shown in Figure 2.7.

The accuracy and precision of sensors were determined for four different waveforms i.e. sine, half sine, square and triangular. Sine waves were generated using the HP 3562A

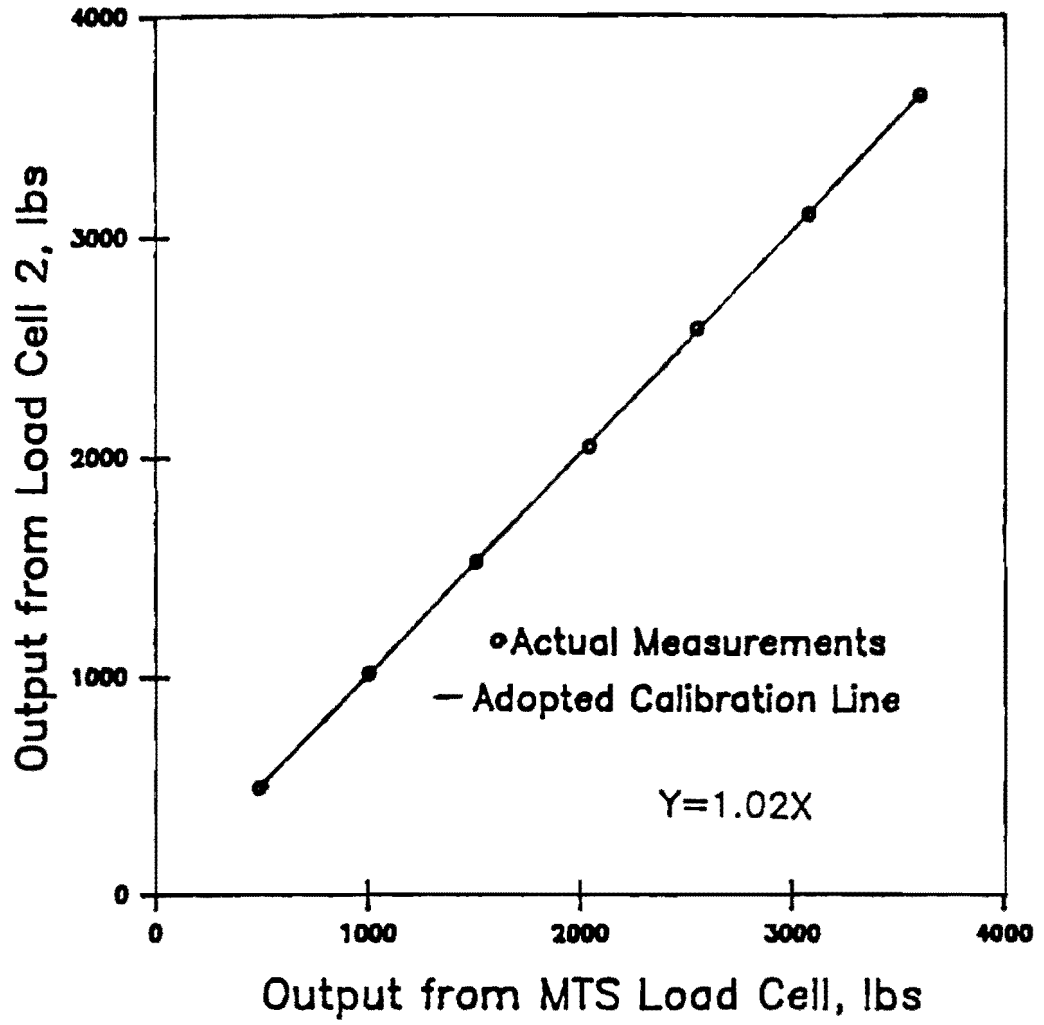
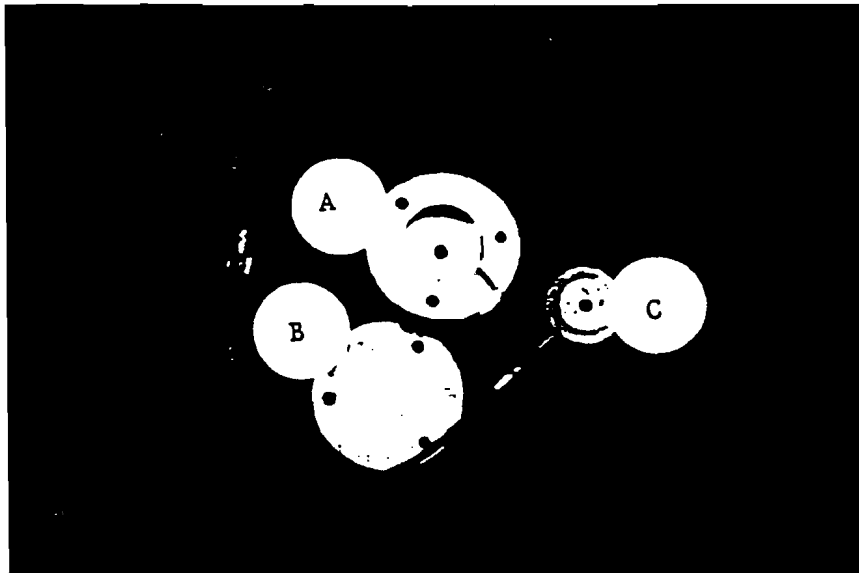


Figure 2.2 Comparison of Loads Measured with Load Cell 2 and MTS Load Cell (Without an Aluminum Casing)



- A - Aluminum Casing
- B - Aluminum Cover for Load Cell
- C - Load Cell

Figure 2.3 A View of Aluminum Casing Used for Load cell Calibration

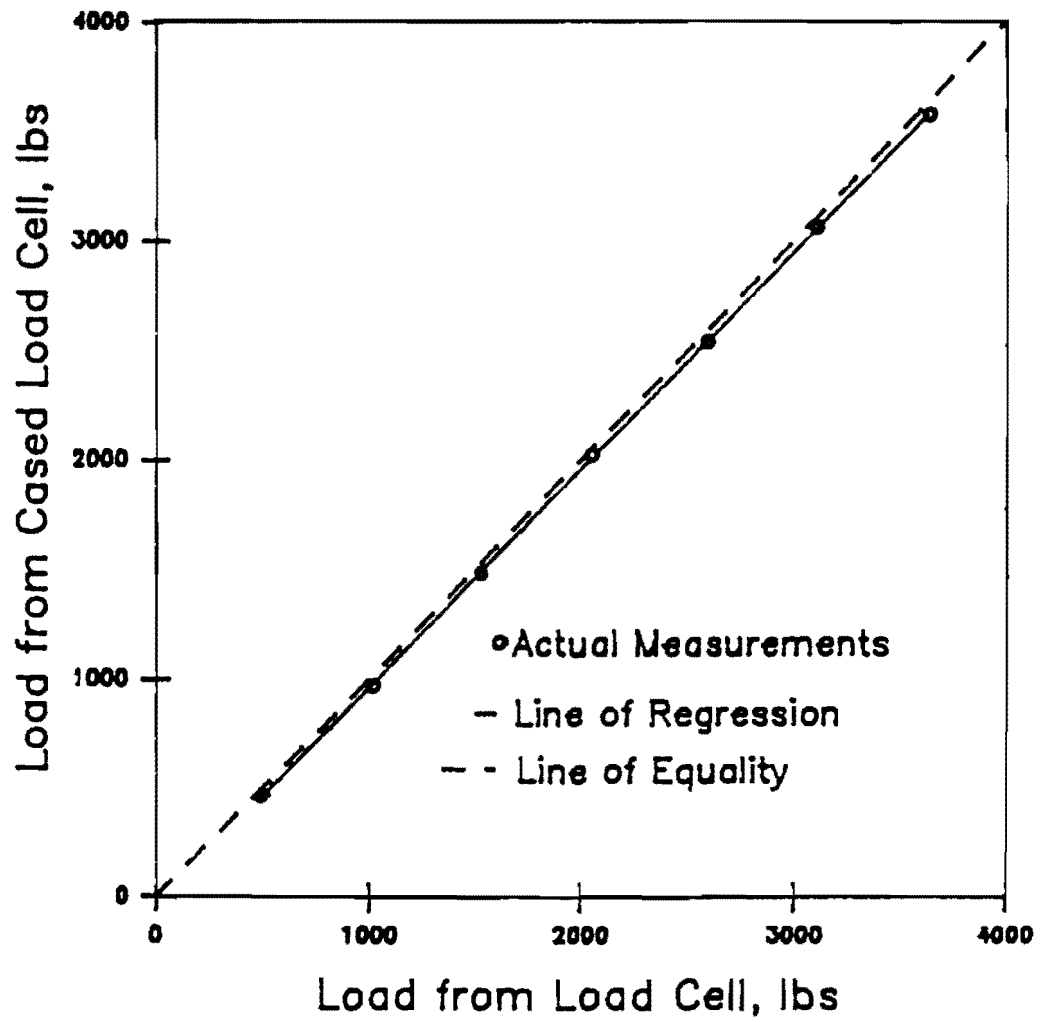


Figure 2.4 Evaluation of Effects of Mounting Load Cells within an Aluminum Plate.

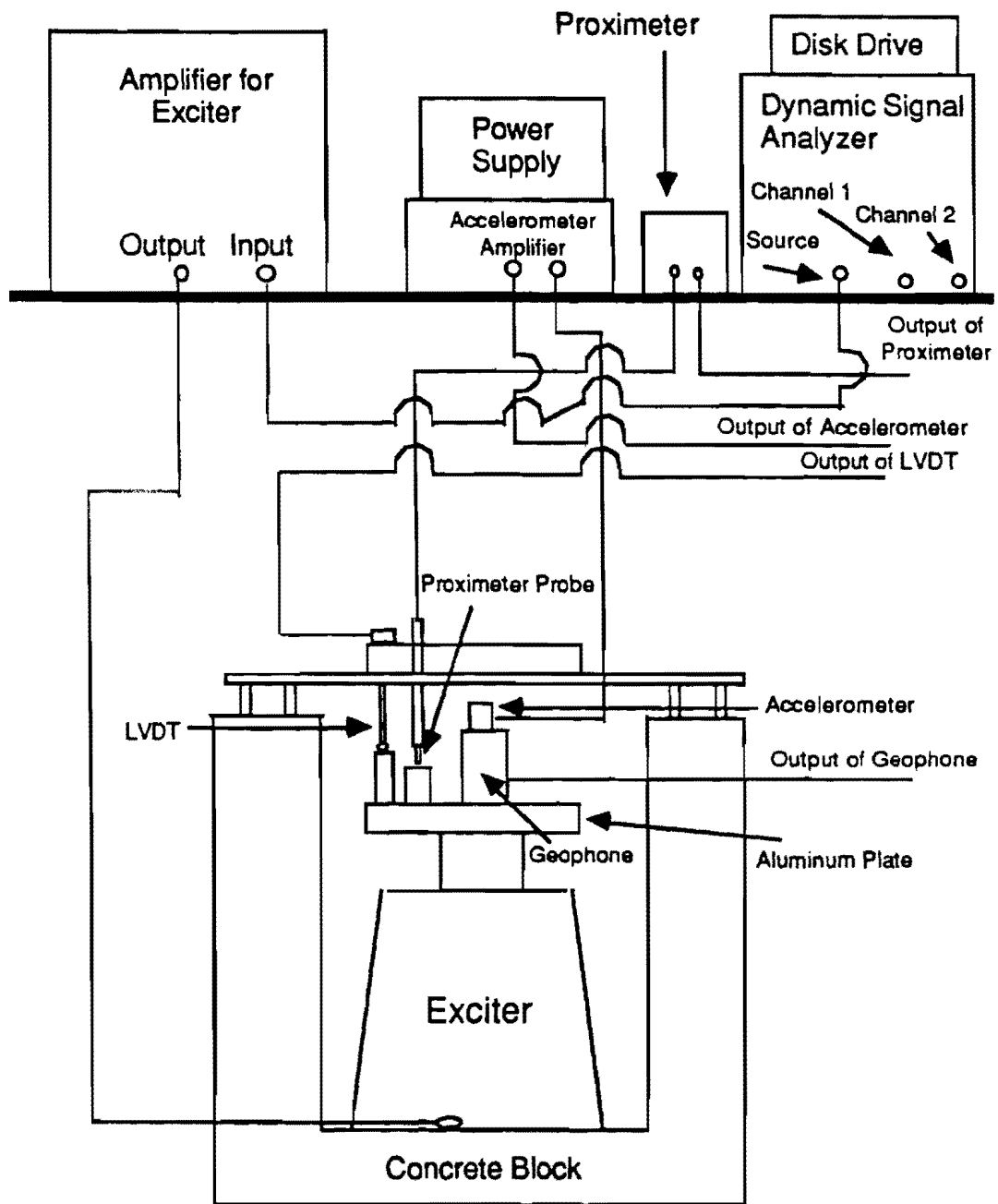
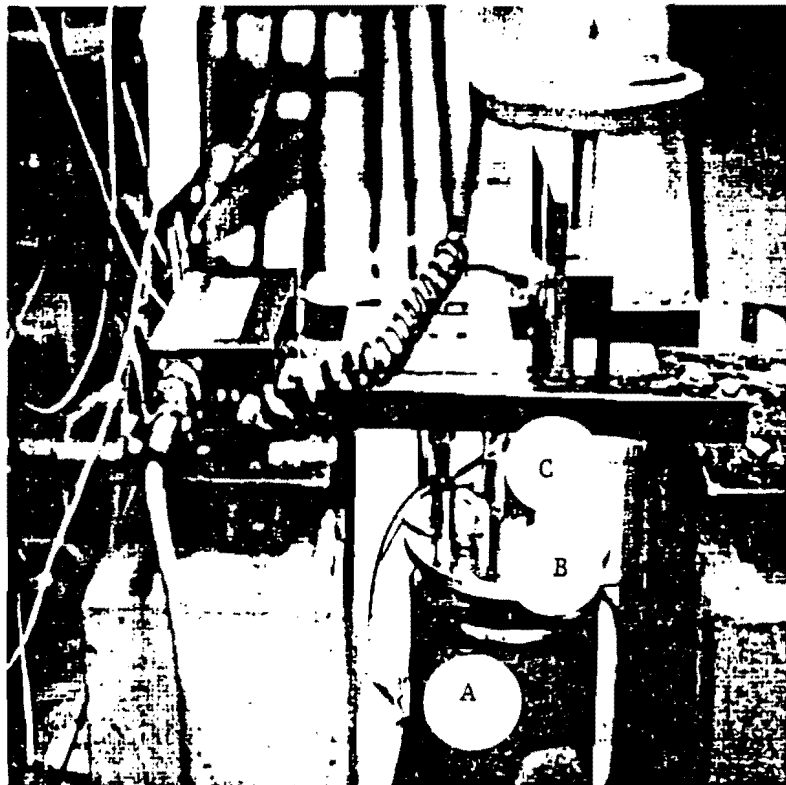
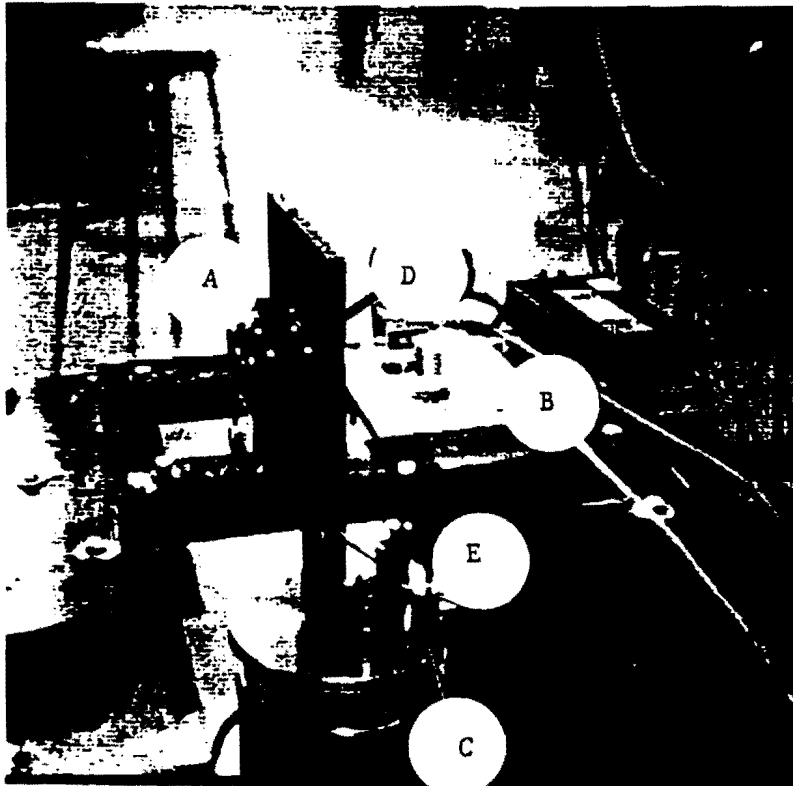


Figure 2.5 Sketch of the Experimental Setup Used in This Study



- A - Exciter
- B - Geophone
- C - Accelerometer

Figure 2.6 Setup Used for Comparison of Different Sensors



- A - Laser Optocator
- B - Top Aluminum Plate
- C - Bottom Aluminum Plate
- D - LVDT
- E - Proximeter

Figure 2.7 Setup Used for Mounting Laser Optocator

analyzer and the other waveforms were generated using model 75 Wavetek arbitrary waveform generator. The procedure used to obtain deflection values is different for each device as well as for each waveform.

The procedures used to determine deflections for each sensor are discussed in the Appendix D for the benefit of the reader.

CHAPTER THREE

EVALUATION OF DEFLECTION MEASURING SENSORS

3.1 INTRODUCTION

Five different sensors were evaluated to find the most accurate and precise sensor which can be sensibly used for absolute calibration of the Falling Weight Deflectometer and the Dynaflect devices. The test setup for the experiment as well as the data reduction scheme were discussed in Chapter Two. In this chapter, results of this evaluation are presented.

3.2 DESCRIPTION OF DATA COLLECTED

In order to fully evaluate five candidate sensors, several parameters were considered. The parameters studied were the amplitude of vibration, the type of excitation, and the frequency content of vibration. Tests were carried out in the laboratory environment so that these variables can be easily controlled.

The amplitude of vibration was varied between 1 to 25 mils. Such a broad range of amplitude was studied to ensure proper response of the sensors to small as well as large amplitudes. Small amplitudes of vibration would allow us to examine the effects of background noise (signal-to-noise ratio) on each sensor. Tests at large vibration amplitudes were carried out to determine the range of usefulness of each sensor. Amplitudes larger than 25 mils were not utilized because they were not considered of any practical interest in this process.

Different types of excitation were investigated to determine the versatility of each sensor for use with different types of nondestructive testing devices. The steady-state vibration and impulse (transient) motions were examined. Three type of impulses, i.e. half-sine, triangular and square, were used. The steady-state vibration is utilized by several NDT devices such as the Dynaflect and road rator. It is well known that the FWD devices impart impulsive loads to pavements.

The effect of frequency content on the behavior of each sensor was studied also. For the steady-state tests, the frequency of vibration was varied between 5 Hz to 100 Hz. The lower limit signifies the lower limit of operation of the shaker's amplifier. The amplifier cannot adequately amplify steady-state signals below 5 Hz. The upper bound (100 Hz) is practically the highest frequency of interest in the deflection based tests.

For the impulse tests, the duration of impulse was varied from 12.5 msec to 175 msec, to cover the frequency ranges of interest in nondestructive testing methods.

3.2.1 Steady State Experiments

Two series of tests were carried out using the steady state vibration setup. In the first series, the laser device was not utilized because of the high costs associated with the

rental of the device (\$300 per week). In the second series of tests, the laser device was added to the testing sequence. Due to time limitations, the extent of deflection data collected with the laser device, is relatively limited.

All combinations of frequency and amplitude evaluated in the steady-state tests in the absence of the laser device are presented in Table 3.1. Typically, at each frequency, measurements in the range of amplitudes of 1 to 25 mils were carried out. As indicated before, frequencies below 5 Hz and above 100 Hz were not considered. The amplitude of vibration was limited to about 20 to 25 mils. At a frequency of 100 Hz, displacements larger than 5 mils could not be generated due to the shaker's characteristics.

An example of data collected at each frequency and each amplitude is shown in Table 3.2. Two geophones (denoted as Geo 1 and Geo 2), two accelerometers (denoted as Acc 1 and Acc 2), an LVDT and a Proximeter (denoted as Prox) were used in all tests.

The recording device used in this experiment was a two-channel spectral analyzer. Therefore, only two devices at one time could be compared. To remove any bias in data due to sequence of testing, a randomized order was developed for comparison of deflections. This sequence is depicted in columns 2 and 3 of Table 3.2. Each sensor was compared twice with the other five sensors. The actual deflections from each pair of sensors are reflected in columns 4 and 5 of Table 3.2. The difference between the deflections of the two sensors was calculated and reported in column 6.

The proximeter device was selected as the reference sensor to facilitate the evaluation process. The proximeter sensors can accurately measure small deflections in the laboratory environment because of their noncontact nature. An example of comparison of deflections obtained from the proximeter and other sensors are shown in Table 3.3 for the data presented in Table 3.2.

In the next step, the average, standard deviation and variance of deflections were calculated for each sensor. As reflected in Table 3.2, each device was utilized 10 times for comparison purposes. As an example, the statistical information obtained from data shown in Table 3.2 is shown in Table 3.4. It can be seen that the average varies between 4.78 mils and 4.95 mils, about 0.2 mils difference, and that overall the variance is less than 0.13 percent.

The second series of tests were carried out adding a laser device to the sensors mentioned before. The laser device was rented for two weeks from a vendor. Therefore, the number of tests had to be modified and reduced. Shown in Table 3.5 is the compilation of all steady-state tests carried out in the presence of the laser device.

An example of data collected at one frequency and one amplitude in the presence of the laser device is shown in Table 3.6. In these tests, each device was simply compared with the laser once. As such, six deflections were obtained from laser device for each set-up. The statistical information with regards to these six measurements was calculated for evaluation purposes. This information is reflected in Table 3.6 also. As before, the two

Table 3.1 Summary of Steady-State Tests Carried out in the Absence of Laser Device

Frequency (Hz)	Approximate Deflection (mils)				
5	1	5	10	18	25
10	1	5	10	18	25
15	5	8	10	15	--
20	5	10	14	22	--
30	4	15	22	--	--
40	1	5	10	22	--
50	1	5	10	18	25
75	1	5	10	18	--
100	1	5	--	--	--

Table 3.2 Testing Sequence Used in Steady-State Deflection Measurements at Each Frequency and Amplitude (in the Absence of Laser Device)

Date of Experiment: 10.02.89
Frequency Used : 05 Hz

Diskette No.: 67
Source Level: 0.020 Volts

File No.	Device Used		Deflection (mil)		Difference (percent) [†]
	Channel 1	Channel 2	Channel 1	Channel 2	
1	Acc 1	Geo 1	1.48	1.51	-1.75
3	Prox	Acc 2	1.53	1.53	-0.13
5	LVDT	Acc 2	1.49	1.51	-1.34
7	Geo 2	Geo 1	1.50	1.50	-0.07
9	Prox	Geo 2	1.53	1.49	2.71
11	LVDT	Acc 1	1.50	1.47	2.33
13	Prox	LVDT	1.53	1.49	2.61
15	LVDT	Acc 1	1.51	1.48	1.99
17	Acc 1	Geo 2	1.50	1.49	0.40
19	Prox	Geo 1	1.53	1.51	1.50
21	Acc 1	Geo 1	1.49	1.51	-1.34
23	LVDT	Prox	1.50	1.53	-2.00
25	Geo 2	Acc 1	1.52	1.51	0.66
27	Prox	Acc 1	1.54	1.49	3.12
29	Acc 1	Acc 2	1.48	1.52	-2.70
31	Acc 2	Prox	1.54	1.53	0.46
33	Prox	Geo 2	1.54	1.50	2.34
35	Acc 2	Geo 2	1.52	1.51	0.66
37	Acc 1	Prox	1.50	1.54	-2.40
39	LVDT	Geo 1	1.51	1.52	-0.93
41	Acc 2	Geo 1	1.56	1.53	1.99
43	LVDT	Acc 2	1.51	1.54	-1.99
45	Geo 2	Geo 1	1.53	1.52	0.33
47	Acc 2	Geo 2	1.54	1.51	2.21
49	Acc 1	Acc 2	1.50	1.53	-1.73
51	Acc 2	Geo 1	1.54	1.52	1.30
53	Prox	Geo 1	1.55	1.52	1.94
55	LVDT	Geo 2	1.52	1.51	0.59
57	LVDT	Geo 1	1.51	1.52	-0.93
59	Geo 2	LVDT	1.53	1.51	1.31

[†]Difference={Channel 1-Channel 2}*100/Channel 1

Accelerometer Serial No.: 23641 & 42 ; Prox. Serial No.: 18745
Geophone No.: 1 & 2 ; LVDT Serial No.: 4745

Table 3.3 Comparison of Deflections for Proximeter and Other Sensors (for Data Reflected in Table 3.2)

Date of Experiment: 10.02.89
Frequency Used : 05 Hz

Diskette No.: 67
Source Level: 0.020 Volts

File No.	Device Used		Deflection (mil)		Difference (percent) [†]
	Channel 1	Channel 2	Channel 1	Channel 2	
3	Prox	Acc 2	1.53	1.53	-0.13
9	Prox	Geo 2	1.53	1.49	2.71
13	Prox	LVDT	1.53	1.49	2.61
19	Prox	Geo 1	1.53	1.51	1.50
23	LVDT	Prox	1.50	1.53	1.96
27	Prox	Acc 1	1.54	1.49	3.12
31	Acc 2	Prox	1.54	1.53	-0.46
33	Prox	Geo 2	1.54	1.50	2.34
37	Acc 1	Prox	1.50	1.54	2.34
53	Prox	Geo 1	1.55	1.52	1.94

Table 3.4 Evaluation of Variation in Deflections Measured by Each Sensor (for Data Reflected in Table 3.2)

Test No.	Device Used	Average Deflection (mil)	Standard Deviation (mil)	Variance (percent)
1	Accelerometer 1	1.49	0.01	0.02
2	Accelerometer 2	1.53	0.01	0.02
3	Geophone 1	1.52	0.01	0.01
4	Geophone 2	1.51	0.01	0.02
5	Proximeter	1.53	0.01	0.00
6	L.V.D.T.	1.51	0.01	0.01

[†]Difference = $\{(\text{Prox. defl.}) - (\text{Other Device defl.})\} * 100 / (\text{Prox. defl.})$

Accelerometer Serial No's: 23641 & 42 ; Prox. Serial No.: 18745
Geophone No's: 1 & 2 ; LVDT Serial No.: 4745

Table 3.5 Summary of Steady-State Tests Carried out in the presence of Laser Device.

Frequency (Hz)	Approximate Deflection (mils)	
5	5	18
10	5	18
15	5	18
20	5	18
30	5	18
40	5	18
50	5	18
75	5	18

Table 3.6 Testing Sequence Used in Steady-State Deflection Measurements at Each Frequency and Amplitude (in the Presence of Laser Device)

Date of Experiment: 9.13.89 Diskette No.: LAS29
 Frequency Used : 10 Hz Source Level: 0.045 Volts

Test No.	Device Used		Deflection (mil)		Difference (percent) ⁺
	Channel 1*	Channel 2	Channel 1	Channel 2	
1	Laser	Geo 1	5.19	5.13	1.16
2	Laser	Prox.	5.20	5.12	1.54
3	Laser	Acc 2	5.19	5.23	-0.77
4	Laser	LVDT	5.19	5.12	1.35
5	Laser	Geo 2	5.19	5.13	1.16
6	Laser	Acc 1	5.20	5.08	2.23

* Average = 5.19 mil
 Standard Deviation = 0.00 mil
 Variance = 0.00 percent

⁺Difference=(Channel 1-Channel 2)*100/Channel 1

Accelerometer Serial No's: 23641 & 42 ; Prox. Serial No.: 18745
 Geophone No's: 1&2; LVDT Serial No.: 4745; Laser Serial No. 2201

devices that were compared are shown in Columns 2 and 3; measured deflections with the corresponding sensors are shown in Columns 4 and 5; and finally, the differences in deflections are reflected in Column 6.

3.2.2 Impulse Experiments.

Each sensor was subjected to three different types of impulse for evaluation purposes. These impulse types were half-sine, square, and triangular.

The pulse width was varied between 12.5 msec to 175 msec to cover a wide range of frequencies. Typically, the pulse width for loads applied with the FWD varies between 25 msec and 75 msec. Therefore, this experiment should cover all ranges of interest in pavement evaluation. Normally, as the pulse width increases the dominant frequency content of the pulse decreases. As an example a pulse width of 25 msec correspond to frequencies in the range of zero to about 25 Hz. However a pulse of 175 msec corresponds to frequency range of zero to 2 Hz.

Nominal deflections used were 5, 15 and 25 mils. As for steady-state tests, lower limit (5 mils) is used to evaluate the effects of undesirable external electrical and environmental noise and the upper limit is used to evaluate the working range of each sensor.

Tests with the impulse motion were carried out in two phases: without the laser device and with the laser device. A matrix of all tests carried out with the half-sine impulse in the absence of the laser device is shown in Table 3.7. The half-sine impulse tests are quite comprehensive because this is the shape of the pulse typically used in the NDT devices.

In the absence of laser device, the sequence of tests carried out at any given impulse width and amplitude was identical to that of the steady-state tests (Table 3.2). An example of data collected at a pulse width of 25 msec and a nominal deflection of 5 mils is shown in Table 3.8. The difference between deflections measured with all devices is less than 2 percent, except for accelerometers 1 and 2. The reason for the lack of performance of accelerometers in this range has been described in Chapter One.

Once again, the proximeter was used as the reference source to demonstrate the differences in the measured deflections. As an example, Table 3.9 demonstrates the difference in deflections between each sensor and the proximeter for data shown in Table 3.8. In the last step, the statistical information with regards to measurements made by each device was determined. As an example, the mean, standard deviation and variance for each device used in Table 3.8 are summarized in Table 3.10.

Different tests carried out with the square and triangular impulses in the absence of the laser device are shown in Table 3.7. The process of data collection and reduction is identical to those of half-sine and is not repeated herein.

In the presence of the laser device, the amount of data collected was minimized because of monetary constraints. Tests carried out with each type of impulse are summarized in

**Table 3.7 Summary of Impulse Tests Carried out in the
Absence of Laser Device.**

Pulse Width (mSec)	Deflection (mils)			Type of Impulse*
	5	15	25	
12.5	5	15	25	1
25	5	15	25	1,2,3
50	5	15	25	1,2,3
75	5	15	25	1,2,3
100	5	15	25	1,2,3
112.5	5	15	25	1
125	5	15	25	1,2
150	5	15	25	1
175	5	15	25	1,2

* Types of Impulse: 1 = Half-Sine
2 = Square
3 = Triangular

Table 3.11. As for the steady-state tests, each device was compared with the laser device only once. An example of this process is given in Table 3.12 for a half-sine impulse with a pulse width of 25 msec and for a nominal deflection of 5 mils. The statistical information associated with the repetition of these tests is given in the table as well.

3.3 Precision and Accuracy of Deflection Sensors

As mentioned before, five candidate sensors were evaluated so that the optimum sensor to be used for the calibration device can be determined. In this section, the effects of factors such as amplitude of deflection, frequency content, type of impulse on the precision and accuracy of the five sensors are presented.

The data collection methodology and the data reduction process for each sensor were described in Chapter Two. For completeness, a series of steady-state deflection data collected and reduced for a frequency of 10 Hz and a nominal deflection of 25 mils are included in Appendix D. The frequency of 10 Hz was selected because it reasonably resembles the frequency of vibration of a Dynaflect. Similarly, a series of deflection data collected with the impulsive motion of 25 msec pulse width and nominal deflection of 25 mils in the raw and reduced forms are included in Appendix D. The reader is encouraged to inspect Appendix D to get a feel for the amount of distortion in the outcome of each sensor. The distortion is mainly due to signal processing as well as background mechanical and electrical noise.

3.3.1 Steady-State Deflections

As mentioned in the previous section, for each frequency and each amplitude, deflections were measured ten times. The precision of each sensor in terms of variance of the ten repetitions (six repetitions for the laser device) at any given frequency and nominal deflection was determined. The variances determined in this manner are illustrated as a function of frequency in Figures 3.1 to 3.6 for two accelerometers (ACC1 and ACC2), two geophones (GEO1 and GEO2), an LVDT and the laser device, respectively. The raw data used to evaluate the accuracy and precision of each sensor are included in Appendix E. A comprehensive analysis of the precision and accuracy are included in Appendices F and G.

The two accelerometers more or less exhibit similar variability in deflections (Figures 3.1a and 3.2a). For all deflection levels, the variance is less than 1 percent translating to a maximum standard deviation of 0.2 mils (for 20 mils of deflection). This 0.2 mils is well within the level of background noise. It can be seen that at several frequencies, the variance increases with an increase in the amplitude of vibration. The reason for this matter is not known at this time. However, the opposite trend is generally expected because as the amplitude of vibration increases the signal-to-noise ratio increases; resulting in less variability in data.

The two geophones exhibit similar behaviors also (Figures 3.3a and 3.4a). In all but a few cases, the variance is less than 0.5 percent, and never exceeds 1 percent. As a result,

Table 3.11 Summary of Impulse Tests Carried out in the Presence of Laser Device.

Pulse Width (mSec)	Deflection (mils)			Type of Impulse
	5	15	25	
12.5	5	15	25	1
25	5	15	25	1,2,3
50	5	15	25	1,2,3
75	5	15	25	1
100	5	15	25	1,2,3

* Types of Impulse: 1 = Half-Sine
 2 = Square
 3 = Triangular

Table 3.12 Comparison of Deflections from Laser and Other Sensors

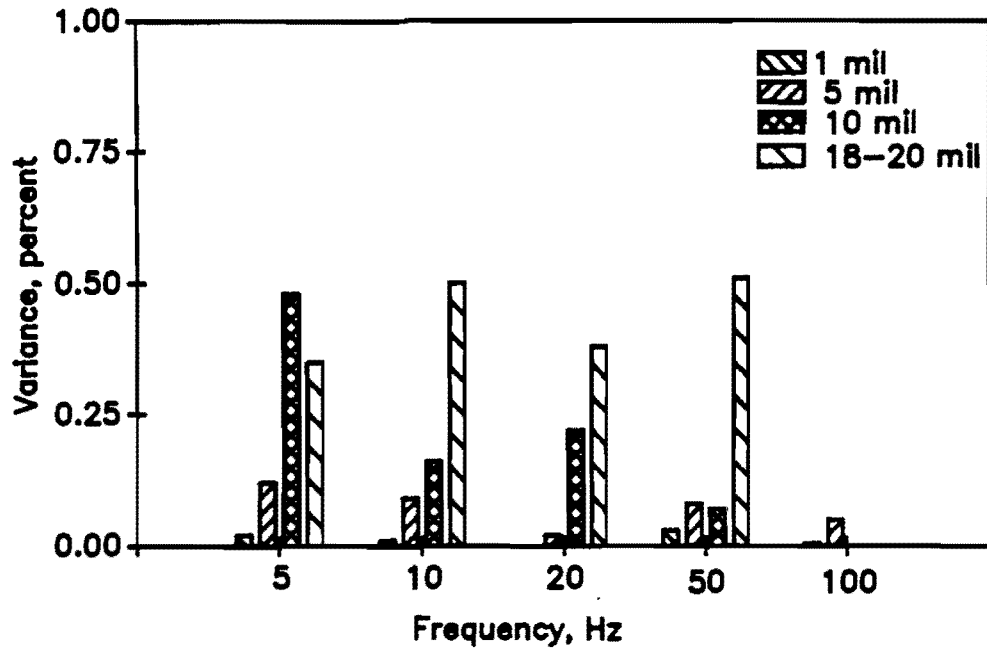
Date of Experiment: 9.9.89 Diskette No.: LAS09
 Type of Signal : Half Sine Source Level: 0.03025 Volts
 Pulse Width:025 ms.

Test No.	Device Used		Deflection (mil)		Difference (percent) ⁺
	Channel 1*	Channel 2	Channel 1	Channel 2	
1	Laser	Geo 1	5.25	5.15	1.88
2	Laser	Prox.	5.27	5.09	3.42
3	Laser	Acc 2	5.34	5.88	-10.07
4	Laser	LVDT	5.24	5.18	1.09
5	Laser	Geo 2	5.28	5.33	-0.99
6	Laser	Acc 1	5.33	5.28	0.96

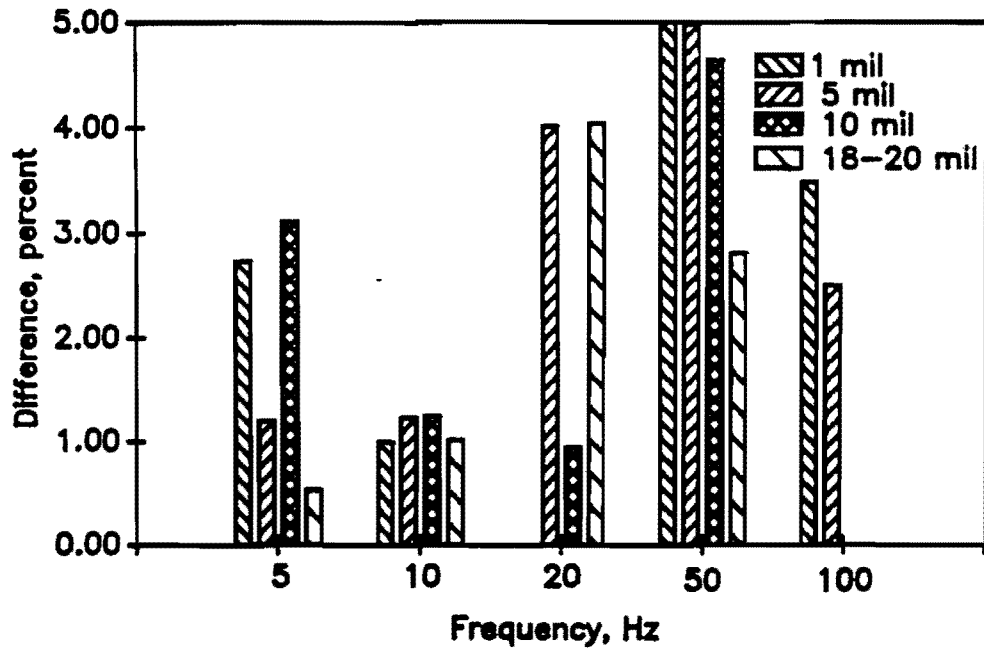
* Average = 5.28 mil
 Standard Deviation = 0.04 mil
 Variance = 0.17 percent

⁺Difference={Channel 1-Channel 2}*100/Channel 1

Accelerometer Serial No's: 23641 & 42 ; Prox. Serial No.: 18745
 Geophone No's: 1&2; LVDT Serial No.: 4745; Laser Serial No. 2201

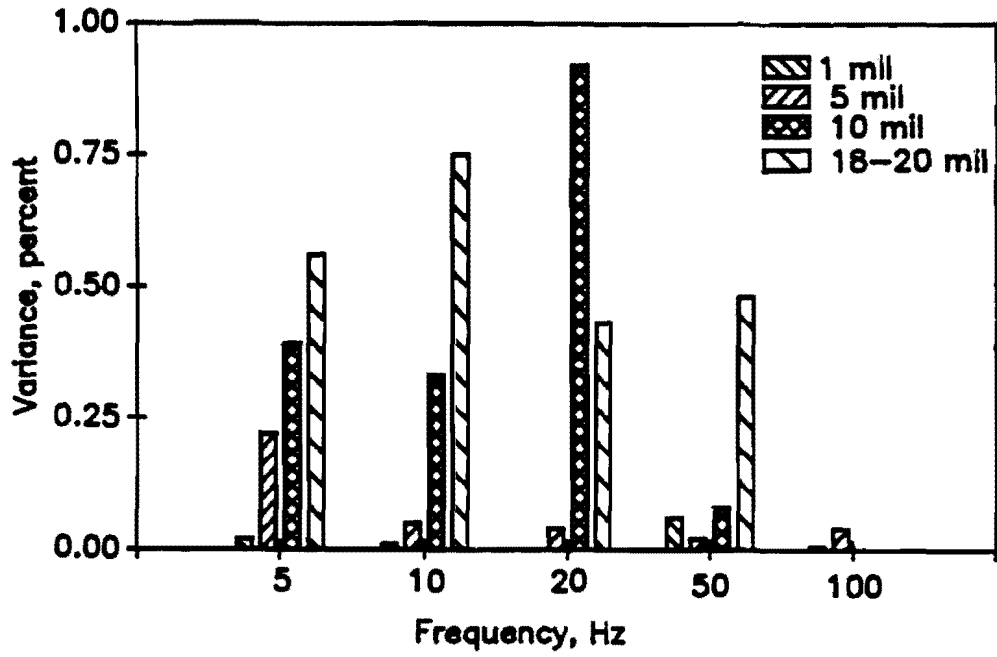


a) Variance

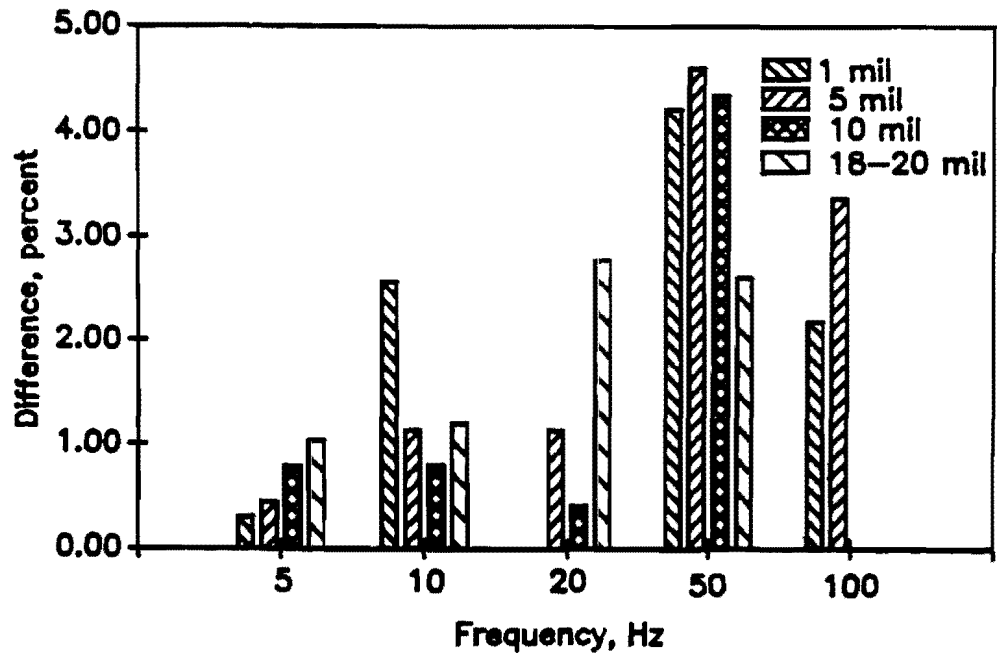


b) Difference from Proximeter Deflections

Figure 3.1 Evaluation of Accuracy and Precision of Accelerometer 1 Under Steady-State Loading

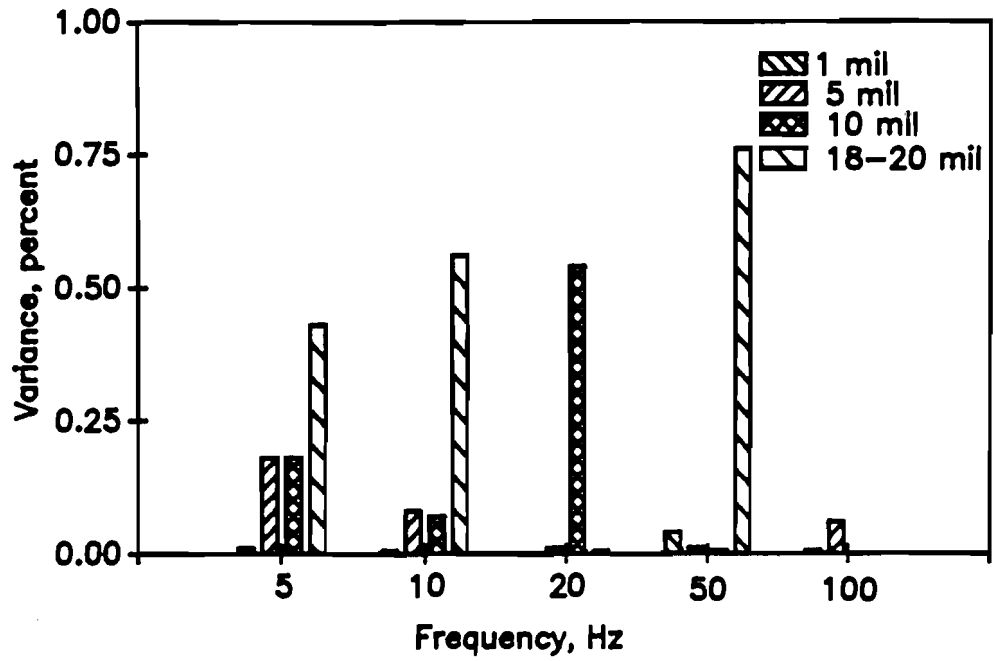


a) Variance

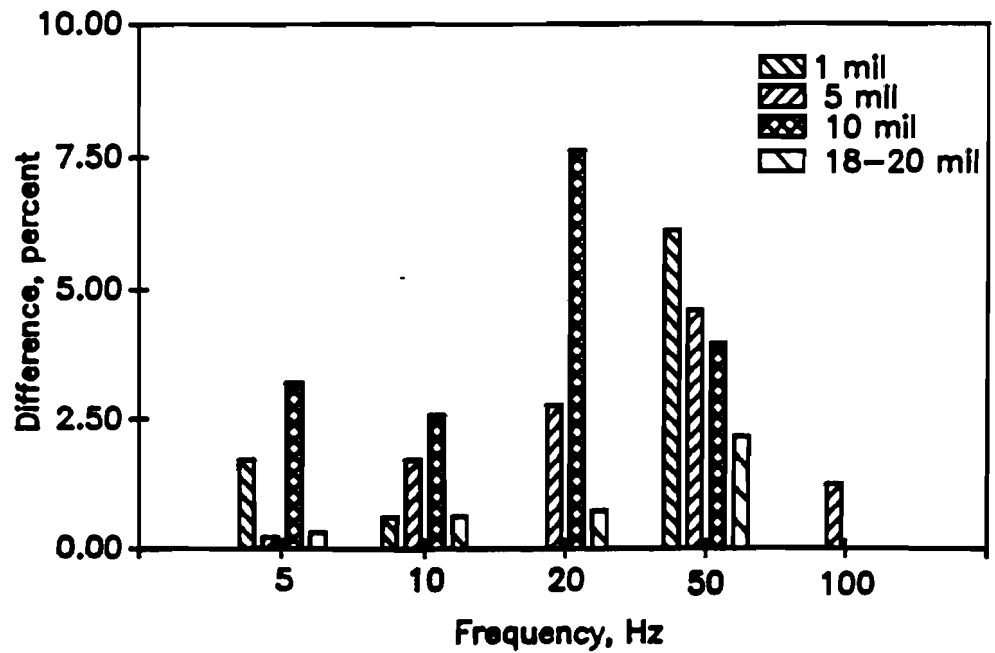


b) Difference from Proximeter Deflections

Figure 3.2 Evaluation of Accuracy and Precision of Accelerometer 2 Under Steady-State Loading

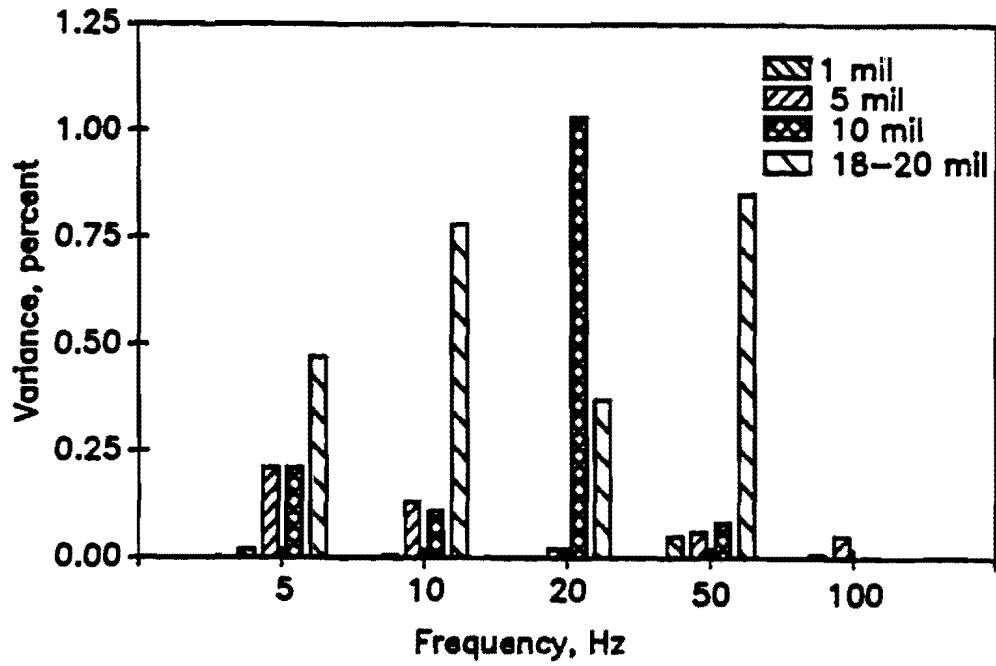


a) Variance

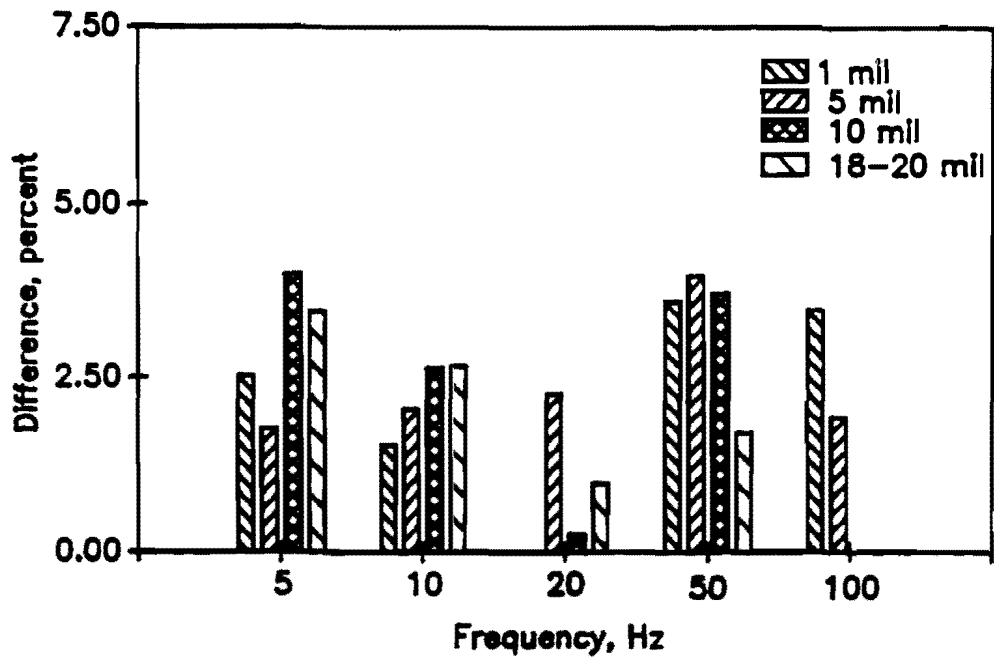


b) Difference from Proximeter Deflections

Figure 3.3 Evaluation of Accuracy and Precision of Geophone 1 Under Steady-State Loading

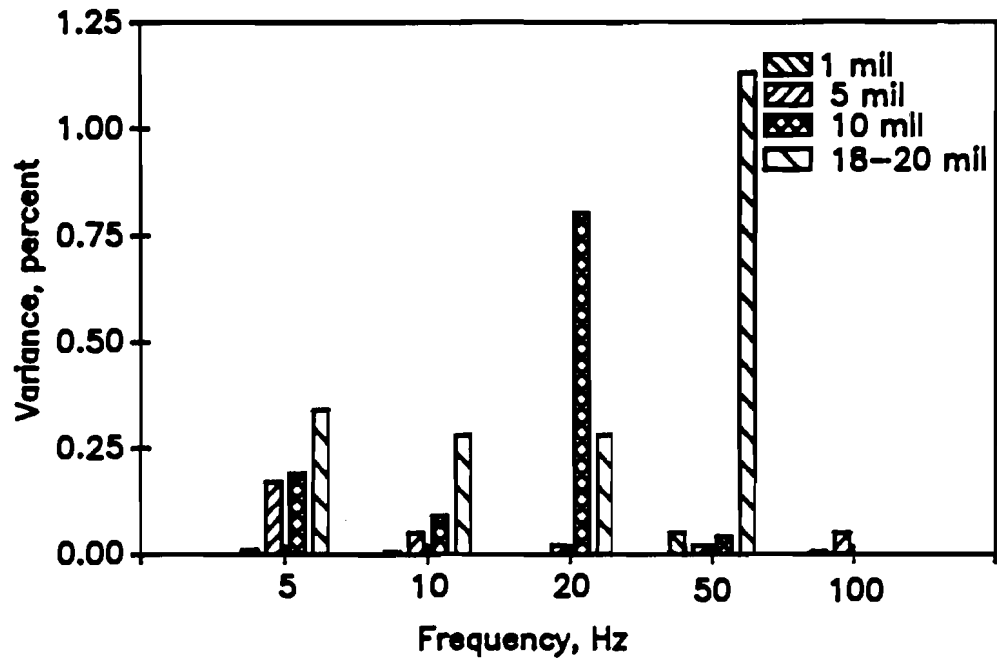


a) Variance

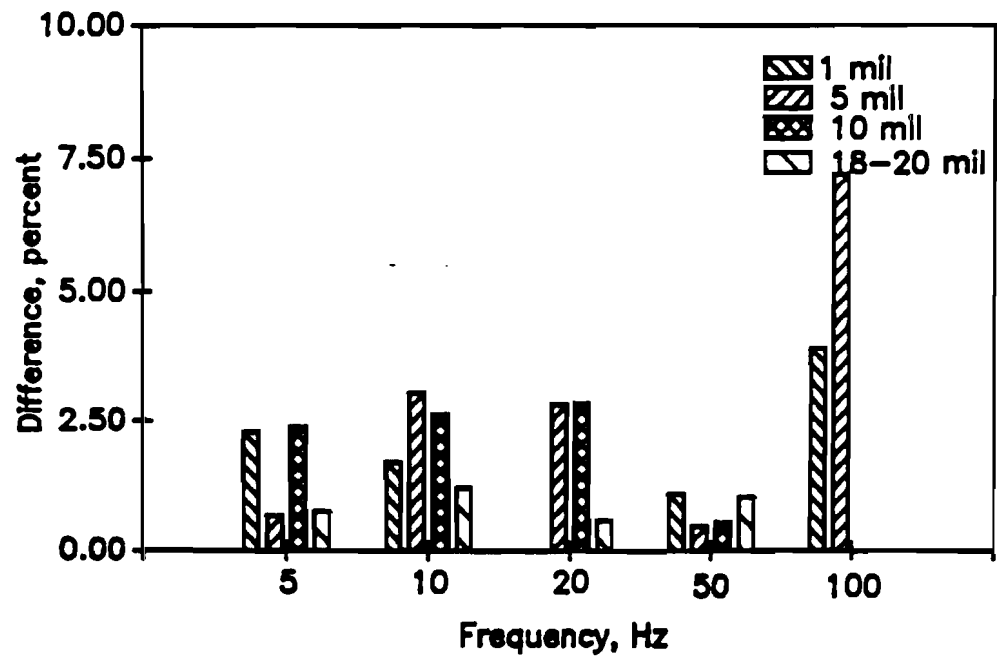


b) Difference from Proximeter Deflections

Figure 3.4 Evaluation of Accuracy and Precision of Geophone 2 Under Steady-State Loading

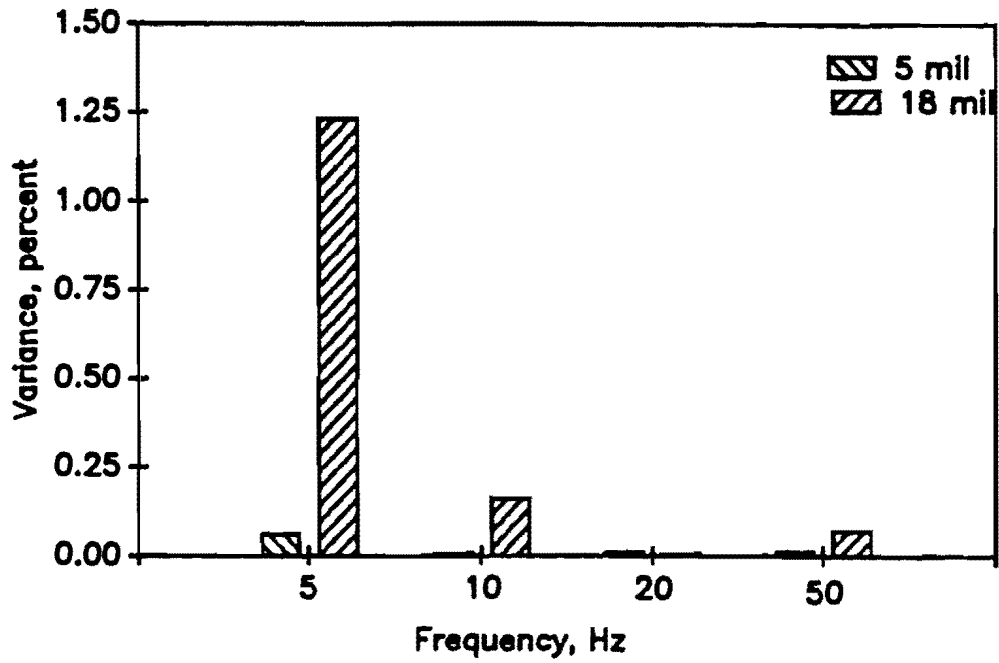


a) Variance

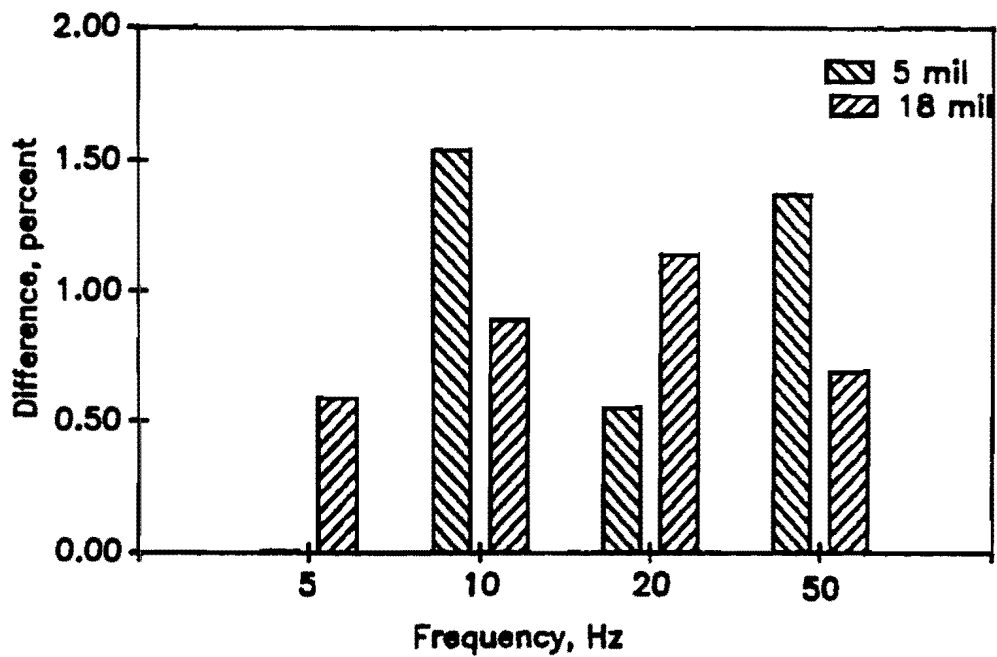


b) Difference from Proximeter Deflections

Figure 3.5 Evaluation of Accuracy and Precision of LVDT Under Steady-State Loading



a) Variance



b) Difference from Proximeter Deflections

Figure 3.6 Evaluation of Accuracy and Precision of Laser Under Steady-State Loading

the variation in deflections from geophones is well within background noise. As for the accelerometers, the higher variances are normally associated with higher deflection levels.

The LVDT device also performs well under the steady-state loads (Figure 3.5a). The variances are usually less than 0.5 percent, except two cases where the variances are about 1 percent.

The laser device exhibits very little variance in all but one case (Figure 3.6a). As a matter of fact, in most cases the variance is almost zero.

The precision of the proximeter is quite good and is in the order of 0.5 percent as shown in Figure 3.7. At high amplitude of vibration, the variance is about 0.75 percent which is still quite small.

The accuracy of each device was determined by comparing deflections measured with each device against those measured with the proximeter. The variances obtained with the proximeter is shown in Figure 3.7. The proximeter has been known as one of the most accurate and precise deflection measuring devices in the laboratory environment because of its noncontact nature. These comparisons are presented in a graphical form in Figures 3.1 through 3.6 for the two accelerometers, two geophones the LVDT, and the laser device, respectively.

The accuracy of the two accelerometers is similar (Figures 3.1b and 3.2b). The maximum difference between deflections measured by the accelerometers and the proximeter is about five percent. But generally, the differences are within three percent.

The accuracy of the geophones, as compared with the proximeter, is generally within four percent except in two cases for Geophone 1 where the differences are six and 7.5 percent (Figures 3.3b and 3.4b).

The LVDT has an accuracy of about 2.5 percent when compared with the proximeter (Figure 3.5b). However, at a frequency of 100 Hz the LVDT becomes less accurate when the deviation from the deflections of the proximeter is about five percent. A frequency of 100 Hz is quite close to the cut-off frequency of the LVDT.

The laser device compares very favorably with the proximeter as indicated in Figure 3.6b. In all cases, deflections from the two devices do not differ with more than 1.5 percent. Due to the limited availability of the laser device, the proximeter was used as the reference sensor.

3.3.2. Half-sine impulse

Precision and accuracy of the six sensors mentioned above were also evaluated under a half-sine impulse. The results are summarized in Figure 3.8 through 3.13 for the two accelerometers, two geophones, the LVDT and the laser device, respectively. The raw

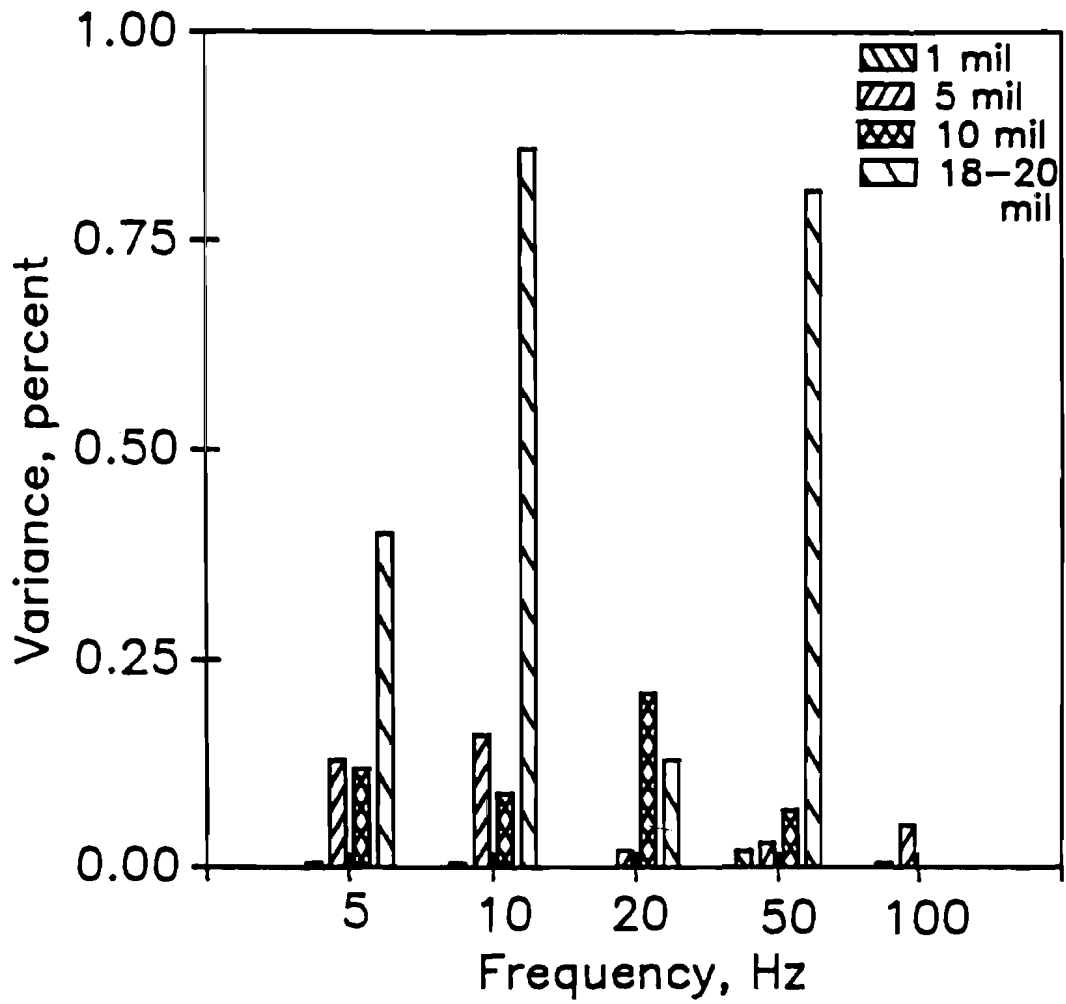
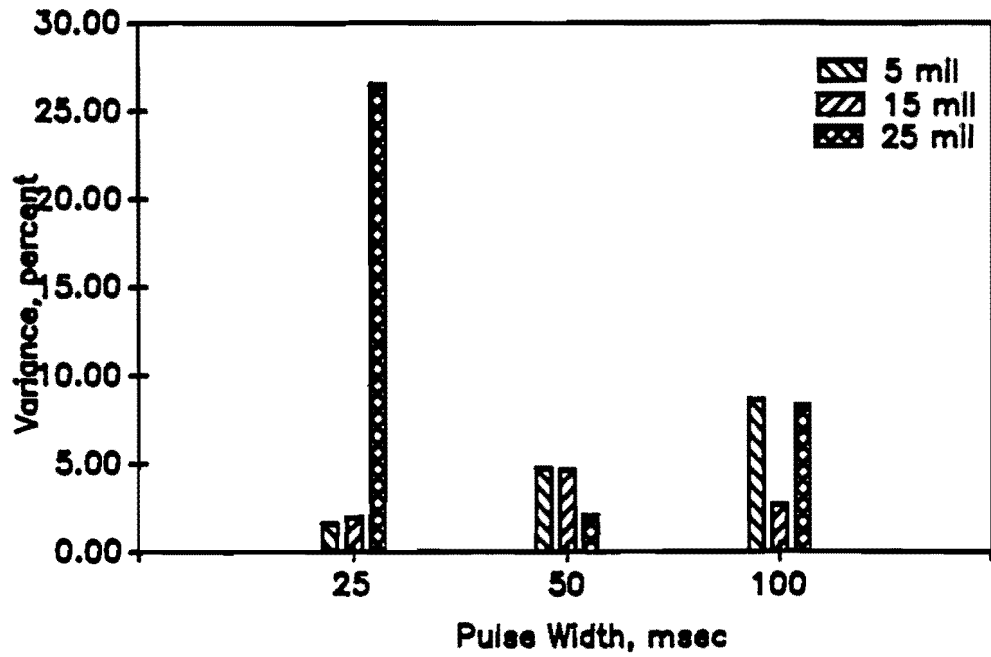
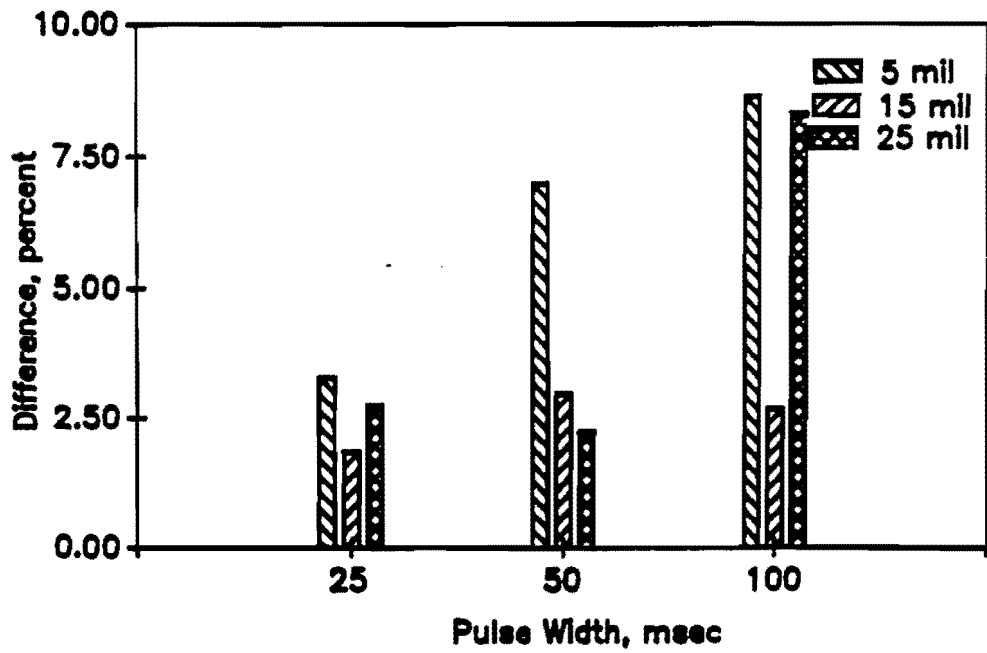


Figure 3.7 Variability in Deflection Measured with Proximeter as a Function of Frequency and Amplitude

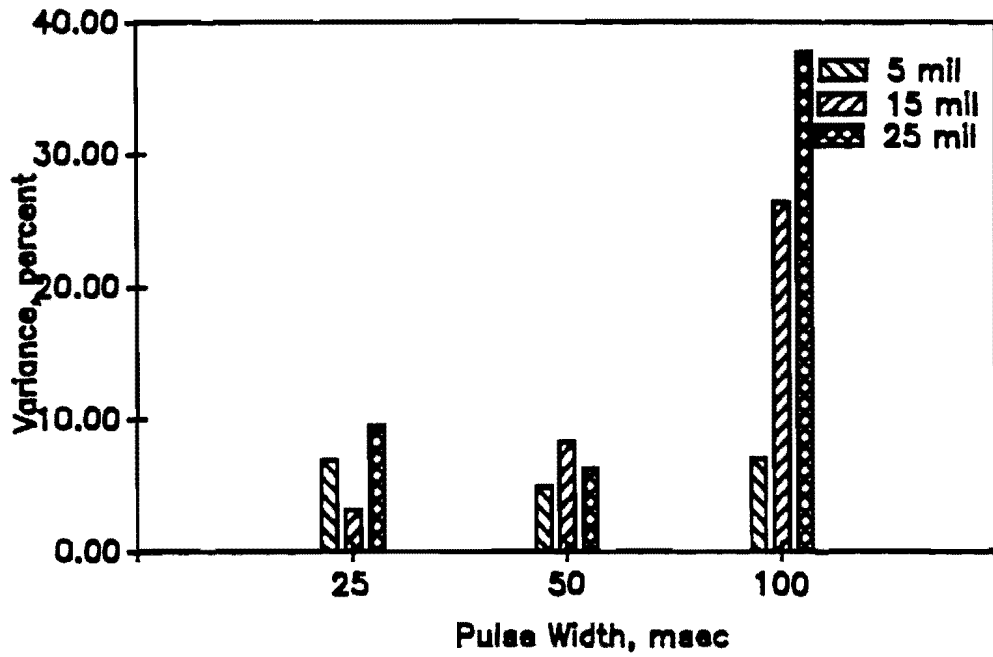


a) Variance

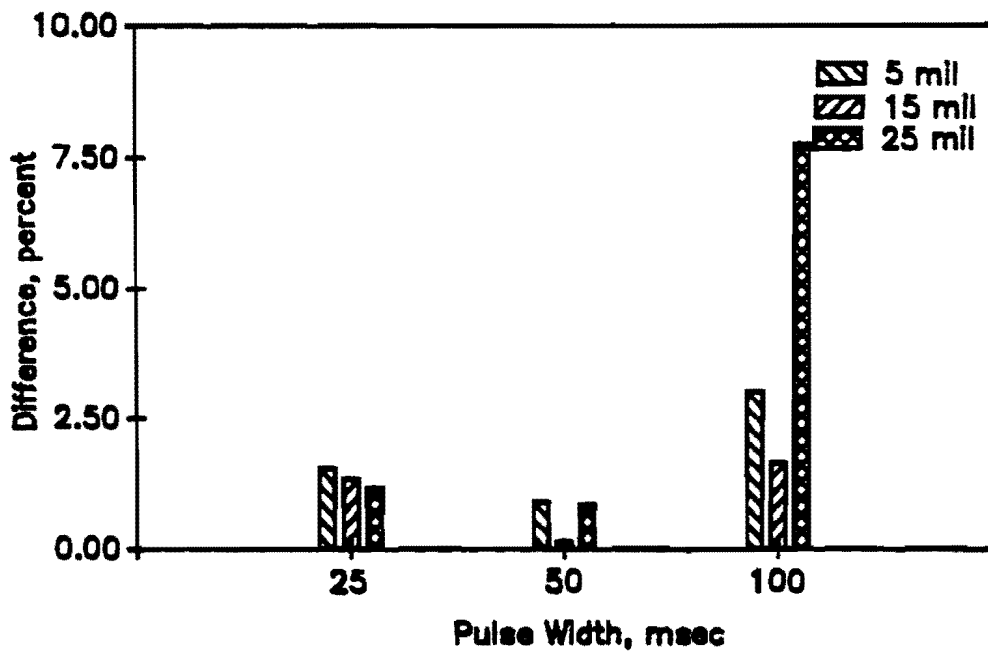


b) Difference from Proximeter Deflections

Figure 3.8 Evaluation of Accuracy and Precision of Accelerometer 1 Under Half-Sine Pulse Loading

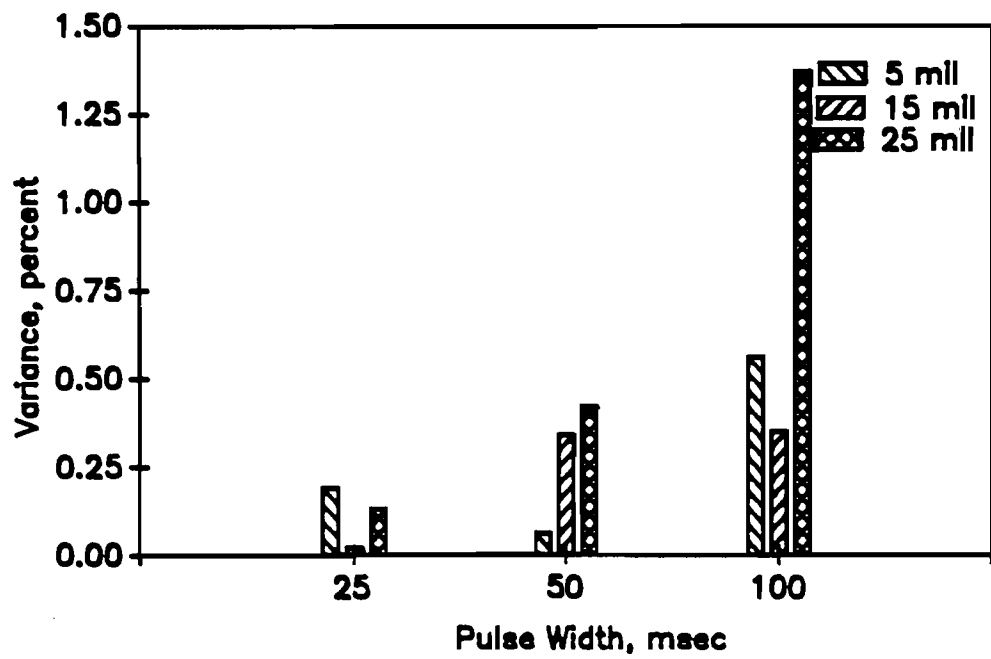


a) Variance

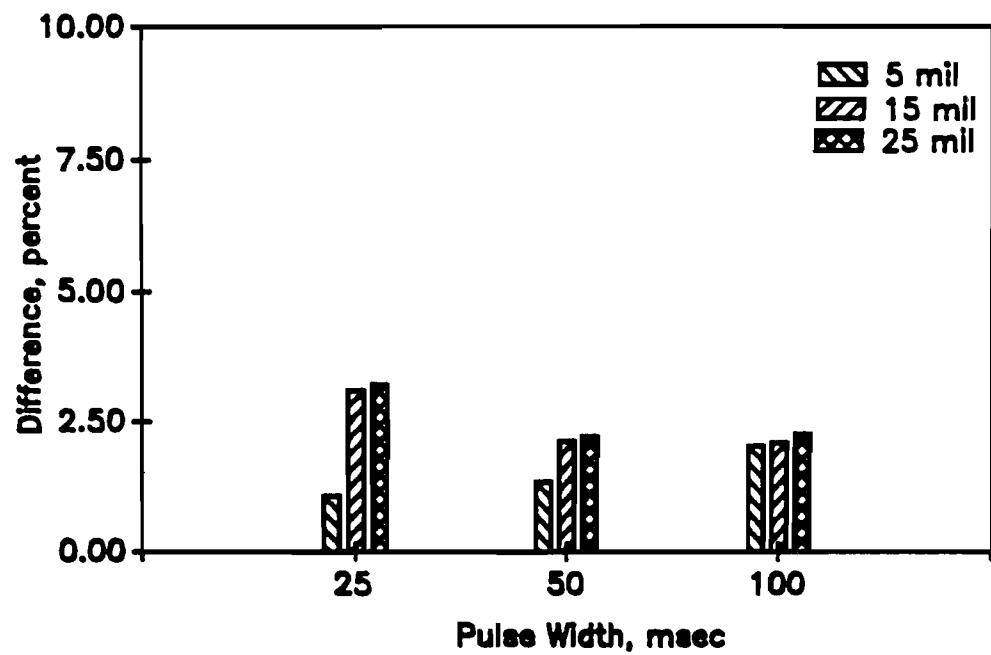


b) Difference from Proximeter Deflections

Figure 3.9 Evaluation of Accuracy and Precision of Accelerometer 2 Under Half-Sine Pulse Loading

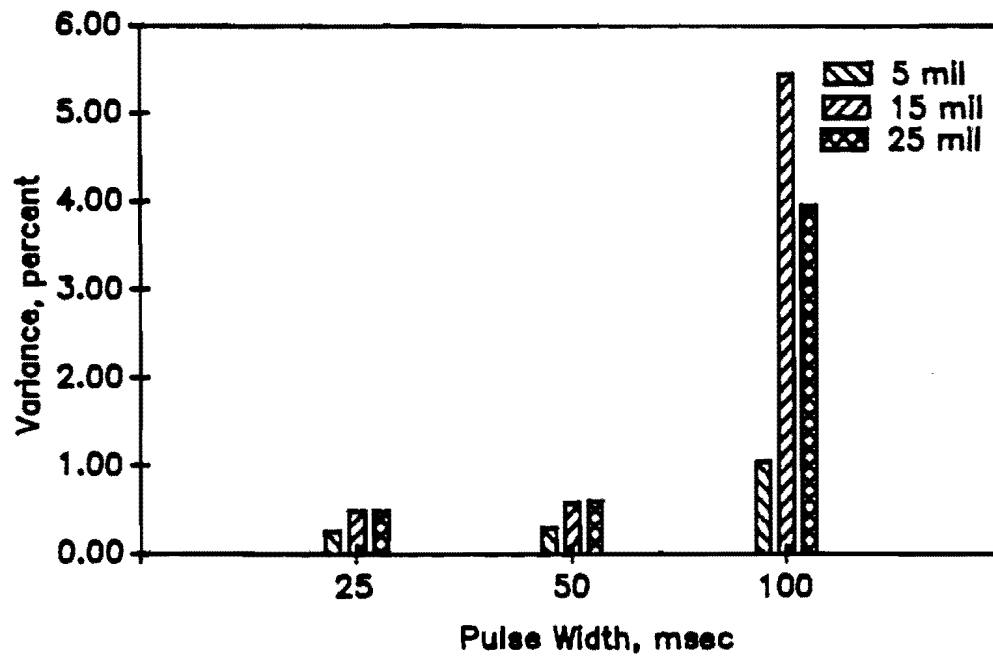


a) Variance

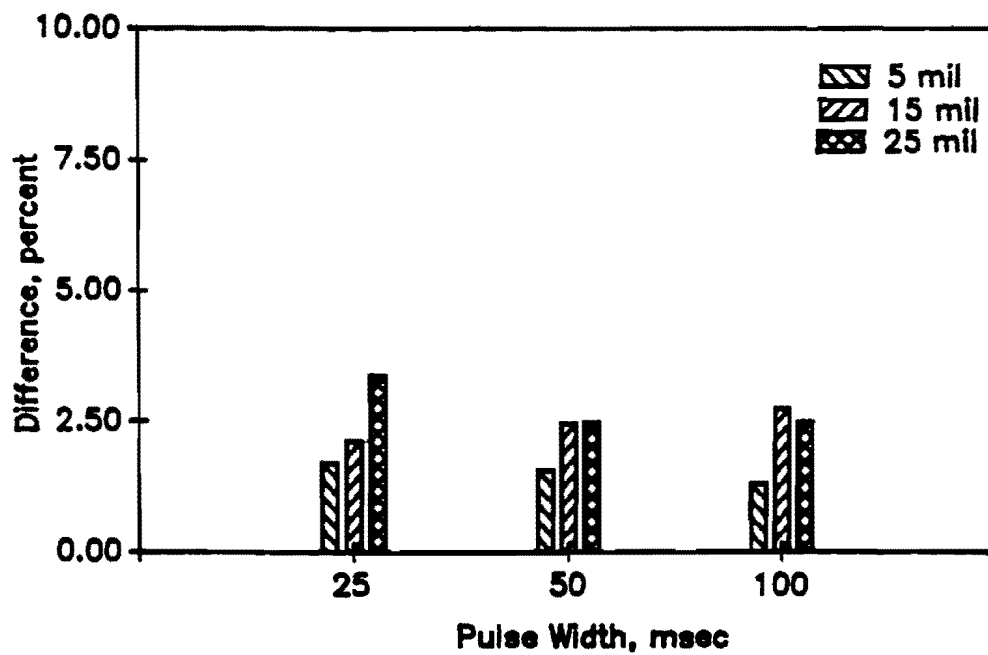


b) Difference from Proximeter Deflections

Figure 3.10 Evaluation of Accuracy and Precision of Geophone 1 Under Half-Sine Pulse Loading

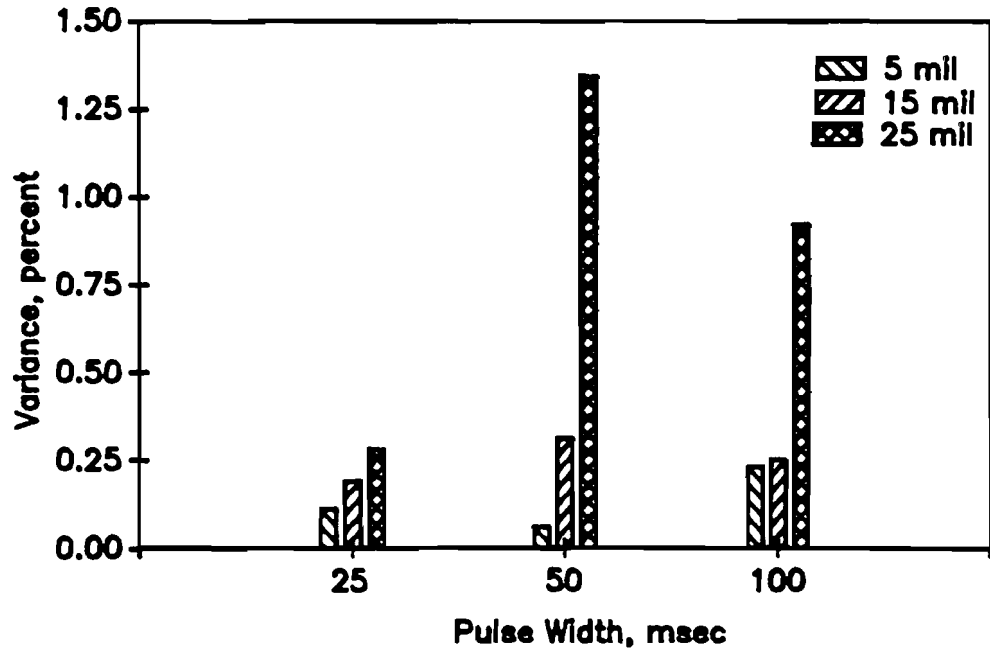


a) Variance

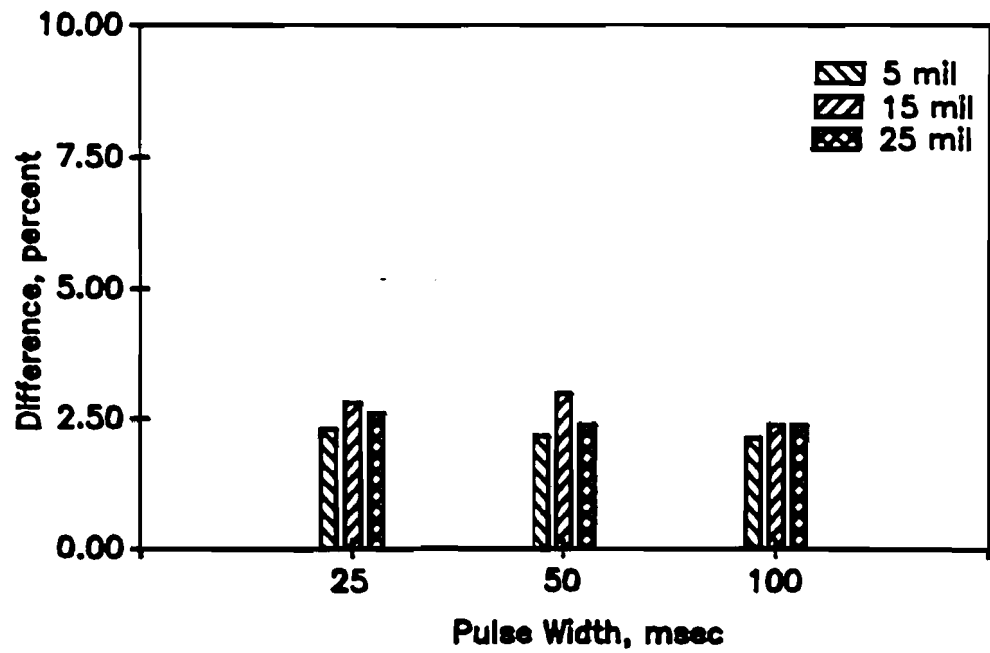


b) Difference from Proximeter Deflections

Figure 3.11 Evaluation of Accuracy and Precision of Geophone 2 Under Half-Sine Pulse Loading

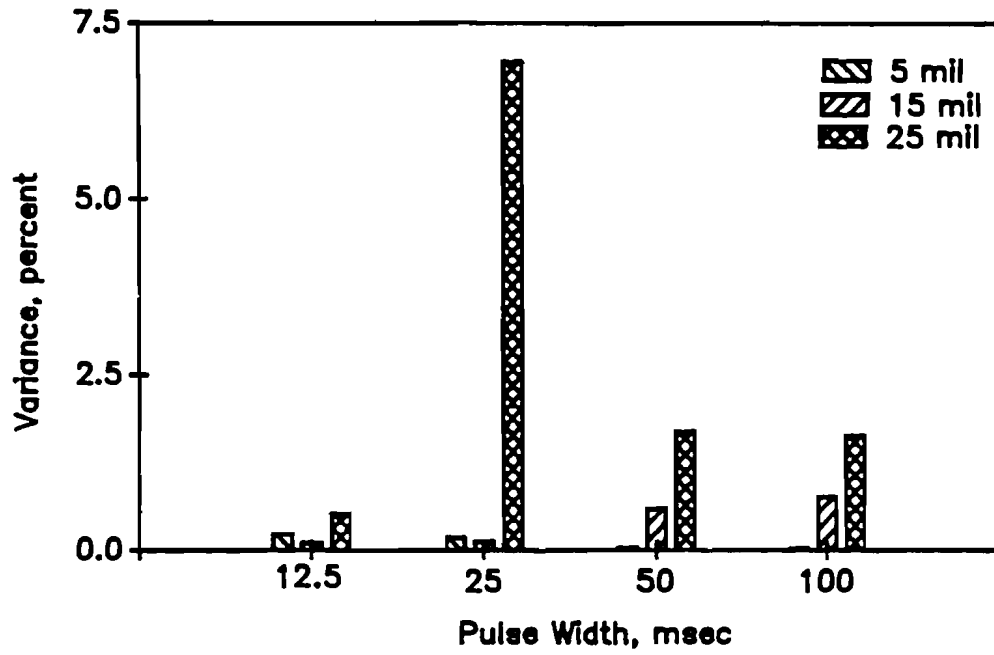


a) Variance

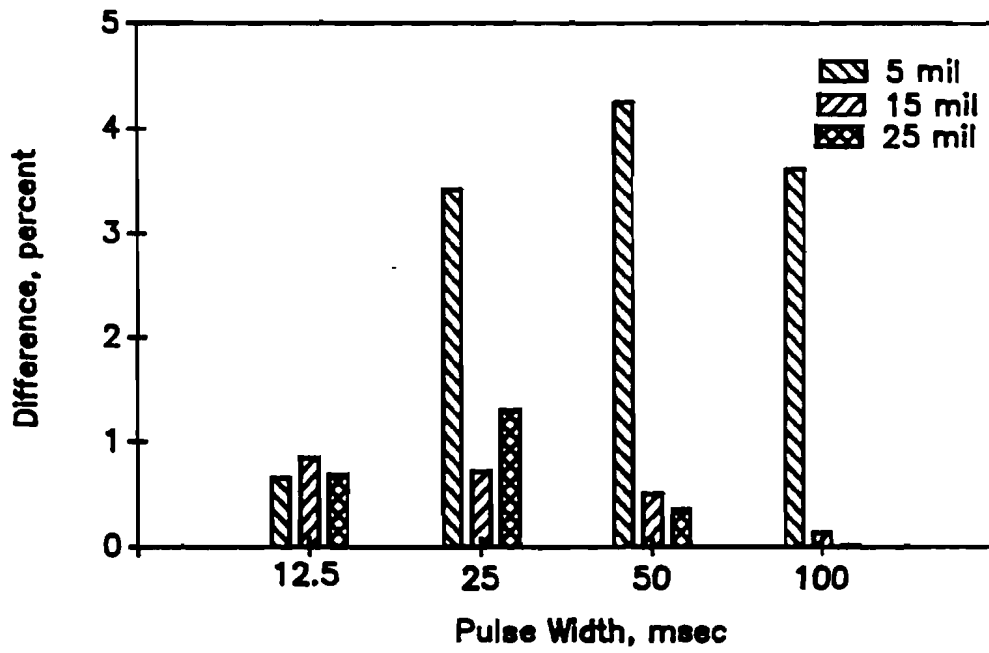


b) Difference from Proximeter Deflections

Figure 3.12 Evaluation of Accuracy and Precison of LVDT Under Half-Sine Pulse Loading



a) Variance



b) Difference from Proximeter Deflections

Figure 3.13 Evaluation of Accuracy and Precision of Laser Under Half-Sine Pulse Loading

data from which the accuracy and precision were evaluated are included in Appendix H. A comprehensive analysis of the precision and accuracy are included in Appendices I and J.

The two accelerometers exhibited quite large variation in deflections as depicted in Figures 3.8a and 3.9a. It can be seen that variances in excess of five percent are not uncommon. Also, the two accelerometers do not exhibit similar trends.

Contrary to the accelerometers, the variances measured with the geophones are less than 2 percent in all cases (Figures 3.10a and 3.11a). Such a small variation can easily be attributed to background noise. As a matter of fact in most cases the variance is below 0.5 percent.

The LVDT is quite precise also. The maximum variance is about 1.25 percent (Figure 3.12a), and typically, less than 0.5 percent.

The laser device is not as repeatable as it was under the steady-state conditions. However, as depicted in Figure 3.13a, in all conditions (but one) the repeatability of data is within 1.5 percent.

The precision of the proximeter is depicted in Figure 3.14. For all the experiments carried out with this device, the maximum variance is about 0.60 percent, which is very small.

The accuracy of the two accelerometers is unacceptably low for an impulse width of 100 msec (Figure 3.8b and 3.9b). As mentioned in Appendix B, for large pulse widths, vibrations are not accurately measured with an accelerometer. The accuracy of the accelerometers at shorter pulse widths is within three percent.

The accuracy of the geophones and the LVDT are quite good and deflections measured with both sensors are within 2.5 percent of deflections measured with a proximeter in almost all cases (Figures 3.10b through 3.12b). Therefore, one may confidently use a geophone or an LVDT for accurate measurement of deflections under half-sine pulses.

The accuracy of the laser device as compared with a proximeter normally varies between 0.5 and 4 percent (Figure 3.13b). Therefore, it seems that a geophone or an LVDT may result in a better and more consistent accuracy.

3.3.3 Square and Triangular Pulses

The results from limited experiments with the square and triangular pulses are summarized in Figures 3.15 through 3.21 for the square pulses and Figures 3.22 through 3.28 for the triangular pulses. The raw data collected with these two pulses are included in Appendix H. A comprehensive analysis of data in terms of accuracy and precision are presented in Appendices K through N.

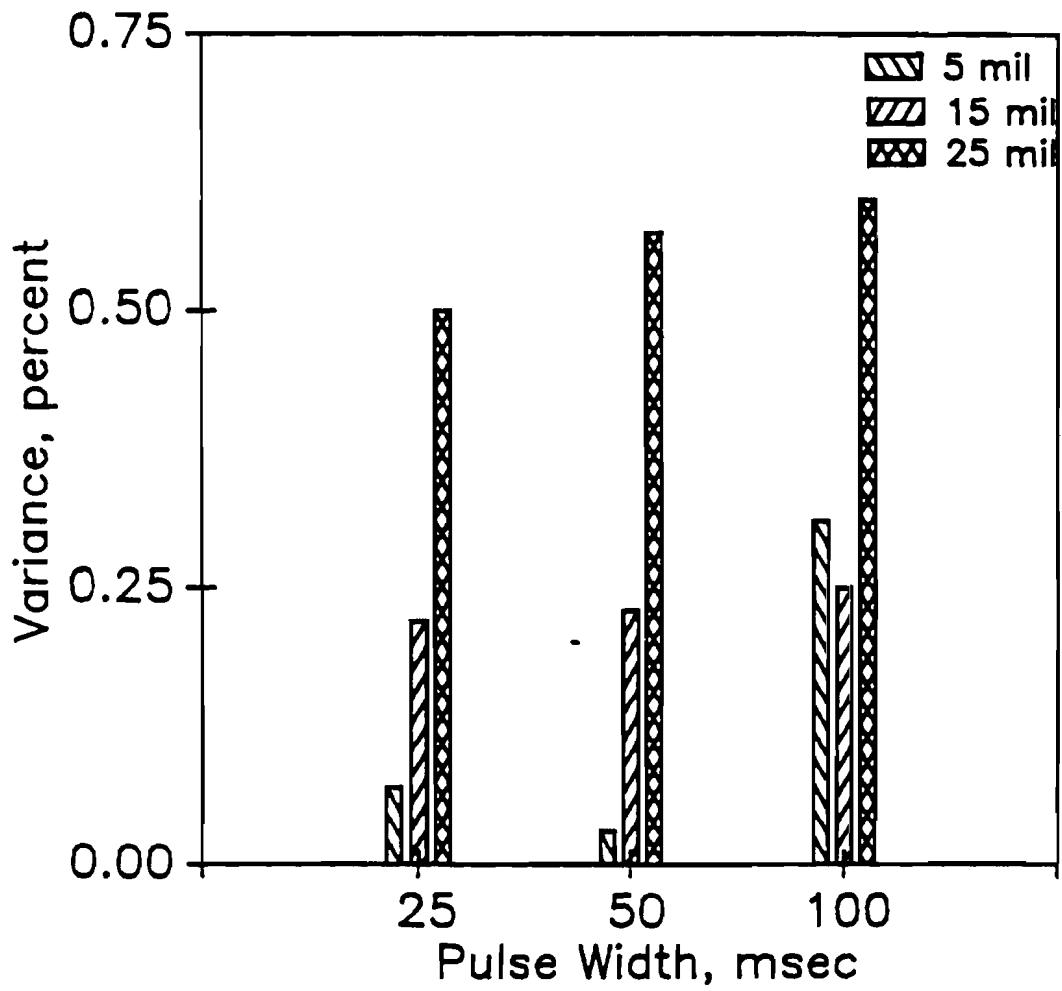
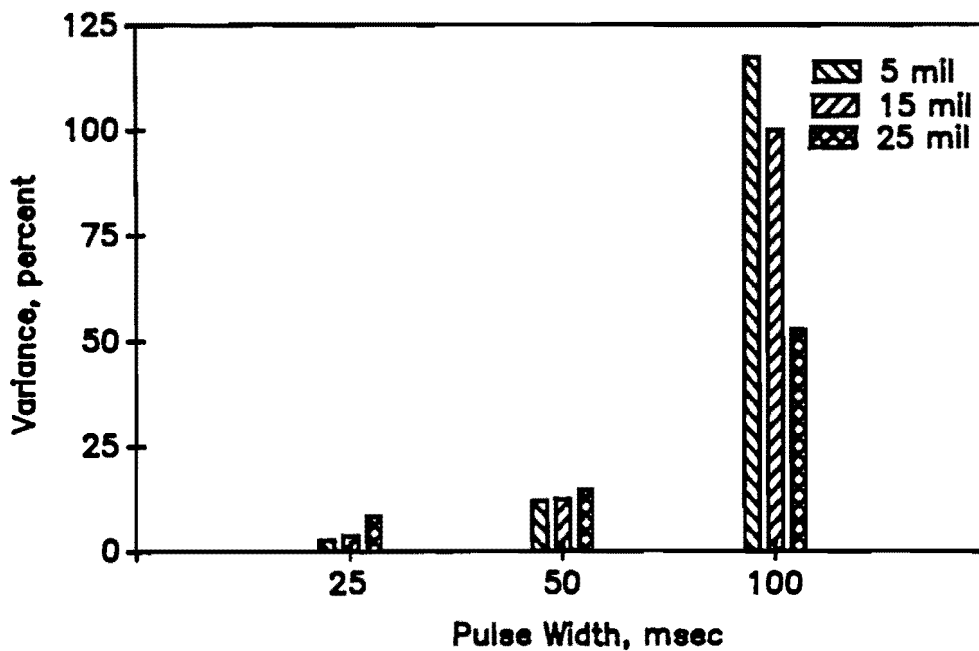
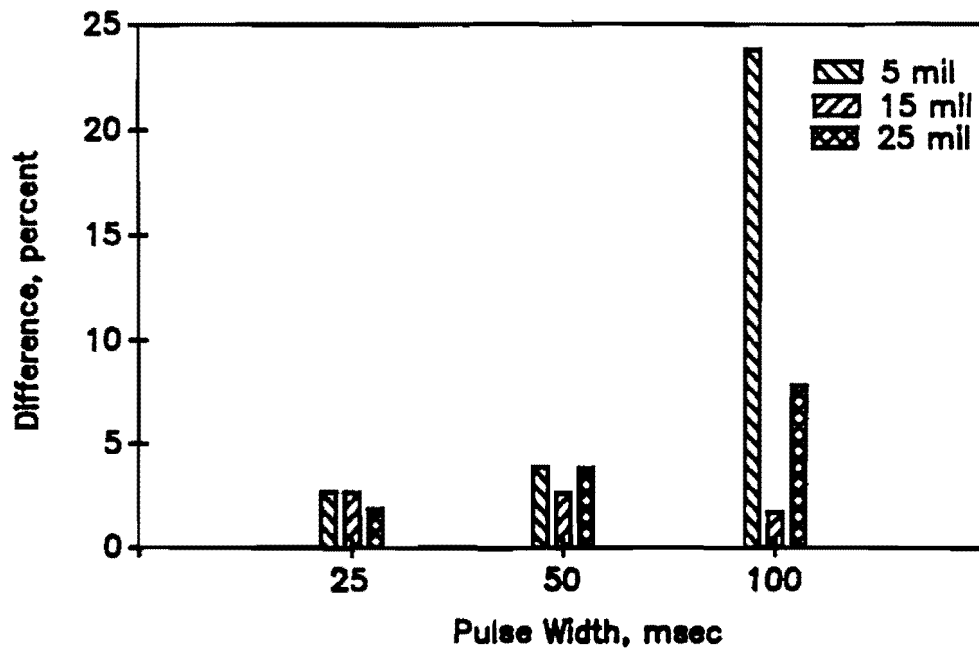


Figure 3.14 Variability in Deflection Measured with Proximeter as a Function of Half-Sine Impulse

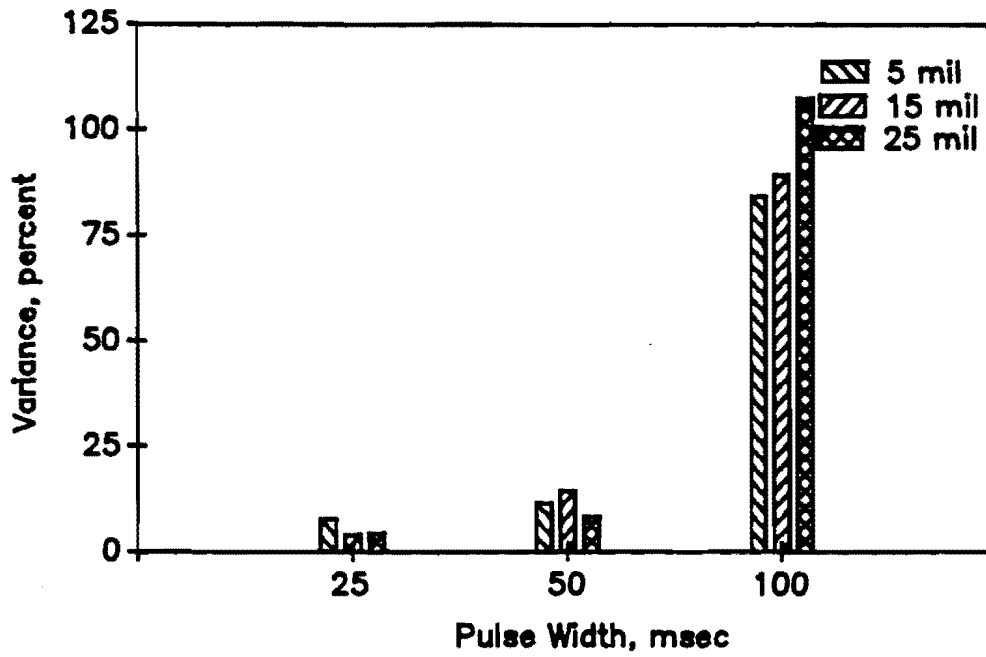


a) Variance

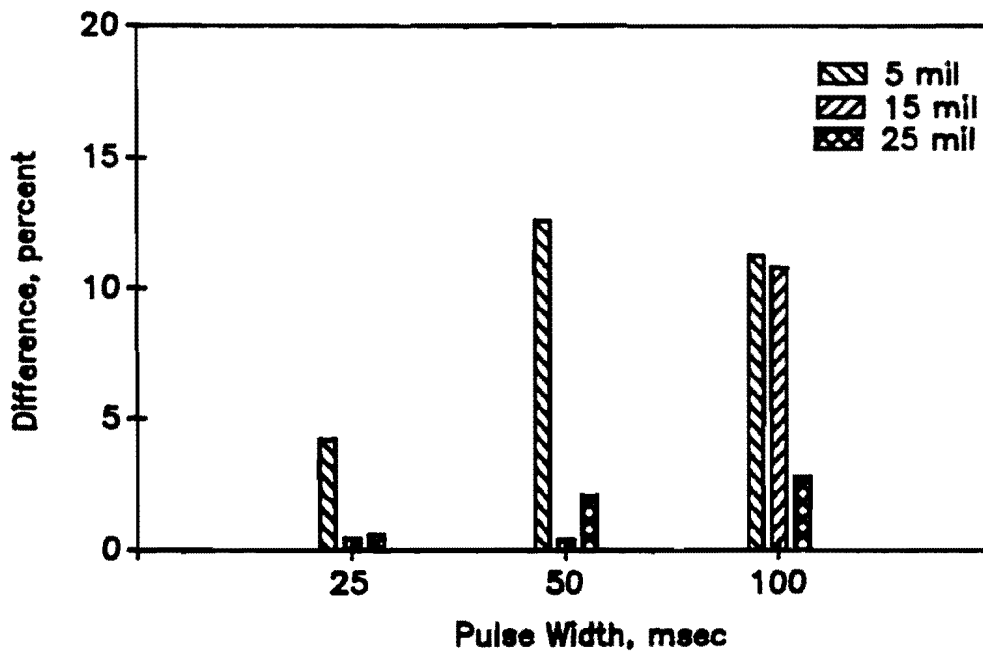


b) Difference from Proximeter Deflections

Figure 3.15 Evaluation of Accuracy and Precision of Accelerometer 1 Under Triangular Loading

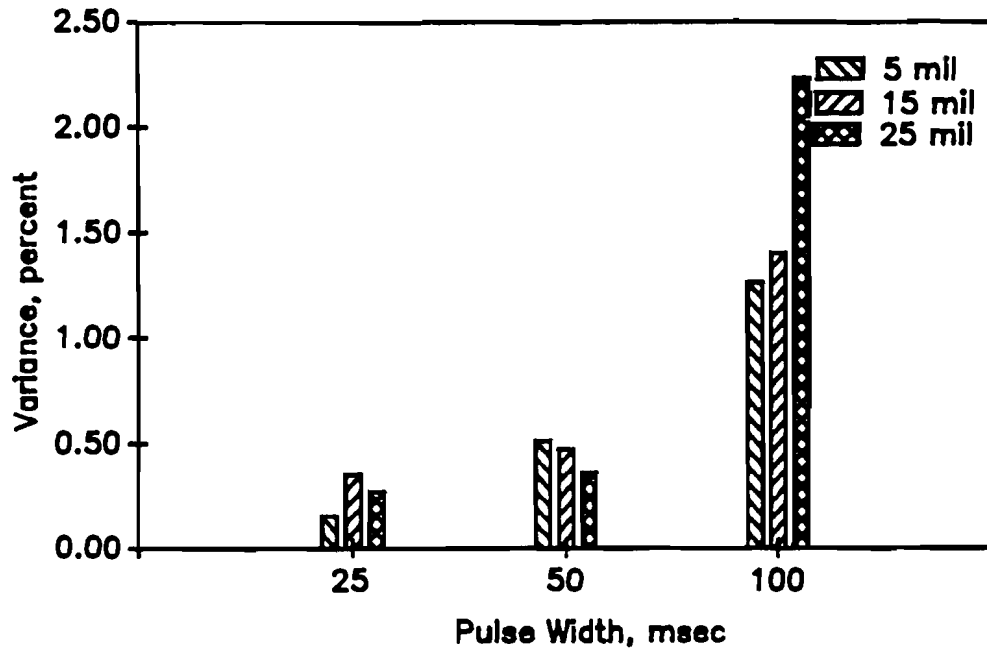


a) Variance

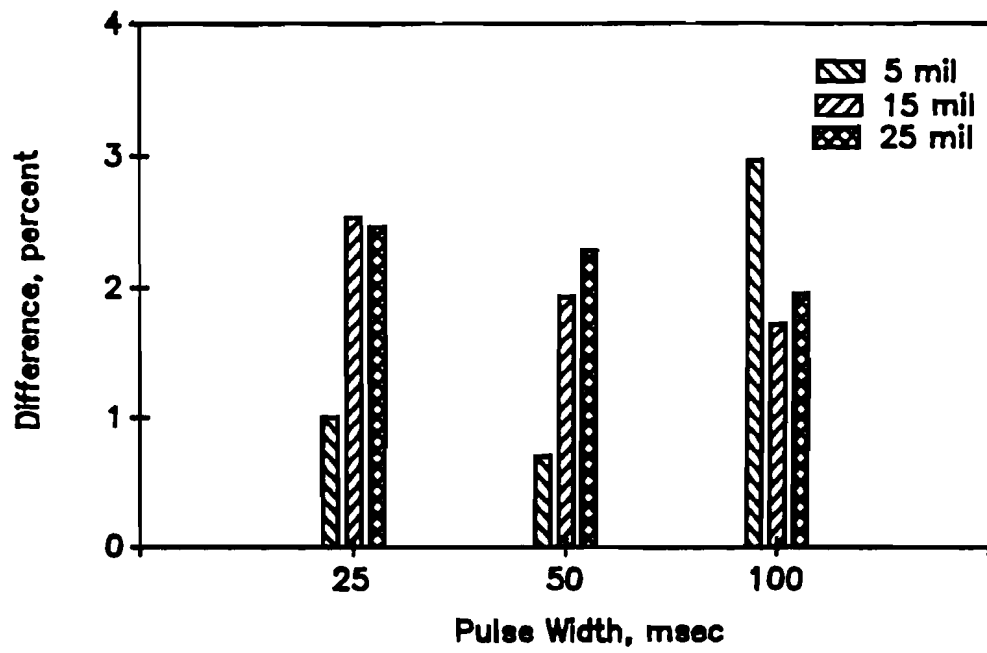


b) Difference from Proximeter Deflections

Figure 3.16 Evaluation of Accuracy and Precision of Accelerometer 2 Under Square Loading

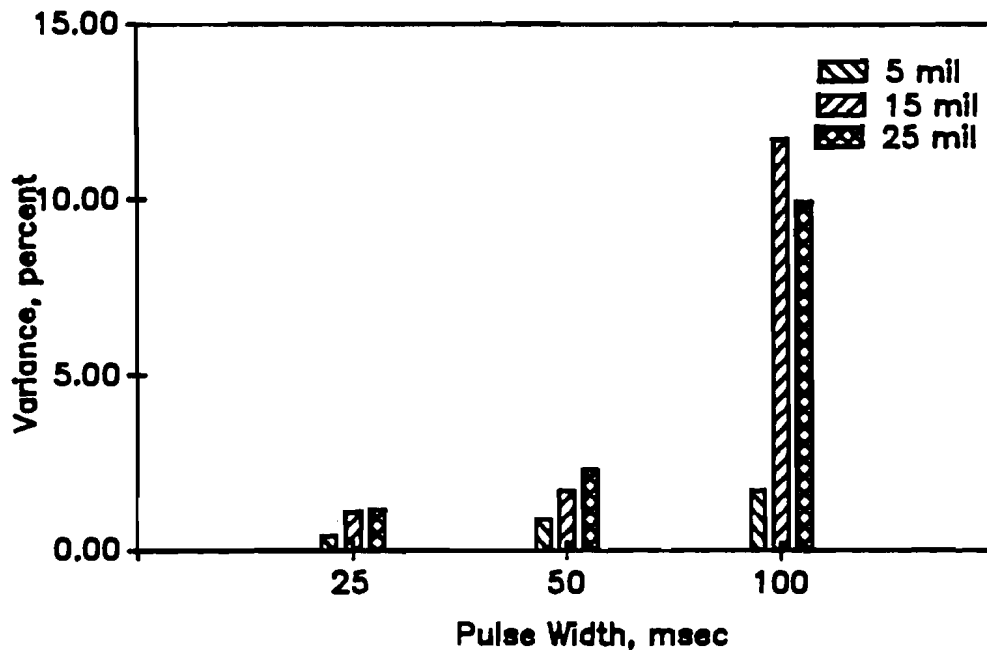


a) Variance

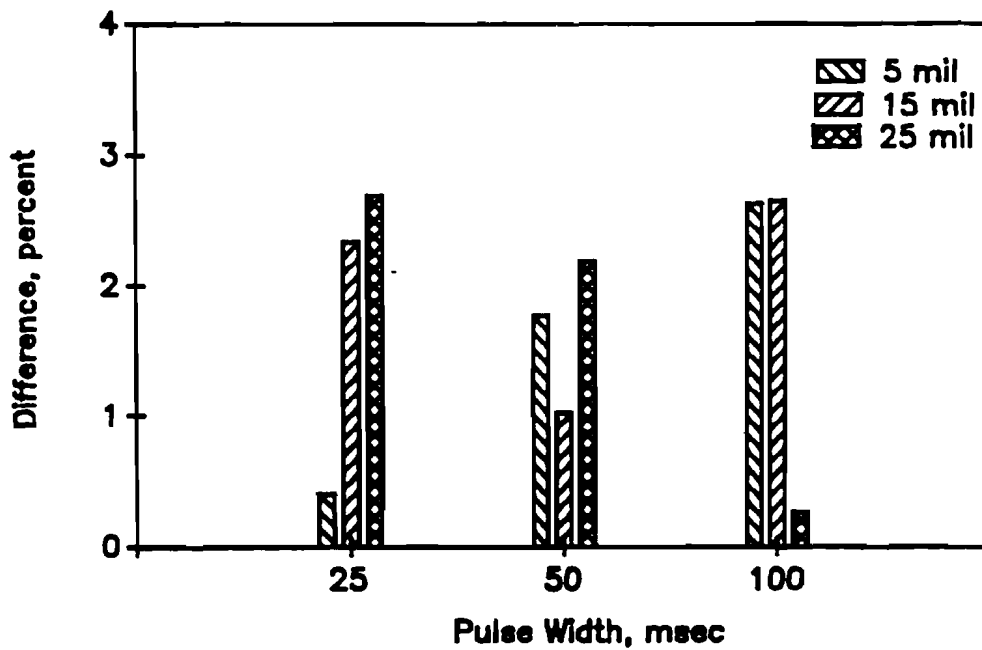


b) Difference from Proximeter Deflections

Figure 3.17 Evaluation of Accuracy and Precision of Geophone 1 Under Square Loading

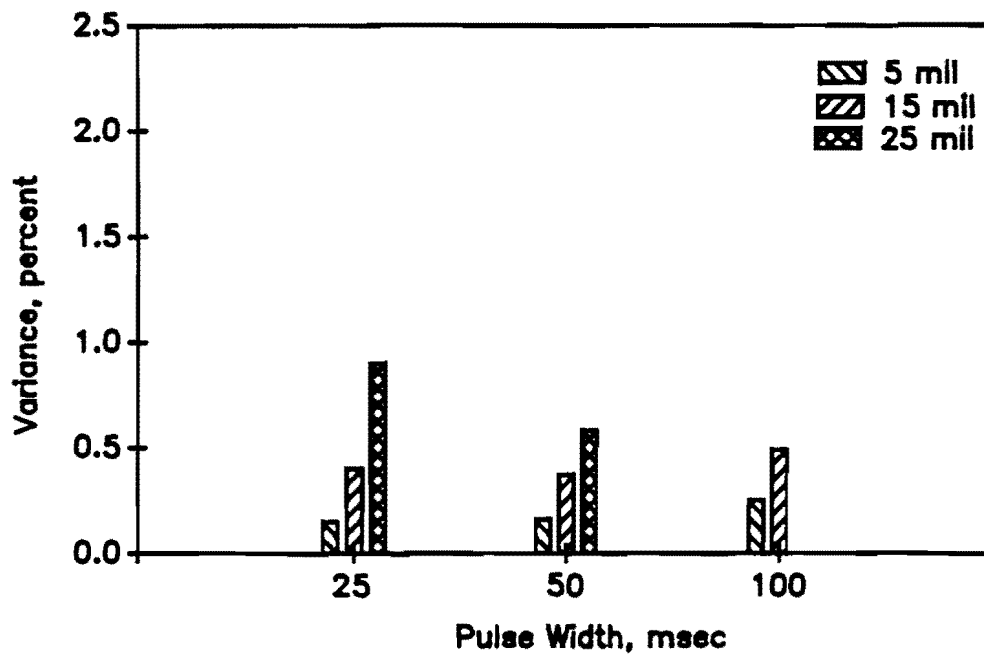


a) Variance

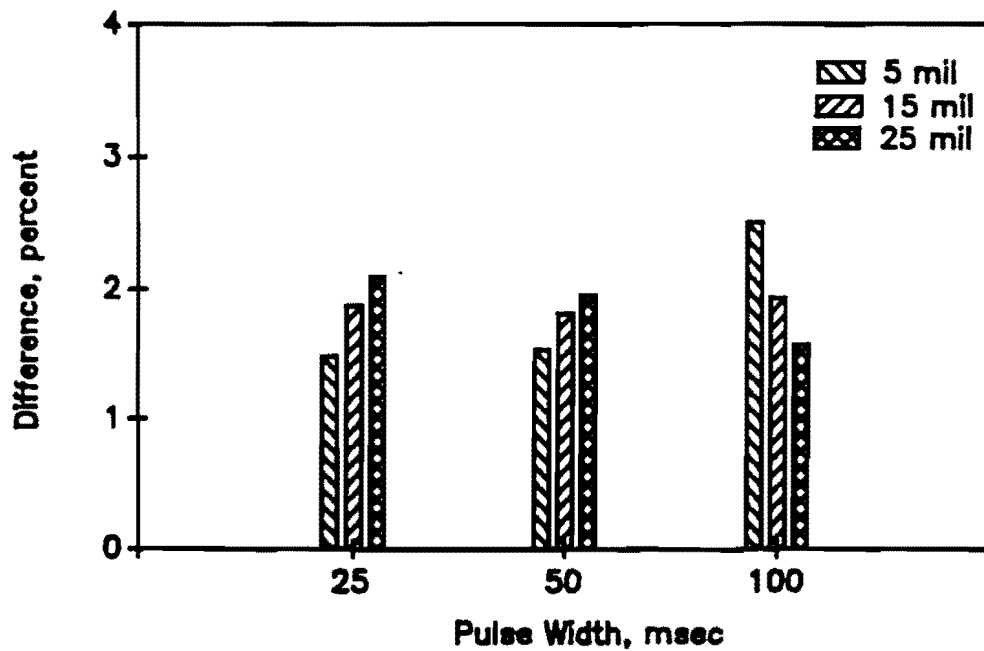


b) Difference from Proximeter Deflections

Figure 3.18 Evaluation of Accuracy and Precision of Geophone 2 Under Square Loading

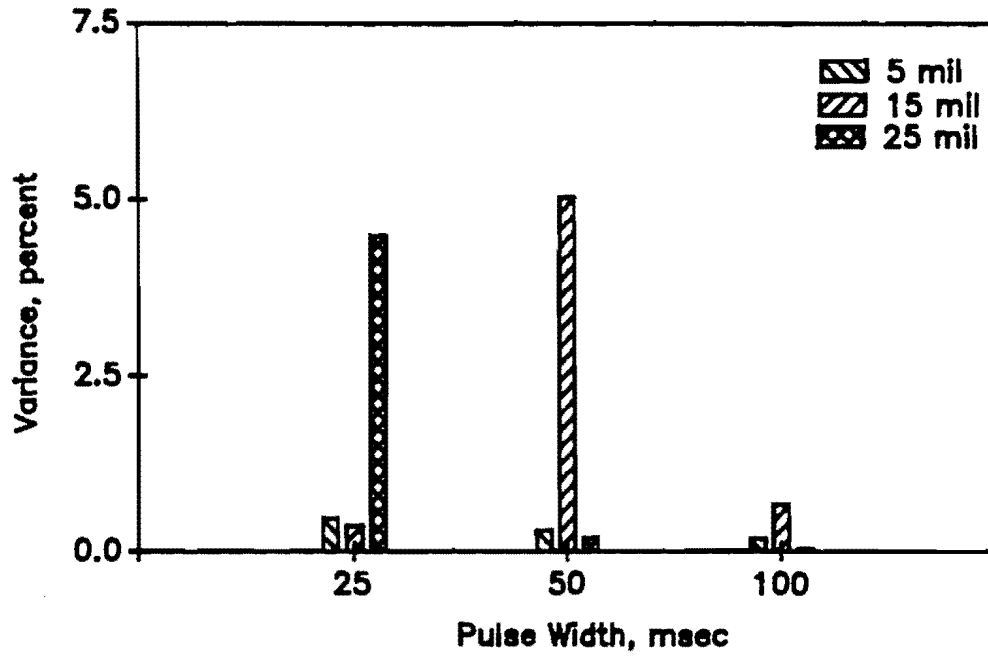


a) Variance

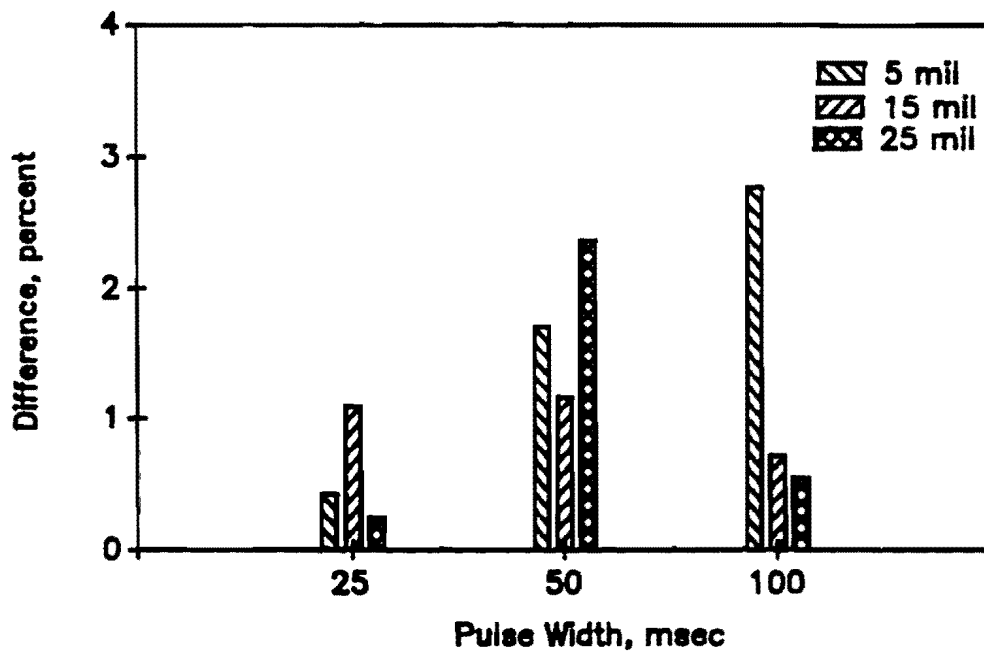


b) Difference from Proximeter Deflections

Figure 3.19 Evaluation of Accuracy and Precision of LVDT Under Square Loading



a) Variance



b) Difference from Proximeter Deflections

Figure 3.20 Evaluation of Accuracy and Precision of Laser Under Square Loading

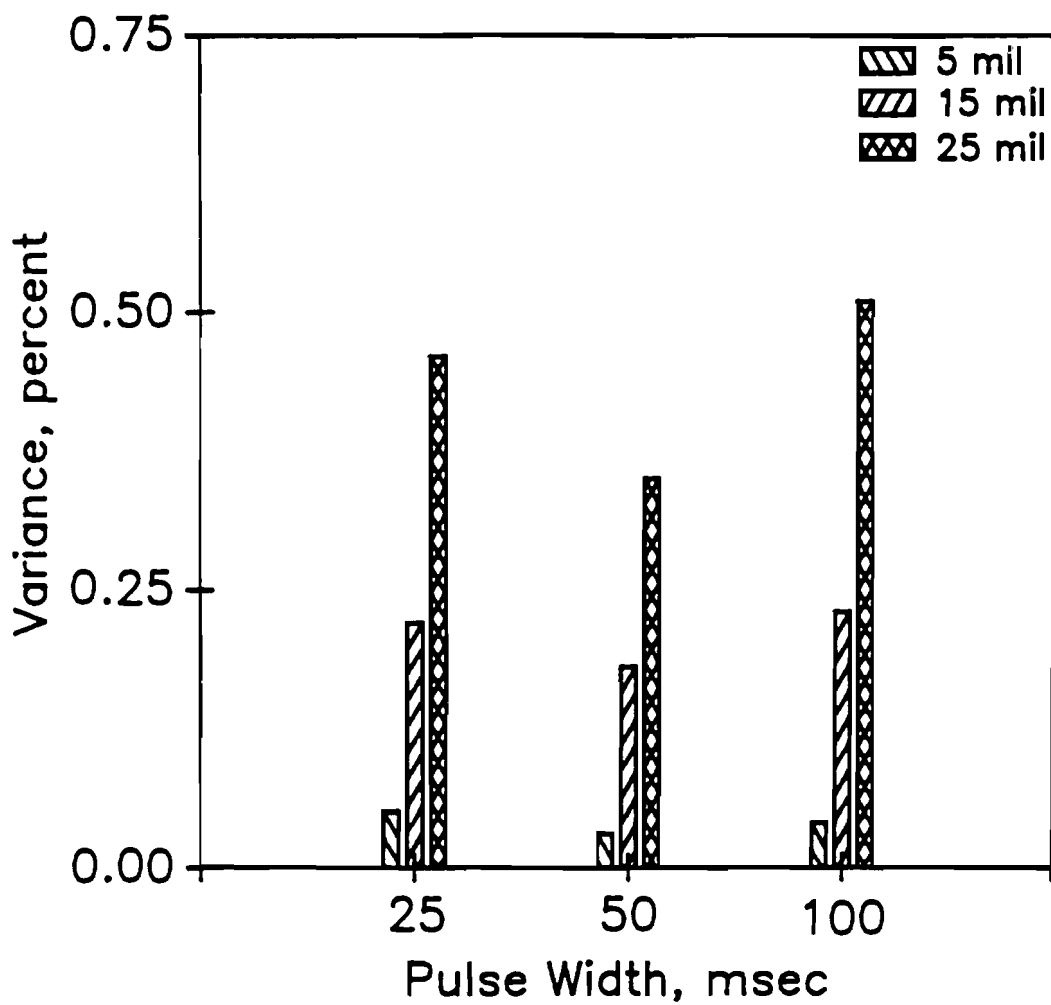
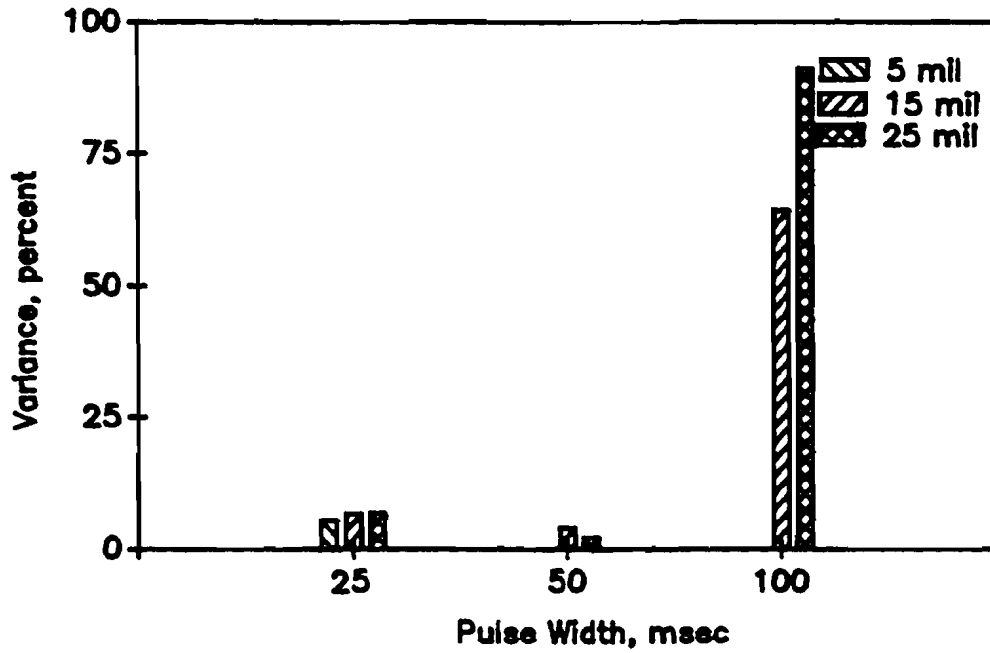
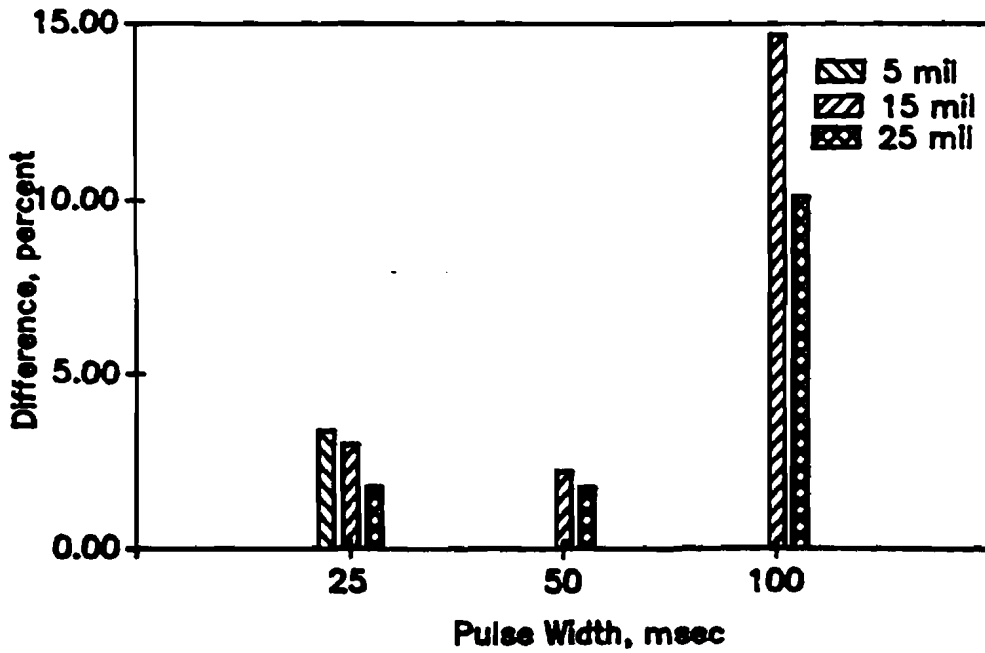


Figure 3.21 Variability in Deflection Measured with Proximeter as a Function of Frequency and Amplitude

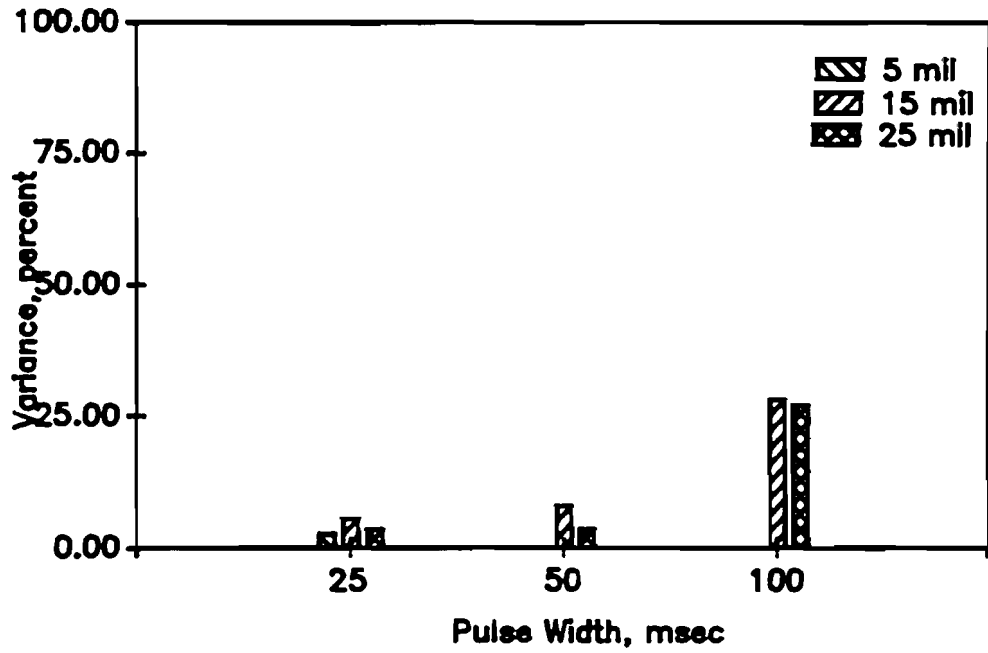


a) Variance

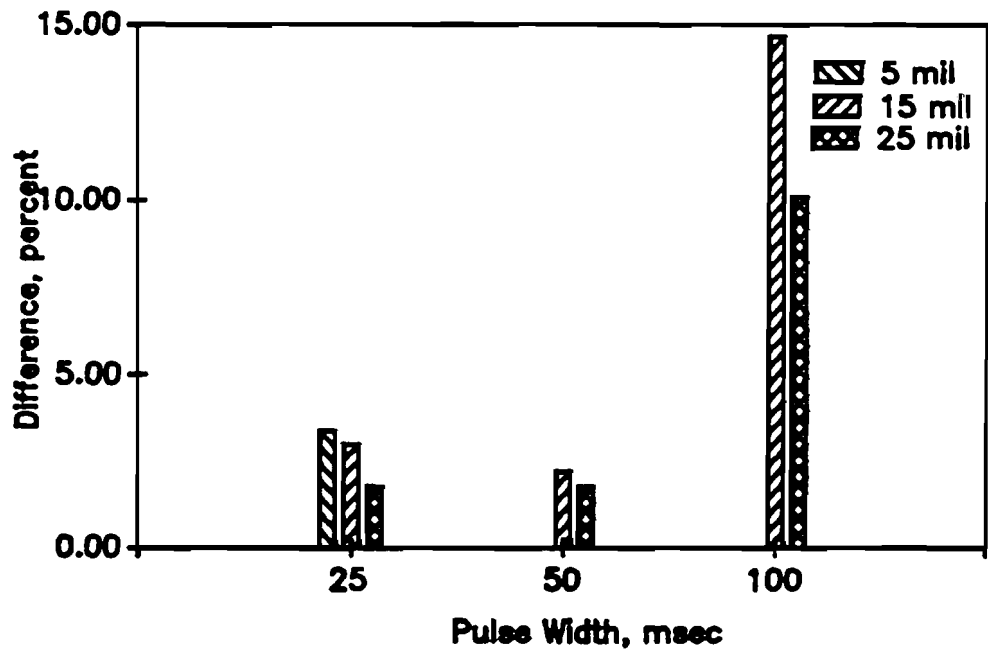


b) Difference from Proximeter Deflections

Figure 3.22 Evaluation of Accuracy and Precision of Accelerometer 1 Under Triangular Pulse Loading

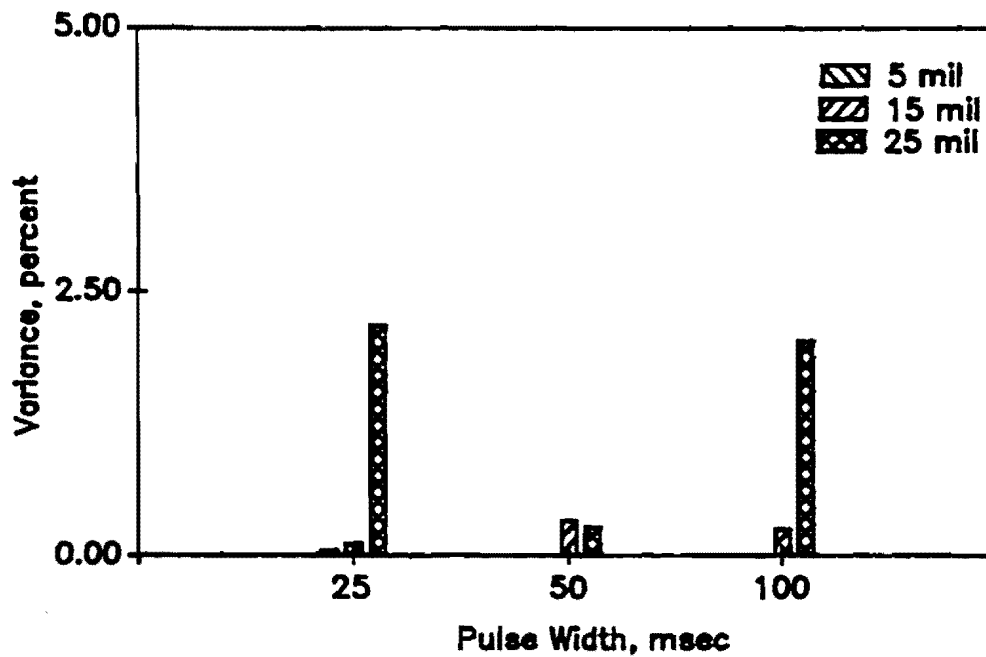


a) Variance

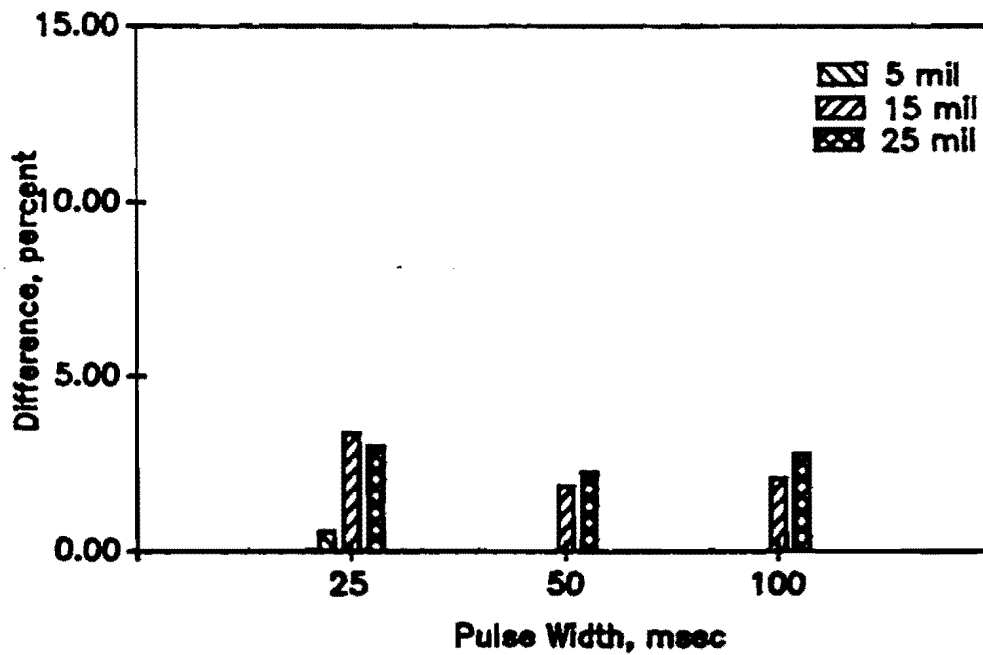


b) Difference from Proximeter Deflections

Figure 3.23 Evaluation of Accuracy and Precision of Accelerometer 2 Under Triangular Pulse Loading

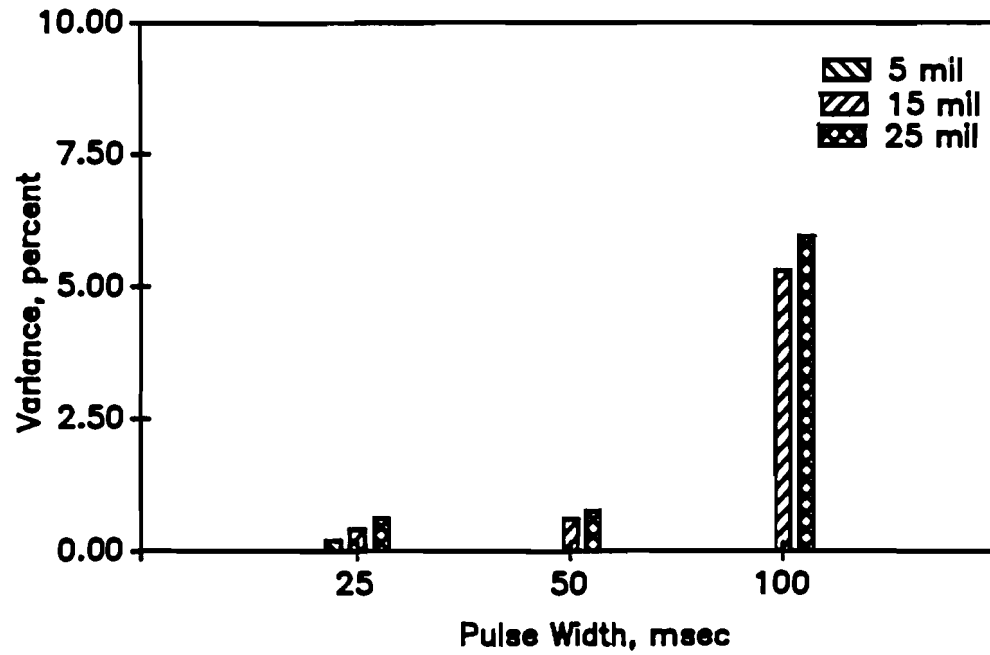


a) Variance

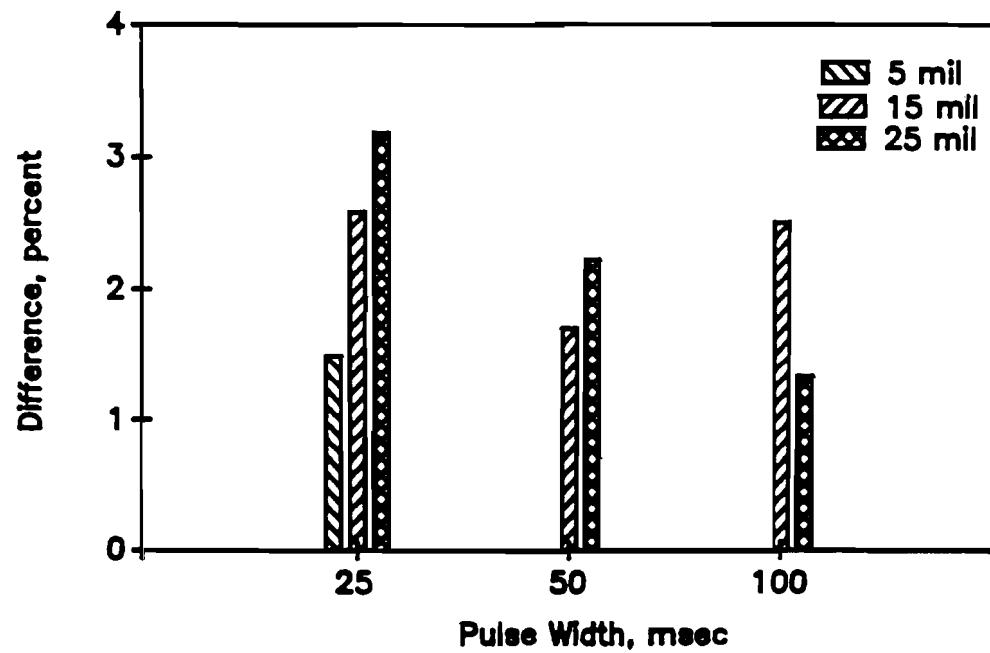


b) Difference from Proximeter Deflections

Figure 3.24 Evaluation of Accuracy and Precision of Geophone 1 Under Triangular Pulse Loading

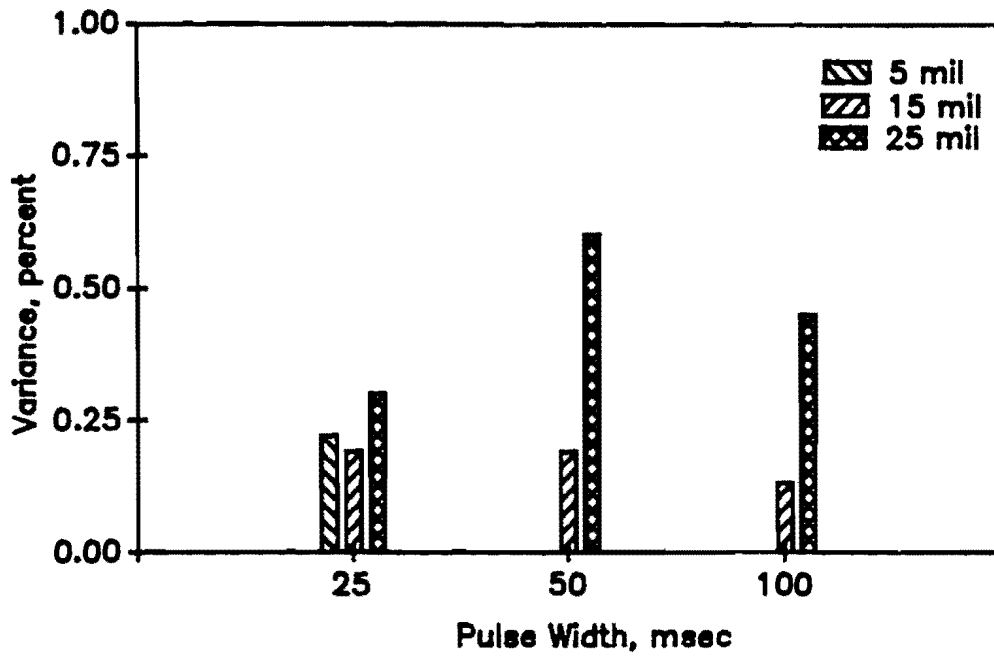


a) Variance

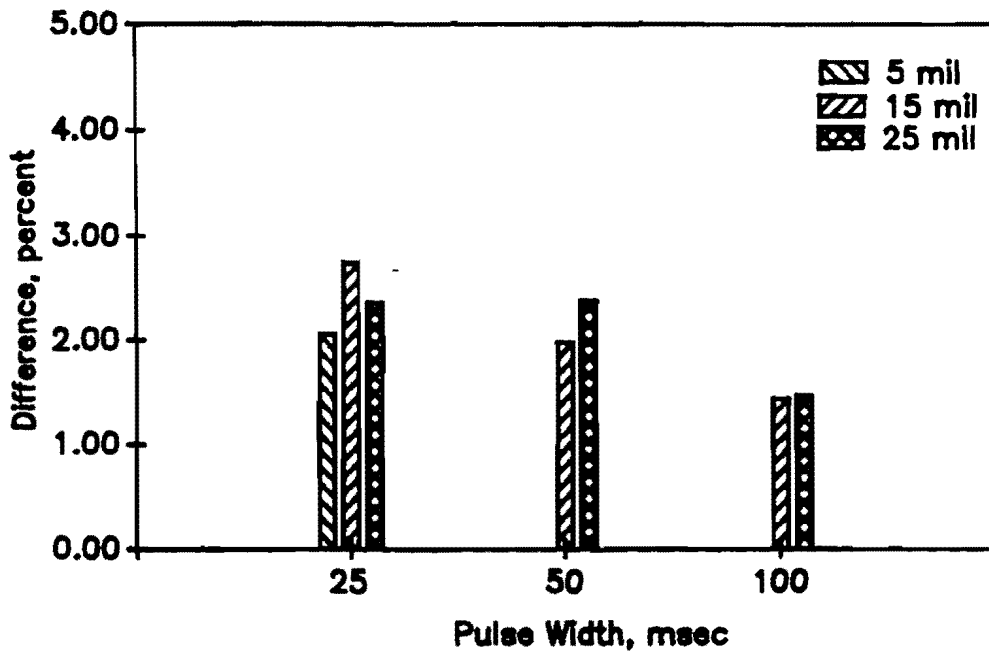


b) Difference from Proximeter Deflections

Figure 3.25 Evaluation of Accuracy and Precision of Geophone 2 Under Triangular Pulse Loading

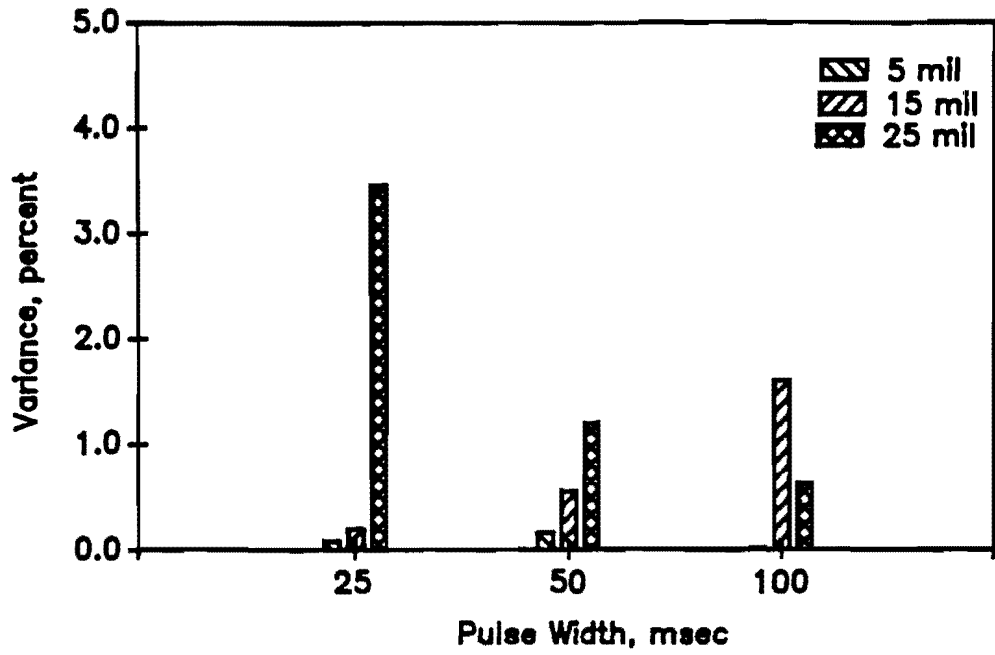


a) Variance

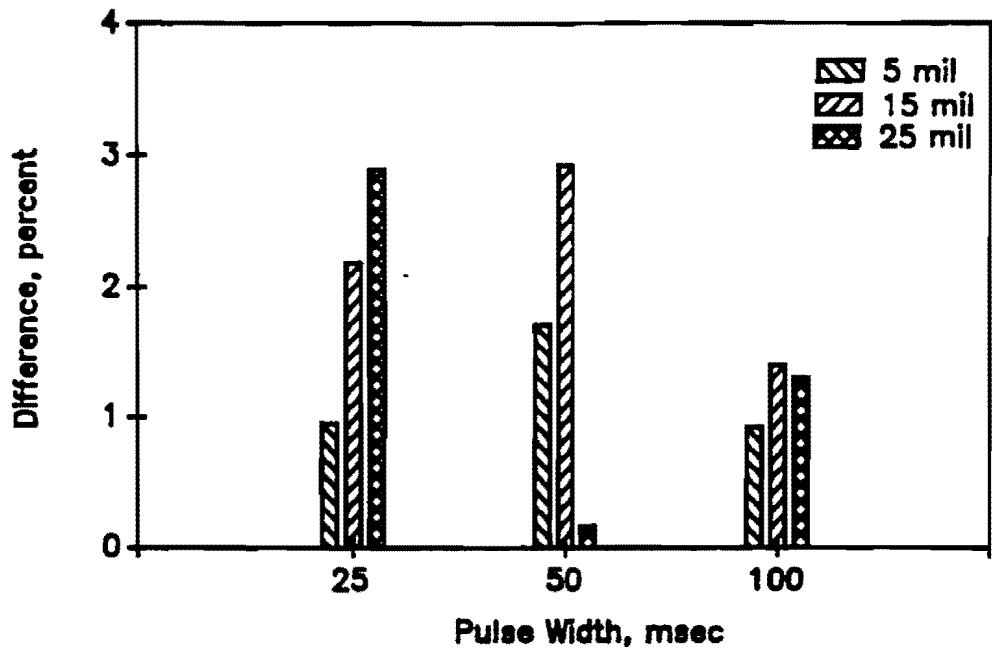


b) Difference from Proximeter Deflections

Figure 3.26 Evaluation of Accuracy and Precision of LVDT Under Triangular Pulse Loading



a) Variance



b) Difference from Proximeter Deflections

Figure 3.27 Evaluation of Accuracy and Precision of Laser Under Triangular Pulse Loading

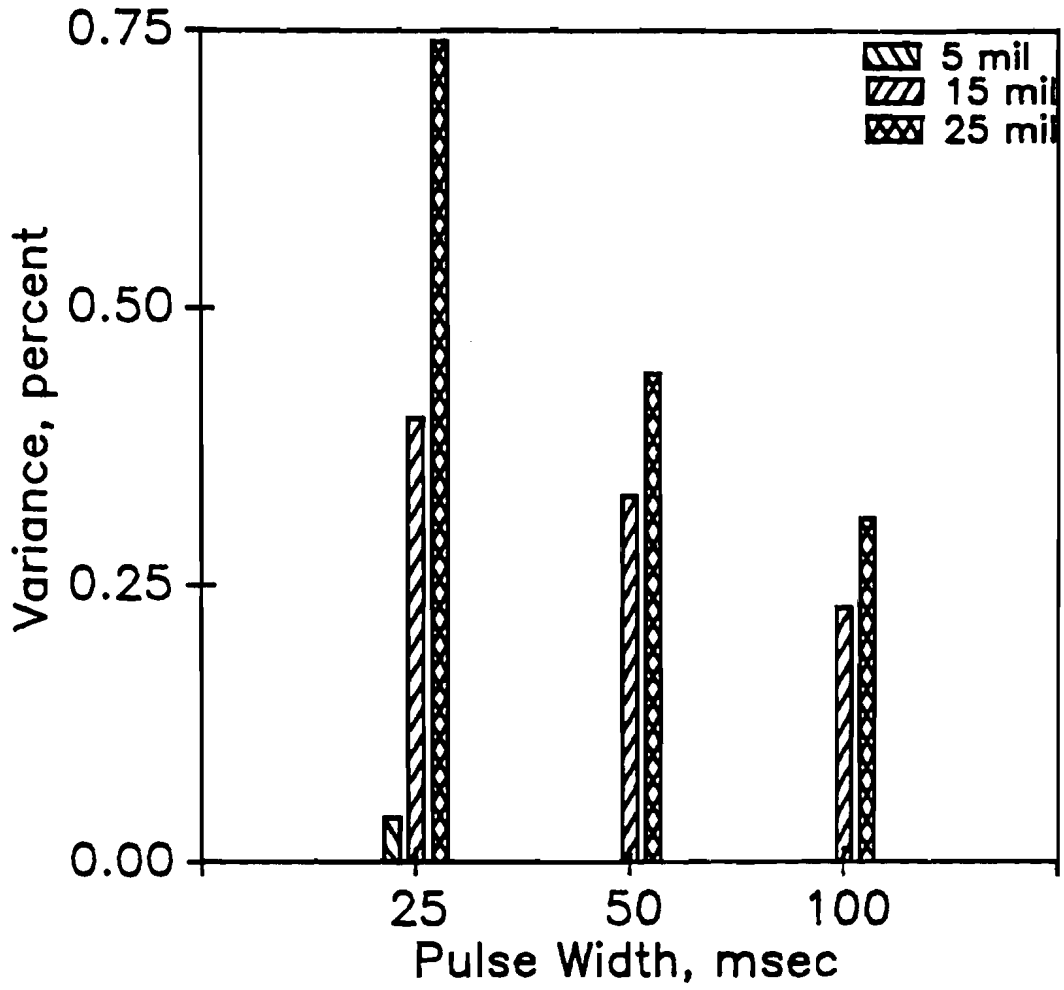


Figure 3.28 Variability in Deflection Measured with Proximeter as a Function of Half-Sine Impulse

The general trends from these two types of pulses is similar to those of the half-sine pulse. For the sake of brevity only an overall evaluation is included herein. Basically, the accelerometers are the least precise sensors and as the pulse width increases (frequency content decreases) the precision decreases (Figures 3.15, 3.16, 3.22 and 3.23). The laser device exhibits the second least favorable precision (Figures 3.20 and 3.27). The most precise sensor is the proximeter (Figures 3.21 and 3.28) followed by the LVDT (Figures 3.19 and 3.26). Closely following the LVDT are the geophones (Figures 3.17, 3.18, 3.24 and 3.25).

CHAPTER FOUR

CONCLUSIONS

Accelerometers are well-calibrated sensors because their calibration curves can be traced to the National Bureau of Standards. However, piezoelectric accelerometers are not capable of accurately measuring motions of large duration because of reasons given in Appendix B.

Accelerometers used in this study function in the frequency range of 10 to 10 kHz. A significant portion of the energy imparted to a pavement by impulsive NDT device is below 10 Hz limit and the Dynaflect device vibrates at a frequency of 8 Hz. The original cost of the accelerometers is high and the connecting micro-dot coaxial cables used for connecting the accelerometers to the amplifiers are not very field-worthy. The cost of the coaxial cable itself is almost the same as the cost of a geophone.

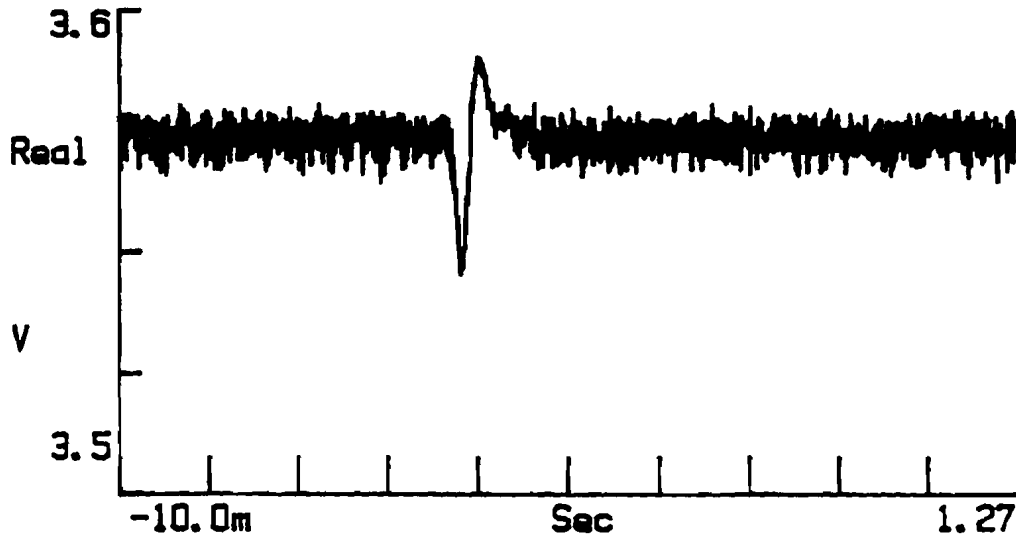
Proximeter is a good tool for measuring deflection in the laboratory. However, the mounting of a proximeter is a problem in the field. In other words, the gap between the proximeter probe and target material should be well controlled throughout the experiment. Also, the input power supply should be of high quality to maintain a constant voltage. The gap between the proximeter and probe is small (about 1 mm), therefore, chances of damaging the probe in the field are high. The proximeter probe should be mounted perfectly horizontal which may be difficult in a field environment.

The LVDT is a good sensing device because of its infinitesimal resolution. But the LVDT suffers from mounting problems similar to those of the proximeter. It is possible to design and construct a mounting system. However, the cost may be prohibitive.

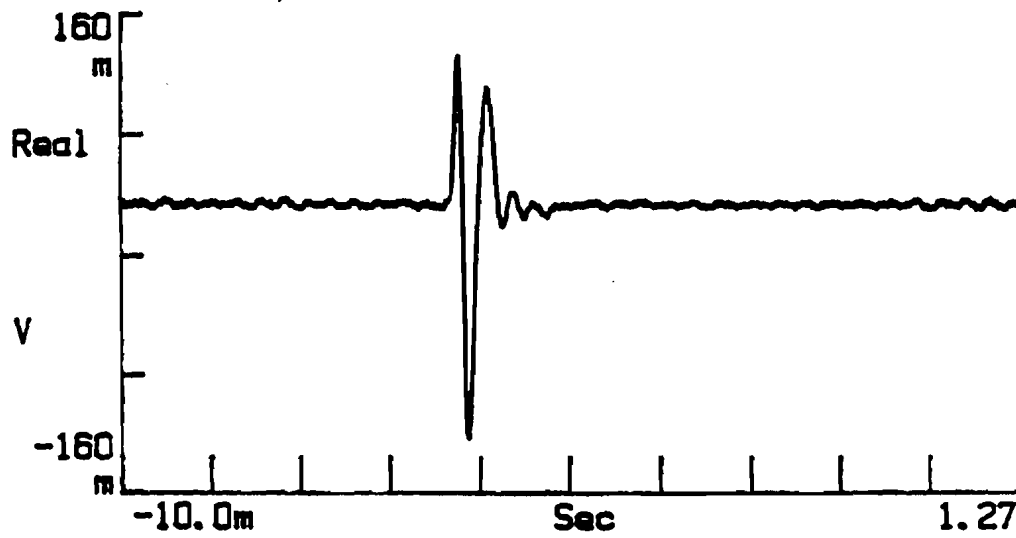
Laser is an accurate and precise sensor. However, the laser optocator needs an extremely smooth surface as a target (which pavement is not). In the laboratory, a properly machined plate was used. Even under this condition, the data obtained from laser for 1 mil deflection had a very poor resolution as shown in Figure 4.1. Of course, once again, the mounting problems needs to be addressed. In addition, the cost of laser is high as compared to other devices.

Contrary to the previous three sensors, geophones do not suffer from mounting problems. But, the data reduction process is rather complicated. However, as described in Chapter Five a proper algorithm has been developed for this task.

The advantages and disadvantages of all sensors as well as their direct and indirect costs are included in Table 4.1. From the discussion in the previous two sections and from Table 4.1, it can be concluded that geophones are the most practical sensors amongst all sensors evaluated. The geophone is rugged enough for the field testing. Geophones cost less than any other sensor. The geophone does not need any special type of mounting fixture as it can be attached to the pavement anywhere with the help of



a) Laser



b) Geophone 2

Figure 4.1 Comparison of Data Obtained from Laser and Geophone, for Half-Sine (Pulse Width 25 mSec), at 1 mil Deflection

Table 4.1 Comparison of Different Characteristics of Five Sensors Evaluated

Sensor	Accelerometer	LVDT	Geophone	Proxi-meter	LASER
Cost	\$350	\$350	\$40	\$400	> \$10,000
Supporting Device(s)	Power Amplifier (\$300)	Power Supply (\$400)	--	Power Supply (\$400)	--
Precision, Steady State	Moderate	Good	Good	V. Good	Excellent
Precision, Impulse	Poor	Good	Good	V. Good	Good
Accuracy, Steady State	Moderate	Good	Good	Excellent	Excellent
Accuracy, Impulse	Poor	Good	Good	Good	Good
Field Worthiness	Good	Moderate	V.Good	Moderate	Poor
Mounting	Very Easy	Difficult	Very Easy	Difficult	Difficult
Ease of Calibration	Moderate	Moderate	Moderate	Moderate	N/A

* Special equipment required

modelling clay. No post or pre amplification or signal conditioning is needed for collection of data; resulting in large savings.

REFERENCES

1. Doebelin, Ernest O., " Measurement System Application and Design," Third Edition, Published by the McGraw Hill Book Company, 1983.
2. Herceg, Edward E., " Hand Book of Measurement and Control," First Edition, Fourth Printing, 1986.
3. Hordeski, Michael E., " Transducers for Automation," First Edition, Published by Van Nostrand Reinhold Company, 1987.
4. Koopmans, Lambert H., " An Introduction to Contemporary Statistics," First Edition, Published by Buxbury Press, 1981.
5. Mark Products, " Geophone General Information," Mark Products, Inc., Houston, Tx., 1985.
6. Nazarian S., Stoke, K.H.,II, " A Theoretical Sensitivity study of the Falling Weight Deflectometer Device on Determining Moduli of Farm-to-Market Roads," Technical Memorandum IAC 936-4, Center for Transportation Research, The University of Texas at Austin, 1986.
7. Norton, Harry N., " Sensor and Analyzer Handbook," First Edition, Published by the Prentice Hall, Inc., Englewood Cliffs, 1982.
8. Ross A. Benstsen, Soheil Nazarian, J Andrew Harrison, " Reliability Testing of Seven Nondestructive Testing of Devices," Nondestructive Testing of Pavements and Backcalculation of Moduli, ASTM STP 1026, A.J. Bush, III and G.Y. Baladi, Eds., American Society for Testing and Materials, Philadelphia, 1989, pp 41-58.
9. Selecom, " Laser Optocator Product Information," Selective Electronic Inc., 1989.
10. Uddin, W., " A Structural System for Pavements Based on Dynamic Deflections," Ph.D Dissertation, The University of Texas, Austin, Tx., 1983.